

# Chitosan Hydrogel Improves Bioavailability of Megosin

Original Paper

Sultanova E. M.<sup>1</sup>, Salakhutdinova M. K.<sup>1</sup>, Oshchepkova Y. I.<sup>1</sup>,  
Asrorov A. M.<sup>1,✉</sup>, Oripova M. J.<sup>1</sup>, Ishimov U. J.<sup>1</sup>, Salikhov S. I.<sup>1</sup><sup>1</sup>Laboratory of Proteins and Peptides Chemistry, Institute  
of Bioorganic chemistry, Academy of Sciences  
of Uzbekistan, 100125, Tashkent, Uzbekistan<sup>2</sup>State Key Laboratory of Drug Research, Shanghai  
Institute of Materia Medica, Chinese Academy of  
Sciences, 501 Haik Road, Shanghai 201203, China

Received 10 May, 2019, accepted 14 January, 2020

**Abstract** **Background:** The aim of this study was to obtain chitosan hydrogels containing megosin, an antiviral medicinal substance, to prolong its bioavailability. Megosin as an immunomodulating agent possesses at least twice higher virostatic and virucidal activities than gossypol, the megosin precursor, and other imine derivatives of gossypol.

**Materials and Methods:** Chitosan, used in this paper, was obtained by deacetylation of chitin; megosin was obtained on the bases of gossypol. Different concentrations of sodium triphosphate (STPP) were used as the cross-linking agent. The release of megosin from hydrogel samples into blood was conducted on five white rats in four groups.

**Results:** Infrared spectral data demonstrated cross-linkage that the band responsible for NH bending of the uncross-linked chitosan reduced its intensity and moved to a lower wavelength, 1636 cm<sup>-1</sup>. It has been proven that megosin contained in gels does not penetrate into the blood and organs after vaginal administration. Release kinetics of megosin from chitosan hydrogels revealed that within 7 h, up to 52% of megosin is allowed into acidic solution (pH 4.5).

**Conclusion:** This study demonstrates the possibility to prolong bioavailability of megosin for at least 7 h, during which time it is not released into blood. The obtained results show the possibility to use the gel composition to treat vaginal herpes.

**Keywords** Chitosan hydrogel – megosin – vaginal herpes

## INTRODUCTION

One of the most common diseases of viral etiology is genital herpes (Sauerbrei, 2016). Acyclic nucleoside antiviral drugs such as acyclovir, valacyclovir, and famciclovir have long been used effectively to treat genital herpes (Pasternak 2010). However, an increasing number of viruses resistant to acyclovir and similar drugs have recently appeared. It was found that in patients with recurrent herpes, the process of formation of interferon is significantly reduced in comparison with healthy people (Sauerbrei, 2016). Therefore, in the treatment of herpes, endogenous interferon inducers have been paid more attention (Katzenel and Leib, 2016; Rasmussen et al., 2007).

Interferons lower the proliferation of herpes virus *in vitro*. Therefore, topical application of gels containing interferon a inducers, several times a day, is a relatively effective treatment for genital herpes (Shperling and Sharopina, 2009). The other effective antiviral drug, megosin (Fig. 1), is able to induce  $\alpha$ ,  $\beta$ ,  $\gamma$  interferons in the body. Therefore, megosin, affecting the

interferon system, exerts its indirect antiviral effect (Baram et al., 2004).

Ordinary conventional vaginal delivery systems like creams, foams, and gels cannot remain for a longer time within the body due to self-cleaning of the vaginal tract. This reduces the retention period of the drug, increases the dose and frequency of drug, and consequently leads to inconvenience when used. Thus, chitosan, a natural cationic amino polysaccharide, used in medicine and pharmaceuticals due to its properties such as biodegradability (Kumar et al., 2004), biocompatibility, lack of toxicity, mucoadhesion (Aranaz et al., 2009; Sonia and Sharma, 2011), and ability to exert antioxidant (Ngo et al., 2014), antibacterial (Martins et al., 2014), and antiviral effects (Ai et al., 2008), is expected to be an efficient agent.

The synergy of the antibacterial properties of chitosan and the antiviral properties of megosin will provide a more effective treatment of genital herpes. The use of mucoadhesive vaginal gel with a slow release of the megosin prolongs the action of

\* E-mail: akmal84a@gmail.com

© European Pharmaceutical Journal

the drug and improves bioavailability (Yellanki et al., 2010). In combination with medicinal substances, chitosan is able to prolong their action (Ahmadi et al., 2015).

The aim of the work is to develop a vaginal gel with mucoadhesive, antibacterial, and antiviral properties to provide longer action at the site of infection using the natural polymer chitosan and the antiviral drug megosin.

## MATERIALS AND METHODS

Megosin was obtained from Institute of Bioorganic Chemistry, Academy of Sciences of Uzbekistan. All other reagents were of analytical grade and used without any further purification.

### Preparation of a vaginal gel

Megosin gel was prepared using chitosan as a gelling agent. Chitosan was dispersed in acetic acid (1%–4%) and was then left overnight to provide complete solubility. Megosin was initially dissolved in 50% ethanol and added to the polymer base with continuous stirring. Two milliliters of an aqueous solution of sodium tripolyphosphate (STPP) (1.4%–5.6%) was added to 10 ml of a chitosan solution of a certain concentration in an aqueous solution of acetic acid at constant stirring.

### Quantification of megosin

An exact amount of the gel was weighed and dissolved in 0.1% acetic acid with lauryl sulfate (1% w/v). After appropriate dilution, the megosin content was analyzed spectrophotometrically (UV-5100 / Vis, Metash, China) at 384 nm.

### Obtaining chitosan from chitin

Chitosan was obtained by deacetylation of chitin. An exact amount of chitin (from Sigma), ground until 0.2–0.3 mm, was treated with 120 ml 50% NaOH at 130°C for 1 h. Chitosan was washed out with water until its pH reached 5; it was then centrifuged and dried. The degree of deacetylation was determined by potentiometric titration. For that, an exact amount of chitosan was diluted in 20 ml of 0.1 M HCl and the obtained solution was titrated with 0.05 M NaOH by adding 0.1 ml solution, stirring every 30 seconds (Czechowska-Biskup et al., 2012).

### Kinetics of megosin release from the gel

Exact amounts of gel samples were placed in a dialysis bag (Serva Feinbiochemica D-6900, 16 × 0.5 m), permeable to passage of substances with a MW less than 10 kDa, and dialyzed against 0.58 mM lactic acid (pH 4.5) and kept at a temperature of 37°C. At certain time intervals, aliquots from the solution were taken and the quantity of the released

megosin was determined spectrophotometrically at 384 nm. The calibration curve for megosin was established.

### Stability of megosin

Megosin was extracted from the freeze-dried gels with a mixture of acetone and water (7:3 v/v). The obtained samples of extracts were analyzed by HPLC (Agilent Technologies 1200 chromatographer with DAD detector. Column: 9.4 × 250 mm Eclipse XDB C18, 5 μm. Mobile phase: A—0.1% trifluoroacetic acid, B—acetonitrile. The flow rate is 2.5 ml/min). We used 10% to 15% acetonitrile as gradient elution for 28 minutes, absorption at 254 nm, referent—360 nm.

### Infrared spectra

Infrared spectra of megosin, chitosan, and the hydrogel on their bases were measured at room temperature on a Fourier infrared spectrometer (Prestige 21, Shimadzu, Japan) with a resolution of 2 cm<sup>-1</sup> and number of scans of 60. Samples were prepared by standard methods in a matrix of fused NaCl.

### Penetration of megosin from chitosan hydrogel into blood

One gram of gel containing 100 μg megosin was introduced intervaginally to white rats weighing 180–200 g. After 7 h, the rats were decapitated and blood, kidneys, and liver samples were collected. Blood and organs were lyophilized, crushed, and extracted with acetone: water solution (3:1, v/v). Quantity analysis of megosin was carried out by HPLC.

## RESULTS AND DISCUSSION

The degree of deacetylation of chitosan was 88%. The alkali amount required for linkage with amino groups of chitosan was determined based on graphs of electrical conductivity in the exact amount of the solution.

We obtained megosin-containing chitosan hydrogels cross-linked with STPP (ionic cross-linking). For the formation of hydrogels containing megosin, we used different concentrations of chitosan, megosin, and STPP (Table 1).

The results showed the highest release level of megosin in 4% chitosan solutions without STPP and with 1.4% and 2.8% STPP containing 1 mg of megosin. More than half the amount of megosin was found released in these samples for 7 h. When 5.6% STPP is included, fourfold lower drug amounts were found released. We determined similar low-level drug release in 5% chitosan solutions. Gel samples with 2% chitosan solution resulted in a moderate level of drug release in almost all cases. The exception was observed in a 2% chitosan gel with 2.8% STPP inclusion, in which just less than half the drug amount was found released for 7 h (Table 1).

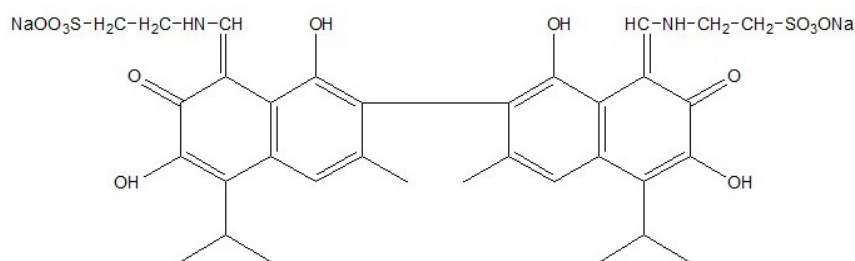


Figure 1: Structure of megosin

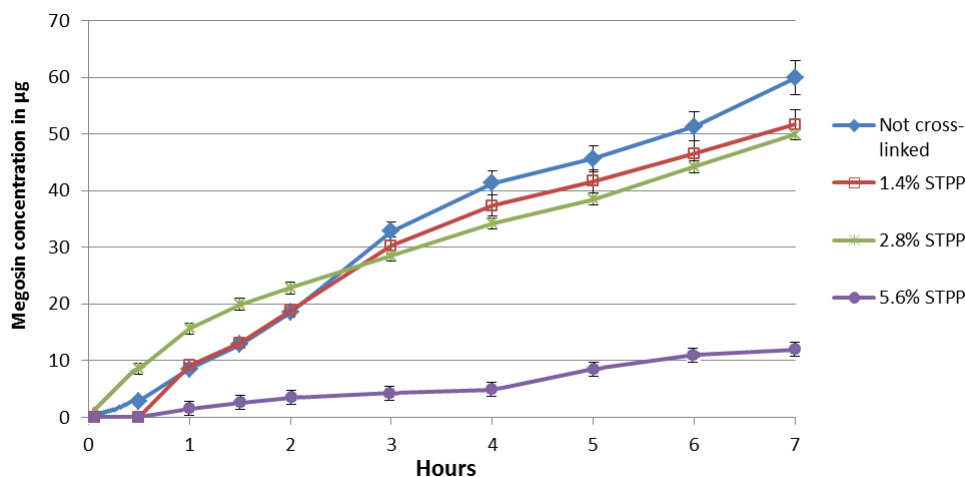


Figure 2: Kinetics of megosin release from 4% chitosan gel samples

Table 1: Releasing level of megosin from chitosan hydrogels

Gel composition			Release percentage of megosin from the gel for 7 h
Chitosan (%)	Megosin (mg)	STPP (%)	
2	1	1.4	20.73 ± 2.33
2	2	1.4	25.88 ± 1.11
2	1	2.8	<b>46.72 ± 2.58</b>
2	2	2.8	32.93 ± 0.89
4	1	0	<b>59.89 ± 1.80</b>
4	1	1.4	<b>51.62 ± 1.68</b>
4	1	2.8	<b>44.91 ± 1.44</b>
4	1	5.6	11.96 ± 0.69
5	1	0	11.07 ± 2.13
5	1	1.4	6.71 ± 0.667

In terms of release yield, gels with 5% chitosan and 5.6% STPP were found the most retaining, likely due to high viscosity and strong cross-linking (Table 1). The kinetics of megosin release from chitosan hydrogel samples for 7 h demonstrated a gradual increase in 4% chitosan solutions (Fig. 2). The process was carried out in conditions mimicking the female body (0.558 mm lactic acid, pH 4.5), For this, a dialysis bag,

containing 1 ml of gel, was immersed in a test tube and 5 ml of lactic acid solution was added. After a certain period of time, the solution was taken. In selected solutions, the absorbance was measured at 384 nm, characteristic for megosin. A pre-constructed calibration curve for megosin was used to determine the concentration.

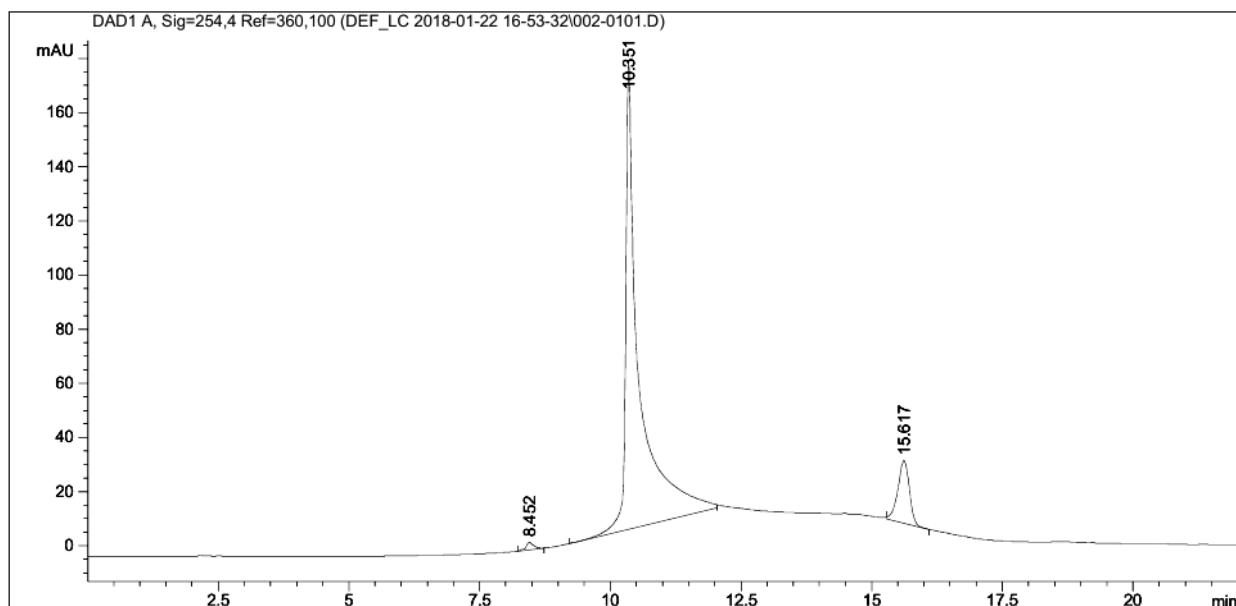


Figure 3: HPLC analysis of megosin in 4% chitosan gel cross-linked with 1.4% STPP

In addition to polar groups ( $\text{NH}_2$  in chitosan and  $\text{SO}_3\text{ONa}$  in megosin) attractions, hydrogen bonds among OH- and NH-groups and van der Waals interactions have been shown to contribute to the retention of megosin in its complex with polyvinylpyrrolidone (Ionov et al., 2009). However, interactions between charged groups likely are the main contributor for the release of the drug in this work, which can be explained by small differences between the non-cross-linked gel and the gel with 1.4% STPP. Moreover, this interaction could lead to higher solubility of megosin in water, which enables its application in biomedicine.

In this work, we determined the stability of megosin in the obtained gels on the 15th day of formation. For this, the exact amount of the gel was taken and freeze-dried. Megosin was extracted with acetone:water system (3:1, v/v). Further, the obtained samples were analyzed by HPLC (Fig. 3).

The HPLC analysis of megosin, isolated from chitosan hydrogel cross-linked with 1.4% STPP, demonstrated its stability and partial degradation in the gel for 15 days. The main peak with a retention time 10.351 is attributed to megosin. The peak at 15.617 is possibly the degradation product of megosin. Further research will clarify its structure and activity.

The IR spectra of megosin, chitosan, and the dried chitosan gel sample containing megosin were obtained (Fig. 4). The structural rearrangement that occurs upon modification of chitosan with STPP is accompanied by changes in the spectra. A low-frequency shift and a noticeable broadening of the absorption bands corresponding to  $\nu$  (NH) vibrations were observed, which indicates the formation of bonds making chitosan cross-linked via  $\text{NH}_2$  group. There is a shift to the low-frequency region of the deformation vibration  $\delta$  (NH) band,

which indicates the involvement of these groups in binding to  $\text{P}_3\text{O}_{10}^{5-}$  anions. In addition, bands appear at  $1217\text{--}1214\text{ cm}^{-1}$ , corresponding to vibrations of  $\nu$  (P = O).

The possible passage of megosin from the chitosan hydrogel into the blood was studied using compositions with the highest release of megosin: 4% chitosan without STPP, 4% chitosan with 1.4% and 2.8%, and 2% chitosan with 2.8% STPP (all with 1 mg megosin). Each group contained at least five experimental animals. The gel was administered intervaginally to white rats. Quantitative determination of megosin was performed by HPLC. No detectable quantity of megosin, released from chitosan hydrogel to blood samples, was found by HPLC analysis.

## CONCLUSION

Thus, we obtained chitosan hydrogels with the antiviral drug megosin. The essential feature of the obtained gel is the ability to swell, mechanical strength, and biodegradation. In addition to the intrinsic properties of chitosan, such as antibacterial and antifungal activity, biocompatibility, and biodegradability, the resulting gels have antiviral properties. Megosin retains its antiviral properties in gels and does not penetrate into the blood. More than half the amount of megosin was found to be released from the gel within 7 h. The use of megosin-containing hydrogel on the basis of chitosan will allow the reduction of the megosin dose and the frequency of the gel so that application of the gel will be more convenient.

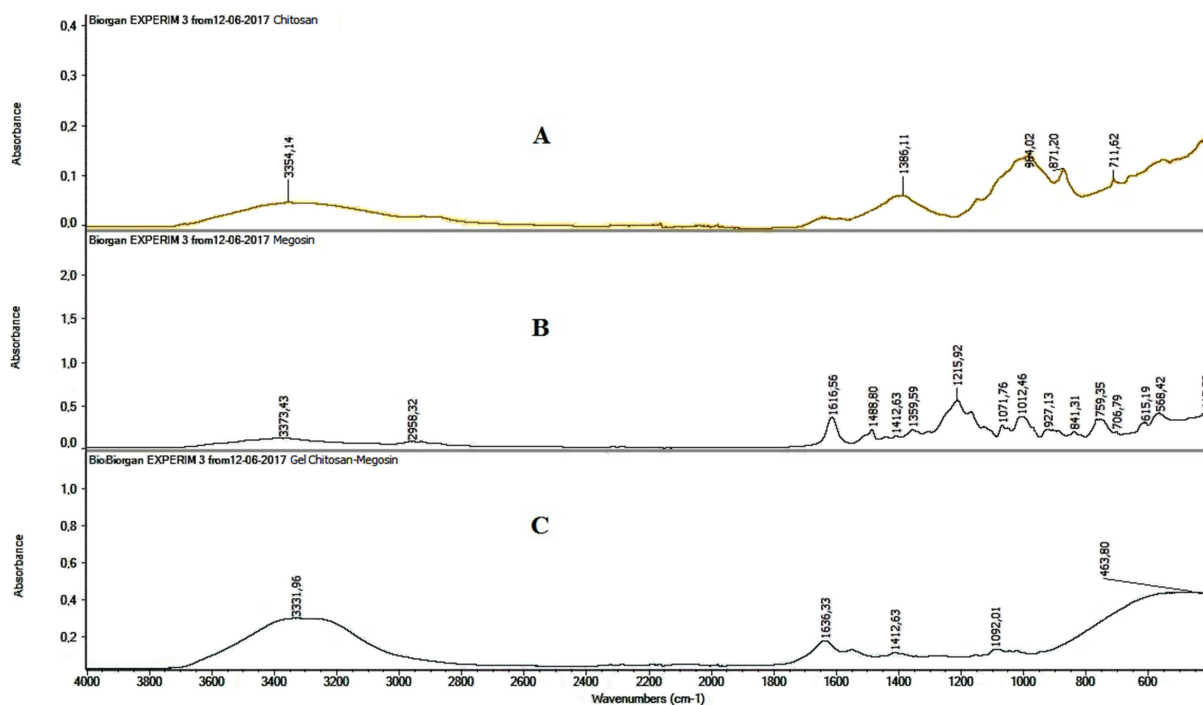


Figure 4: Infrared spectra of chitosan (A), megosin (B), and the dried gel sample on their bases (C)

## ACKNOWLEDGMENTS

The work was supported by the project TA-FA-F6-002-Constructing biomaterials with controllable release of biologically active proteins and polyphenols of Academy of Sciences of Uzbekistan.

We appreciate the support of the CAS President's International Fellowship Initiative (PIFI) Postdoctoral Researchers (2019PB0076) and Shanghai "One Belt One Road" Young Scientist Cooperation Fellowship (18430740800).

We express our sincere thanks to Anzor Sh. Yashinov from Shanghai Institute of Materia Medica (CAS) for critical reading to improve the quality of the paper.

## References

- [1] Sauerbrei A. Optimal management of genital herpes: current perspectives. *Infection and Drug Resistance*. 2016;9:129-141.
- [2] Pasternak B. Use of Acyclovir, Valacyclovir, and Famciclovir in the First Trimester of Pregnancy and the Risk of Birth Defects. *JAMA*. 2010;304:859-866.
- [3] Rasmussen SB, Sørensen LN, Malmgaard L, et al. Type I interferon production during herpes simplex virus infection is controlled by cell-type-specific viral recognition through Toll-like receptor 9, the mitochondrial antiviral signaling protein pathway, and novel recognition systems. *Journal of virology*. 2007;81:13315-13324.
- [4] Katzenell S, Leib DA. Herpes Simplex Virus and Interferon Signaling Induce Novel Autophagic Clusters in Sensory Neurons. *Journal of Virology*. 2016; 90:4706-4719.
- [5] Shperling NV, Sharopina AV. Therapeutic efficiency of preparation of interferon and interferon inducers during genital herpes. *Siberian Medical Journal*. 2009;24: 104-107. (Article in Russian).
- [6] Baram NI, Ismailov AI, Ziyaev KhL, Rezhepov KZh. Biological activity of gossypol and its derivatives. *Chemistry of Natural Compounds*. 2004;40:199-205.
- [7] Kumar MN, Muzzarelli RA, Muzzarelli C, Sashiwa H, Domb AJ. Chitosan chemistry and pharmaceutical perspectives. *Chemical Reviews*. 2004;104:6017-6084.
- [8] Sonia TA, Sharma CP. Chitosan and its derivatives for drug delivery perspective. *Advances in Polymer Science*. 2011;243:23-53.
- [9] Aranaz I, Mengibar M, Harris R et al. Functional characterization of chitin and chitosan. *Current Chemical Biology*. 2009;3:203-230.

- [10] Ngo DH, Kim SK. Antioxidant effects of chitin, chitosan, and their derivatives. In *Advances in Food and Nutrition Research*; Kim SK, Ed., Academic Press: Waltham, MA, USA, 2014;73, pp. 15-31.
- [11] Martins AF, Facchi SP, Follmann HD, Pereira AG, Rubira AF, Muniz EC. Antimicrobial activity of chitosan derivatives containing *N*-quaternized moieties in its backbone: a review. *Int. J. Mol. Sci.* 2014;15:20800-20832.
- [12] Ai H, Wang FR, Yang QS, Zhu F, Le CL. Preparation and biological activities of chitosan from the larvae of housefly, *Musca domestica*. *Carbohydr. Polym.* 2008;72:419-423.
- [13] Yellanki ShK, Nerella NK, Goranti Sh, Kumar Deb S. Development of Metronidazole Intravaginal gel for the treatment of bacterial vaginosis: Effect of Mucoadhesive Natural Polymers on the Release of Metronidazole. *International Journal of Pharm Tech Research.* 2010;2:1746-1750.
- [14] Ahmadi F, Oveisi Z, Samani SM, Amoozgar Z. Chitosan based hydrogels: characteristics and pharmaceutical applications. *Research in pharmaceutical sciences.* 2015;10:1-16.
- [15] Czechowska-Biskup R, Jarosińska D, Rokita B, Ulański P, Rosiak JM. Determination of degree of deacetylation of chitosan - comparison of methods. *Progress on Chemistry and Application of Chitin and its Derivatives.* 2012;XVII:5-19.
- [16] Ionov M, Gordiyenko N, Olchowik E, Baram N, Zijaev Kh, Salakhutdinov B, Bryszewska M, Zamaraeva M. The Immobilization of Gossypol Derivative on N-Polyvinylpyrrolidone Increases its Water Solubility and Modifies Membrane-Active Properties. *Journal of Medicinal Chemistry.* 2009;52: 4119-4125.

# Synthesis, antibacterial and free radical scavenging activity of some newer *N*-((10-nitro-1*H*-indolo [1, 2-*c*]quinazolin-12-yl)methylene)benzenamines

Original Paper

Dixit A.,<sup>1</sup> Pathak D.,<sup>2</sup> Sharma G.K.<sup>1</sup><sup>1</sup>Rajiv Academy for Pharmacy, Mathura, U.P., India<sup>2</sup>Pharmacy College, Saifai, Etawah

Received 20 February, 2019, accepted 11 December, 2019

**Abstract** Present research is oriented on the synthesis of some novel 12-(*N*-arylmethaniminyl)indolo[1,2-*c*]quinazoline analogs (4b1-4b11) and their characterization by <sup>1</sup>H NMR, <sup>13</sup>C NMR, FTIR and mass spectrophotometry. Their free radical scavenging activity and antibacterial potential were also evaluated. Many derivatives have shown a marked free radical scavenging capacity in all the concentrations but specifically compounds 4b7, 4b8 and 4b11 have shown good antioxidant potential with an IC<sub>50</sub> value of 25.18 μmol/L, 28.09 μmol/L & 44.22 μmol/L, respectively (DPPH method) and 39.46 μmol/L, 44.47 μmol/L & 35.61 μmol/L, respectively (H<sub>2</sub>O<sub>2</sub> method). The antibacterial evaluation was carried out against *B. subtilis* and *E. coli* by agar well diffusion method and it revealed that all the compounds in the series were having marked antibacterial activity but compounds 4b9 and 4b11 have shown best antibacterial potential. Then, it was concluded that the derivatives which were containing substituted anilines (4-Nitro, 4-Fluoro, 4-Bromo & 4-Chloro-2-nitro) on the carbon attached on the 12<sup>th</sup> position of indoloquinazoline moiety were having marked potential as an antibacterial and free radical scavenger.

**Keywords** free radical scavenger – antibacterial – DPPH – indoloquinazoline – IC<sub>50</sub>

## INTRODUCTION

Indole is considered as the chief constituent of the alkaloids present in plants (Somei & Yamada, 2003; Gupta et al., 2007). It contains versatile biological activities such as antiviral potential (Cihan-Üstündağ et al., 2019; Xu & Lv, 2009; Ran et al., 2010; Ghosh et al., 2008; Williams et al., 2004), anticancer activity (Gaikwad et al., 2019; El Sayed et al., 2018; Sreenivasulu et al., 2019; Andreani et al., 2008; Slater et al., 2001), antimicrobial study (Chodvadiya et al., 2019; Shirinzadeh et al., 2018; Mathada & Mathada, 2009; Gurkok et al., 2009), antimycobacterial activity (Cihan-Üstündağ et al.; Karah et al., 2007), free radical scavenging activity and antifungal potential (Demurtas et al., 2019; Dekker et al., 1975). The most important pharmacological activities of drugs containing indole moiety are antimicrobial activity and free radical scavenging activity. There are several indole containing structures which are reported by researchers as a good antimicrobial and antifungal agents. Among them, ethyl-3-Indolylacrylate, 5-Bromo-3-(2-Cyanovinyl) indole and 3-(2-Nitrovinyl)indole were those compounds that were active against microbes (Whitehead & Whitesitt, 1974). Haloindoles were found to be effective in between the

concentration of 10-100 μg/ml. In one research study, 3-Acyl-4,7-dihydroxy indoles were reported to be active highly potent against *Escherichia coli* and *Streptococcus pyogenes* (Malesani et al., 1975). 1-Morpholino-3-Carboethoxy-5-hydroxy- 2-methylindole was reported as the most active agent against *Escherichia coli* and *Bacillus cirroflagellosus* (Donawade & Gadaginamath, 2005). 1-(4-Phenyl) and (1-Naphthyl-4*H*-1,2,4-triazole-5-thion-3-yl)indoles were found to be the most potent antimicrobial and antifungal agents (Tsoinis et al., 1997). Some thiosemicarbazide derivatives having indole nucleus and their cyclic 1,2,4-triazole and 1,3,4-thiadiazole analogs were found to have selective action against many microbes and fungi (Varvaresou et al., 2000). Many analogs containing indole moiety fused with various heterocycles were found to be potent antimicrobial agents. Among the reported compounds, 4*H*-pyrano[2,3-*f*] indole, benzotetrahydrocyclohept[1,2-*b*]indole, and 1-triazolylethylbenz[*g*]indole derivatives were reported as some of the most potent classes of antimicrobial compounds (Macchia et al., 1996; Gadaginamath & Kavali 1999; Bhovi & Gadaginamath, 2005). If we talk about another activity, indole

\* E-mail: adixit70@gmail.com

© European Pharmaceutical Journal

has a good candidature for free radical scavenging activity. Literature tells about the involvement of free radicals in various diseases and pathophysiological events including inflammation, cancer, myocardial infarction, arthritis and neurodegenerative disorders (Bast et al., 1991; Bulkley, 1993; Halliwell & Gutteridge, 1998). This involvement of action of free radicals on crucial systems is multiple complex aspects of their involvement in a series of inflammatory disorders (Sreejayan & Rao, 1996) and those disorders which are related to nutrition (McCord, 1993; Cross et al., 1994). Various anti-inflammatory agents are there which act by the free oxygen radicals scavenging action (Santrucek & Krepelka, 1988; Santrunek & Krepelka, 1988). A huge amount of free radicals produced during the inflammation process and out of those wide variety of free radicals there are reactive oxygen species (ROS) such as, superoxide radical ( $O_2^-$ ), hydrogen peroxide ( $H_2O_2$ ), hypochlorous acid (HOCl), singlet oxygen and peroxy radicals, as well as reactive nitrogen species (RNS), like nitric oxide (NO) and peroxy nitrite anion ( $ONOO^-$ ). Actually, ROS and RNS are generated by the endothelial cells, Kupffer cells, neutrophils and macrophages in defense mechanism in the response of infections caused by foreign pathogenic invaders (Nikolic & Breemen, 2001; Vapaatalo, 1986; Halliwell et al., 1988; Mouithys-Mickalad et al., 2000). On the other hand, ROS are also produced by the COX enzyme processes in response to infection and mitochondria are also considered as a source of ROS (Turrens, 2003). These ROS and RNS are involved in a wide variety of diseases and disorders such as cancer, rheumatoid arthritis, and atherosclerosis, Alzheimer and Parkinson's disease, among others (Dedon & Tannenbaum, 2004). In the efforts of finding some more potential of indole nucleus, synthesis of some newer *N*-((10-nitro-1*H*-indolo[1,2-*c*]quinazolin-12-yl)methylene)benzenamine derivatives (4b1-4b11) was done and their antibacterial and antioxidant potential was reported.

## MATERIALS AND METHODS

### Chemistry

The purity of all the synthesized derivatives was determined by thin-layer chromatography on pre-coated silica gel aluminum sheets (Type 60 GF254, Merck) and detection of the spots was done by iodine vapors and UV-Lamp. The melting point was determined by the melting point apparatus and all the melting points were uncorrected. The FTIR spectra were recorded on 470- Shimadzu FTIR spectrophotometer and wavenumber values were expressed in  $cm^{-1}$ . NMR spectra were recorded in DMSO-*d*<sub>6</sub> as a solvent at 300 MHz (<sup>1</sup>H NMR) and 75 MHz (<sup>13</sup>C NMR) on a BRUKER ADVANCE-300 spectrometer. Tetramethylsilane (TMS) was used as an internal standard. Chemical shifts ( $\delta$ ) are shown in parts per million (ppm). Spin multiplicities are given as s (singlet), d (doublet), dd (double doublet), t (triplet) and m (multiplet). Mass spectra were recorded on Shimadzu 2010A LC-MS spectrometer. Elemental

analysis was carried out on Elemental Vario EL III Carlo Erba 1108 and the values were within  $\pm 0.04\%$  of the theoretical values.

### Experimental procedure for the synthesis of 2-(5-nitro-1*H*-indol-2-yl)benzenamine (**1b**)

The mixture of 4-Nitrophenylhydrazine (15 g, 98.03 mmol) and 2-Aminoacetophenone (13.23 g, 98.03 mmol) was refluxed in acetic acid/ethanol mixture for 3 h to give 4-Nitro substituted phenyl hydrazone of 2-Aminoacetophenone. Methanesulfonic acid (220 ml) was heated to 80 °C and phosphorus pentoxide (30 g) was added very slowly with stirring till its complete dissolution (mixture A). The 4-Nitro substituted phenylhydrazone of 2-Aminoacetophenone (20 g) was added slowly to mixture A. The temperature of the reaction was maintained between 80 and 100 °C. Then the solution was heated further at 80 °C for half an hour. Then the reaction mixture cooled to room temperature and then it was poured over crushed ice already containing sodium hydroxide. Then the solid precipitate was filtered, it was washed thoroughly with water, and it was dried to give the crude product which was recrystallized from ethanol. (Yield: 16.20 g, 90 %, M.P. 140-142 °C)

### Experimental procedure for the synthesis of 10-nitro-1*H*-indolo[1,2-*c*]quinazoline (**2b**)

Compound **1b**, 2-(5-nitro-1*H*-indol-2-yl)benzenamine (16 g, 63.24 mmol) was mixed with formic acid (88%, 118 ml) and the solution was heated at 90 °C for 1 h. The reaction mixture was cooled to room temperature and then poured into crushed ice. The solid precipitate was filtered, it was washed thoroughly with water, and it was dried to give the crude product which was recrystallized from ethyl alcohol. (Yield: 12.47 g, 75 %, M.P. 200-202 °C)

### Procedure for the synthesis of 10-nitro-1*H*-indolo[1,2-*c*]quinazoline-12-carbaldehyde (**3b**)

#### Vilsmeier-Haack Formylation

Phosphorous oxychloride (9.72 g, 63.52 mmol) was added slowly to *N,N*-Dimethylformamide (374 ml) at 0 °C and then the solution was stirred for 15 minutes and then it was added dropwise to 10-nitro-*H*-indolo[1,2-*c*]quinazoline (12.47 g, 47.41 mmol). Then, the mixture was stirred for a further 15 minutes and then it was refluxed for 30 minutes. It was then cooled to room temperature and then poured over the crushed ice. The precipitate was then filtered, washed with water (3 x 100 ml) and then it was boiled with aqueous sodium hydroxide (5%, 100 ml). The solid precipitate was then filtered, washed thoroughly with water till it was free from alkali, and then it was dried. The crude material was then recrystallized from ethyl alcohol to give compound 3b (Billimoria & Cava, 1994). (11.44 g, 83 %, M.P. 233-235 °C)

*General procedure for the synthesis of substituted N-((10-nitro-1H-indolo[1,2-c]quinazolin-12-yl)methylene)benzenamines (4b1–4b11)*

An equimolar mixture of 10-nitro-*H*-indolo[1,2-*c*]quinazolin-12-carbaldehyde and substituted anilines in methanol was refluxed for 1 h. It was poured on ice to give the precipitate. The precipitate was then filtered, washed thoroughly with cold water and then it was recrystallized with ethyl alcohol. The percentage yield was obtained in between 80–90 %.

*N-((10-nitro-1H-indolo[1,2-c]quinazolin-12-yl)methylene)benzenamine (4b1)*

Compound 3b (1 g) was refluxed with Aniline (0.31 g).

(Yield: 1.05 g, 84 %); M.P. 251-252 °C; Brown color

FTIR ( $\nu_{\max}$ ,  $\text{cm}^{-1}$ ) 3107 (Aromatic C-H str.), 2938 (Aliphatic C-H str.), 1600 (C=N str.), 1540, 1515 (Aromatic C=C ring str.), 1493, 1350 (N=O str.), 1329 (Aromatic C-N str.);  $^1\text{H}$  NMR (300 MHz, DMSO-*d*6)  $\delta$  ppm: 7.30 (s, 5H), 7.50 (m, 2H), 7.70 (d, 1H), 7.80 (m, 2H), 8.00 (dd,  $J = 8.42, 2.45$  Hz, 2H), 8.50 (s, 1H), 9.23 (s, 1H);  $^{13}\text{C}$  NMR (75 MHz, DMSO-*d*6)  $\delta$  ppm: 102.02, 112.23, 115.35, 116.21, 122.32, 122.41, 125.36, 127.22, 127.18, 127.45, 127.91, 128.65, 130.87, 130.33, 134.77, 136.08, 142.12, 149.21, 149.81, 150.63, 155.74, 160.80; EIMS (m/z):  $[\text{M}]^+$  366.3689,  $[\text{M}+1]^+$  367.3719; Fragments: 262.1336, 217.2027, 189.4612, 163.8462, 108.2225, 104.0144, 45.2915, 27.1215; Anal. calcd. for  $\text{C}_{22}\text{H}_{14}\text{N}_4\text{O}_2$ ; C, 72.12; H, 3.85; O, 8.74; N, 15.29. Found: C, 72.18; H, 3.87; O, 8.70; N, 15.30.

*2-chloro-N-((10-nitro-1H-indolo[1,2-c]quinazolin-12-yl)methylene)benzenamine (4b2)*

Compound 3b (1 g) was refluxed with 2-Chloroaniline (0.43 g).

(Yield: 1.13 g, 82%); M.P. 256-257 °C; Reddish brown color

FTIR ( $\nu_{\max}$ ,  $\text{cm}^{-1}$ ) 3050 (Aromatic C-H str.), 2800 (Aliphatic C-H str.), 1600 (C=N str.), 1544, 1492 (Aromatic C=C ring str.), 1451, 1364 (N=O str.), 1330 (Aromatic C-N str.); 750 (C-Cl str.);  $^1\text{H}$  NMR (300 MHz, DMSO-*d*6)  $\delta$  ppm: 7.10 (d, 1H), 7.10 (m, 2H), 7.30 (d, 1H), 7.50 (s, 1H), 7.58 (t,  $J = 7.12$  Hz, 1H), 7.70 (d, 1H), 7.80 (dd,  $J = 8.29, 2.43$  Hz, 2H), 8.00 (dd,  $J = 8.64, 2.43$  Hz, 2H), 8.50 (s, 1H), 9.23 (s, 1H);  $^{13}\text{C}$  NMR (75 MHz, DMSO-*d*6)  $\delta$  ppm: 102.10, 112.33, 115.20, 116.16, 123.42, 125.66, 127.34, 127.01, 127.55, 127.32, 128.09, 128.67, 128.24, 130.11, 134.55, 136.04, 139.21, 142.78, 149.90, 150.10, 155.55, 160.22; EIMS (m/z):  $[\text{M}]^+$  400.4150,  $[\text{M}+1]^+$  401.2635,  $[\text{M}+2]^+$  402.1035; Fragments: 262.3250, 217.7151, 189.1423, 163.5502, 138.0576, 108.8115, 45.2900, 27.5636; Anal. calcd. for  $\text{C}_{22}\text{H}_{13}\text{ClN}_4\text{O}_2$ ; C, 66.24; H, 3.25; O, 8.31; N, 14.50. Found: C, 66.22; H, 3.93; O, 8.33; N, 9.48.

*3-chloro-N-((10-nitro-1H-indolo[1,2-c]quinazolin-12-yl)methylene)benzenamine (4b3)*

Compound 3b (1 g) was refluxed with 3-Chloroaniline (0.43 g).

(Yield: 1.16 g, 85 %); M.P. 254-255 °C; Dark brown color

FTIR ( $\nu_{\max}$ ,  $\text{cm}^{-1}$ ) 3029 (Aromatic C-H str.), 2929 (Aliphatic C-H str.), 1590 (C=N str.), 1500, 1458 (Aromatic C=C ring str.), 1554, 1326 (N=O str.), 1238 (Aromatic C-N str.), 752 (C-Cl str.);  $^1\text{H}$  NMR (300 MHz, DMSO-*d*6)  $\delta$  ppm: 7.11 (d, 1H), 7.23 (t,  $J = 7.44$  Hz, 1H), 7.35 (t,  $J = 7.41$  Hz, 2H), 7.50 (t,  $J = 7.39$  Hz, 2H), 7.71 (d, 1H), 7.86 (dd,  $J = 8.43, 2.41$  Hz, 2H), 8.01 (dd,  $J = 8.28, 2.42$  Hz, 2H), 8.54 (s, 1H), 9.23 (s, 1H);  $^{13}\text{C}$  NMR (75 MHz, DMSO-*d*6)  $\delta$  ppm: 102.21, 112.36, 115.09, 116.33, 120.40, 122.06, 125.65, 127.56, 127.37, 127.90, 127.24, 128.26, 131.82, 134.18, 135.38, 136.03, 142.19, 149.22, 150.36, 150.43, 155.74, 160.08; EIMS (m/z):  $[\text{M}]^+$  400.4533,  $[\text{M}+1]^+$  401.2345,  $[\text{M}+2]^+$  402.2030; Fragments: 262.4333, 217.5050, 189.1723, 163.5210, 138.1035, 108.2465, 45.3200, 27.8715; Anal. calcd. for  $\text{C}_{22}\text{H}_{13}\text{ClN}_4\text{O}_2$ ; C, 66.24; H, 3.25; O, 8.31; N, 14.50. Found: C, 66.27; H, 3.22; O, 8.33; N, 14.47.

*4-chloro-N-((10-nitro-1H-indolo[1,2-c]quinazolin-12-yl)methylene)benzenamine (4b4)*

Compound 3b (1 g) was refluxed with 4-Chloroaniline (0.43 g).

(Yield: 1.13 g, 83 %); M.P. 253-254 °C; Reddish brown color

FTIR ( $\nu_{\max}$ ,  $\text{cm}^{-1}$ ) 3046 (Aromatic C-H str.), 2928 (Aliphatic C-H str.), 1624 (C=N str.), 1590, 1500 (Aromatic C=C ring str.), 1550, 1350 (N=O str.), 1283 (Aromatic C-N str.), 750 (C-Cl str.);  $^1\text{H}$  NMR (300 MHz, DMSO-*d*6)  $\delta$  ppm: 7.22 (dd,  $J = 8.40, 2.41$  Hz, 2H), 7.35 (dd,  $J = 8.43, 2.38$  Hz, 2H), 7.51 (t, 7.45 Hz, 2H), 7.72 (s, 1H), 7.85 (dd, 8.46, 2.43 Hz, 2H), 8.01 (dd, 8.40, 2.42 Hz, 2H), 8.53 (s, 1H), 9.23 (s, 1H);  $^{13}\text{C}$  NMR (75 MHz, DMSO-*d*6)  $\delta$  ppm: 102.24, 112.09, 115.13, 116.21, 123.14, 123.33, 125.42, 127.35, 127.29, 127.98, 128.37, 130.27, 130.16, 132.22, 134.81, 136.92, 142.33, 147.01, 149.17, 150.29, 155.45, 160.38; EIMS (m/z):  $[\text{M}]^+$  400.4904,  $[\text{M}+1]^+$  401.1802,  $[\text{M}+2]^+$  402.2760; Fragments: 262.4035, 217.2651, 189.1423, 163.5662, 138.0826, 108.1540, 45.6302, 27.3016; Anal. calcd. for  $\text{C}_{22}\text{H}_{13}\text{ClN}_4\text{O}_2$ ; C, 66.24; H, 3.25; O, 8.31; N, 14.50. Found: C, 66.26; H, 3.26; O, 8.35; N, 14.52.

*2-nitro-N-((10-nitro-1H-indolo[1,2-c]quinazolin-12-yl)methylene)benzenamine (4b5)*

Compound 3b (1 g) was refluxed with 2-Nitroaniline (0.47 g).

(Yield: 1.12 g, 80 %); M.P. 245-246 °C; Grey color

FTIR ( $\nu_{\max}$ ,  $\text{cm}^{-1}$ ) 3020 (Aromatic C-H str.), 2954 (Aliphatic C-H str.), 1620 (C=N str.), 1585, 1450 (Aromatic C=C ring str.), 1520, 1322 (N=O str.), 1220 (C-N str.);  $^1\text{H}$  NMR (300 MHz, DMSO-*d*6)  $\delta$  ppm: 7.50 (m, 4H), 7.72 (dd,  $J = 8.43, 2.44$  Hz, 2H), 7.81 (dd,  $J = 8.41, 2.42$  Hz, 2H), 8.01 (dd,  $J = 8.44, 2.44$  Hz, 2H), 8.25 (d, 1H), 8.50 (s, 1H), 9.23 (s, 1H);  $^{13}\text{C}$  NMR (75 MHz, DMSO-*d*6)  $\delta$  ppm: 102.11, 112.22, 115.36, 116.49, 122.32, 123.09, 125.02, 127.00, 127.15, 127.28, 128.82, 128.53, 134.37, 136.19, 136.18, 141.26, 142.31, 144.42, 149.46, 150.50, 155.63, 160.88; EIMS (m/z):  $[\text{M}]^+$  411.7609,  $[\text{M}+1]^+$  412.3619; Fragments: 262.1356, 217.4400, 189.2350, 163.4902, 149.2949, 108.3225, 45.6415, 27.2712; Anal. calcd. for  $\text{C}_{22}\text{H}_{13}\text{N}_5\text{O}_4$ ; C, 64.25; H, 3.62; O, 15.60; N, 17.35. Found: C, 64.27; H, 3.22; O, 15.57; N, 17.38.

**3-nitro-*N*-((10-nitro-1*H*-indolo[1,2-*c*]quinazolin-12-yl)methylene)benzenamine (4b6)**

Compound 3b (1 g) was refluxed with 3-Nitroaniline (0.47 g). (Yield: 1.18 g, 84 %); M.P. 250-252 °C; Greyish green color  
FTIR ( $\nu_{\max}$ ,  $\text{cm}^{-1}$ ) 3046 (Aromatic C-H str.), 2958 (Aliphatic C-H str.), 1651 (C=N str.), 1574, 1419 (Aromatic C=C ring str.), 1508, 1360 (N=O str.), 1174 (C-N str.);  $^1\text{H NMR}$  (300 MHz, DMSO-*d*6)  $\delta$  ppm: 7.58 (m, 3H), 7.72 (dd,  $J = 8.40, 2.45$  Hz, 2H), 7.83 (dd,  $J = 8.42, 2.45$  Hz, 1H), 7.84 (dd,  $J = 8.39, 2.41$  Hz, 1H), 8.01 (dd,  $J = 8.34, 2.29$  Hz, 2H), 8.22 (t,  $J = 7.35$  Hz, 2H), 8.54 (s, 1H), 9.23 (s, 1H);  $^{13}\text{C NMR}$  (75 MHz, DMSO-*d*6)  $\delta$  ppm: 102.25, 112.36, 115.12, 116.57, 117.31, 119.09, 125.26, 127.52, 127.78, 127.91, 128.17, 128.18, 131.31, 134.06, 136.14, 142.77, 149.81, 149.15, 149.48, 150.80, 155.36, 160.66; EIMS (m/z):  $[\text{M}]^+$  411.7618,  $[\text{M}+1]^+$  412.3629; Fragments: 262.2045, 217.3640, 189.2750, 163.5292, 149.2509, 108.3914, 45.6121, 27.2022; Anal. calcd. for  $\text{C}_{22}\text{H}_{13}\text{N}_5\text{O}_4$ ; C, 64.30; H, 3.50; O, 15.56; N, 17.41. Found: C, 64.32; H, 3.47; O, 15.54; N, 17.44.

**4-nitro-*N*-((10-nitro-1*H*-indolo[1,2-*c*]quinazolin-12-yl)methylene)benzenamine (4b7)**

Compound 3b (1 g) was refluxed with 4-Nitroaniline (0.47 g). (Yield: 1.22 g, 87 %); M.P. 252-253 °C; Reddish brown color  
FTIR ( $\nu_{\max}$ ,  $\text{cm}^{-1}$ ) 3085 (Aromatic C-H str.), 2937 (Aliphatic C-H str.), 1670 (C=N str.), 1610, 1421 (Aromatic C=C ring str.), 1554, 1326 (N=O str.), 1292 (C-N str.);  $^1\text{H NMR}$  (300 MHz, DMSO-*d*6)  $\delta$  ppm: 7.51 (m, 4H), 7.73 (d, 1H), 7.83 (dd,  $J = 8.42, 2.40$  Hz, 1H), 7.84 (dd,  $J = 8.39, 2.44$  Hz, 1H), 8.01 (m, 2H), 8.29 (dd,  $J = 8.26, 2.29$  Hz, 2H), 8.53 (s, 1H), 9.23 (s, 1H);  $^{13}\text{C NMR}$  (75 MHz, DMSO-*d*6)  $\delta$  ppm: 102.65, 112.33, 115.18, 116.44, 122.92, 122.29, 123.64, 123.75, 125.19, 127.05, 127.06, 127.20, 128.13, 134.45, 136.61, 142.77, 146.32, 149.48, 150.37, 155.19, 155.29, 160.04; EIMS (m/z):  $[\text{M}]^+$  411.3303,  $[\text{M}+1]^+$  412.2959; Fragments: 262.1136, 217.5940, 189.2050, 163.5450, 149.4862, 108.0545, 45.7124, 27.2821; Anal. calcd. for  $\text{C}_{22}\text{H}_{13}\text{N}_5\text{O}_4$ ; C, 64.30; H, 3.50; O, 15.45; N, 17.41. Found: C, 64.27; H, 3.52; O, 15.42; N, 17.40.

**4-fluoro-*N*-((10-nitro-1*H*-indolo[1,2-*c*]quinazolin-12-yl)methylene)benzenamine (4b8)**

Compound 3b (1 g) was refluxed with 4-Fluoroaniline (0.37 g). (Yield: 1.06 g, 81 %); M.P. 258-259 °C; Grey color  
FTIR ( $\nu_{\max}$ ,  $\text{cm}^{-1}$ ) 3080 (Aromatic C-H str.), 2920 (Aliphatic C-H str.), 1606 (C=N str.), 1558, 1325, (N=O str.), 1433, 1421 (Aromatic C=C ring str.), 1292 (Aromatic C-N str.), 1180 (C-F str.);  $^1\text{H NMR}$  (300 MHz, DMSO-*d*6)  $\delta$  ppm: 7.01 (dd,  $J = 8.29, 2.44$  Hz, 2H), 7.24 (dd,  $J = 8.35, 2.43$  Hz, 2H), 7.50 (s, 1H), 7.58 (t,  $J = 7.40$  Hz, 1H), 7.70 (d, 1H), 7.83 (dd,  $J = 8.22, 2.46$  Hz, 1H), 7.84 (d, 1H), 8.01 (dd,  $J = 8.18, 2.40$  Hz, 2H), 8.53 (s, 1H), 9.23 (s, 1H);  $^{13}\text{C NMR}$  (75 MHz, DMSO-*d*6)  $\delta$  ppm: 102.05, 112.55, 115.69, 116.41, 116.25, 116.32, 123.28, 123.16, 125.07, 127.18, 127.00, 127.30, 128.48, 134.22, 136.31, 142.83, 144.76, 149.51,

150.19, 155.82, 160.20, 161.35; EIMS (m/z):  $[\text{M}]^+$  384.1269,  $[\text{M}+1]^+$  385.3126; Fragments: 262.9936, 217.3023, 189.4712, 163.2262, 122.5622, 108.4945, 45.3815 27.3115; Anal. calcd. for  $\text{C}_{22}\text{H}_{13}\text{FN}_4\text{O}_2$ ; C, 68.75; H, 3.41; O, 8.33; N, 14.58. Found: C, 68.72; H, 3.39; O, 8.30; N, 14.55.

**4-bromo-*N*-((10-nitro-1*H*-indolo[1,2-*c*]quinazolin-12-yl)methylene)benzenamine (4b9)**

Compound 3b (1 g) was refluxed with 4-Bromoaniline (0.59 g). (Yield: 1.30 g, 85 %); M.P. 240-241 °C; Dark brown color  
FTIR ( $\nu_{\max}$ ,  $\text{cm}^{-1}$ ) 3073 (Aromatic C-H str.), 2927 (Aliphatic C-H str.), 1613 (C=N str.), 1588, 1458 (Aromatic C=C ring str.), 1518, 1323, (N=O str.) 1232 (Aromatic C-N str.), 609 (C-Br str.);  $^1\text{H NMR}$  (300 MHz, DMSO-*d*6)  $\delta$  ppm: 7.21 (dd,  $J = 8.44, 2.42$  Hz, 2H), 7.42 (dd,  $J = 8.40, 2.38$  Hz, 2H) 7.50 (s, 1H), 7.58 (t,  $J = 7.50$  Hz, 1H), 7.71 (d, 1H), 7.83 (dd,  $J = 8.56, 2.39$  Hz, 1H), 7.84 (dd,  $J = 8.50, 2.63$  Hz, 1H), 8.01 (dd,  $J = 8.40, 2.41$  Hz, 2H), 8.52 (s, 1H), 9.23 (s, 1H);  $^{13}\text{C NMR}$  (75 MHz, DMSO-*d*6)  $\delta$  ppm: 102.03, 112.26, 115.15, 116.33, 121.27, 124.41, 124.35, 125.83, 127.42, 127.28, 127.06, 128.30, 133.22, 133.12, 134.19, 136.90, 142.39, 148.44, 149.56, 150.07, 155.82, 160.08; EIMS (m/z):  $[\text{M}]^+$  445.1316,  $[\text{M}+1]^+$  446.2617,  $[\text{M}+2]^+$  447.5860; Fragments: 262.2627, 217.3373, 189.0577, 181.4457, 163.3219, 108.2079, 45.0195, 27.1422; Anal. calcd. for  $\text{C}_{22}\text{H}_{13}\text{BrN}_4\text{O}_2$ ; C, 59.34; H, 2.94; O, 7.19; N, 12.58. Found: C, 59.32; H, 2.91; O, 7.16; N, 12.59.

**2-chloro-4-nitro-*N*-((10-nitro-1*H*-indolo[1,2-*c*]quinazolin-12-yl)methylene)benzenamines (4b10)**

3b (1 g) was refluxed with 2-Chloro-4-nitroaniline (0.58 g). (Yield: 1.33 g, 88 %); M.P. 256-257 °C; Reddish brown color  
FTIR ( $\nu_{\max}$ ,  $\text{cm}^{-1}$ ) 3028 (Aromatic C-H str.), 2853 (Aliphatic C-H str.), 1642 (C=N str.), 1563, 1430 (Aromatic C=C ring str.), 1523, 1308 (N=O str.), 1283 (C-N str.), 752 (C-Cl str.);  $^1\text{H NMR}$  (300 MHz, DMSO-*d*6)  $\delta$  ppm: 7.51 (t,  $J = 7.56$  Hz, 2H), 7.58 (t,  $J = 7.39$  Hz, 1H), 7.70 (d, 1H), 7.82 (m, 2H), 8.01 (dd,  $J = 8.30, 2.45$  Hz, 2H), 8.12 (d, 1H), 8.26 (s, 1H), 8.51 (s, 1H), 9.23 (s, 1H);  $^{13}\text{C NMR}$  (75 MHz, DMSO-*d*6)  $\delta$  ppm: 102.11, 112.22, 115.47, 116.66, 120.74, 124.57, 125.33, 125.09, 127.01, 127.18, 127.77, 128.91, 128.28, 134.44, 136.56, 142.00, 145.88, 148.20, 149.01, 150.43, 155.17, 160.84; EIMS (m/z):  $[\text{M}]^+$  445.5030,  $[\text{M}+1]^+$  446.1413,  $[\text{M}+2]^+$  447.2303; Fragments: 262.3925, 217.6756, 189.1023, 182.5222, 163.8866, 108.4325, 45.4560, 27.2202; Anal. calcd. for  $\text{C}_{22}\text{H}_{12}\text{N}_5\text{O}_4\text{Cl}$ ; C, 59.27; H, 2.71; O, 14.38; N, 15.71. Found: C, 59.28; H, 2.70; O, 14.36; N, 15.73.

**4-chloro-2-nitro-*N*-((10-nitro-1*H*-indolo[1,2-*c*]quinazolin-12-yl)methylene)benzenamine (4b11)**

Compound 3b (1 g) was refluxed with 4-Chloro-2-nitroaniline (0.58 g). (Yield: 1.29 g, 85 %); M.P. 255-256 °C; Light brown color

FTIR ( $\nu_{\max}$ ,  $\text{cm}^{-1}$ ) 3023 (Aromatic C-H str.), 2910 (Aliphatic C-H str.), 1612 (C=N str.), 1553, 1423 (Aromatic C=C ring str.), 1513, 1330 (N=O str.), 1285 (C-N str.), 685 (C-Cl str.);  $^1\text{H}$  NMR (300 MHz, DMSO-*d*<sub>6</sub>)  $\delta$  ppm: 7.50 (t,  $J = 7.47$  Hz, 2H), 7.52 (t,  $J = 7.36$  Hz, 1H), 7.71 (d, 1H), 7.87 (m, 2H), 8.01 (dd,  $J = 8.42, 2.38$  Hz, 2H), 8.15 (d, 1H), 8.28 (s, 1H), 8.54 (s, 1H), 9.23 (s, 1H);  $^{13}\text{C}$  NMR (75 MHz, DMSO-*d*<sub>6</sub>)  $\delta$  ppm: 102.05, 112.14, 115.23, 116.14, 124.25, 125.66, 125.25, 127.36, 127.17, 127.46, 128.81, 133.62, 134.77, 136.01, 136.34, 142.71, 142.29, 143.37, 149.45, 150.40, 155.92, 160.14; EIMS ( $m/z$ ):  $[\text{M}]^+$  445.5237,  $[\text{M}+1]^+$  446.2513,  $[\text{M}+2]^+$  447.4463; Fragments: 262.6625, 217.1725, 189.1882, 182.3421, 163.6131, 108.7235, 45.4560, 27.1925; Anal. calcd. for  $\text{C}_{22}\text{H}_{12}\text{N}_5\text{O}_4\text{Cl}$ ; C, 59.27; H, 2.71; O, 14.38; N, 15.71. Found: C, 59.29; H, 2.69; O, 14.37; N, 15.74.

## BIOLOGICAL ACTIVITIES

### Antibacterial activity

Antibacterial activity for all derivatives was done by agar well diffusion method. Ciprofloxacin was used as the reference compound. One gram-negative bacterium (*Escherichia coli*) and a gram-positive bacterium (*Bacillus subtilis*) were taken for activity. These bacteria were obtained from Microbiology Laboratory, National JALMA Institute for Leprosy & Other Mycobacterial Diseases, Agra, India. Solutions of all derivatives having a concentration of 100  $\mu\text{g/ml}$  and 150  $\mu\text{g/ml}$  were prepared in Dimethylsulfoxide (DMSO). Sterilized materials were used. The bacteria were grown in nutrient broth at 37 °C for 24 h. On a water bath, nutrient agar was melted and then cooled to 45 °C. It was then shaken gently. Inoculation of each culture (1.0 ml) was done aseptically and then mixing was done by gentle shaking and then the mixture was poured into the sterilized Petri plates. The material was then allowed to settle for 1–2 h, and then it was cut to make wells of 7 mm. Each compound in the form of the solution was added to each of these wells. Then all plates were incubated at 37 °C for 24 h. After incubation time, the zone of inhibition around each well was measured in millimeters. DMSO was used as a control (Ugur et al., 2000).

Antioxidant activities

### DPPH radical scavenging activity

All the synthesized derivatives were evaluated for their free radical scavenging potential using 0.1 mmol solution of DPPH in methanol. Solutions were kept in darkness for half an hour to form free radicals. Solution of different concentrations were prepared (10, 20, 30, 40 and 50  $\mu\text{g/ml}$ ) for test compounds as well as standard. Then, 1 ml of each test compound solution was added with the same volume of DPPH solution, then the mixture was mixed vigorously and kept for half an hour in the darkroom. The absorbance of all solutions was measured at a wavelength of 517 nm. The same procedure was performed in the triplicate manner ( $n = 3$ ) and the average of the three

readings was shown in the results with standard deviation. The same procedure was carried out with the solutions of ascorbic acid. Percent inhibition was calculated using equation 1 (Kaushik et al., 2016; Malviya et al., 2017).

$$\% \text{ inhibition} = \frac{\text{Absorbance of control} - \text{Absorbance of sample}}{\text{absorbance of control}} \times 100 \quad (1)$$

### $\text{H}_2\text{O}_2$ radical scavenging activity

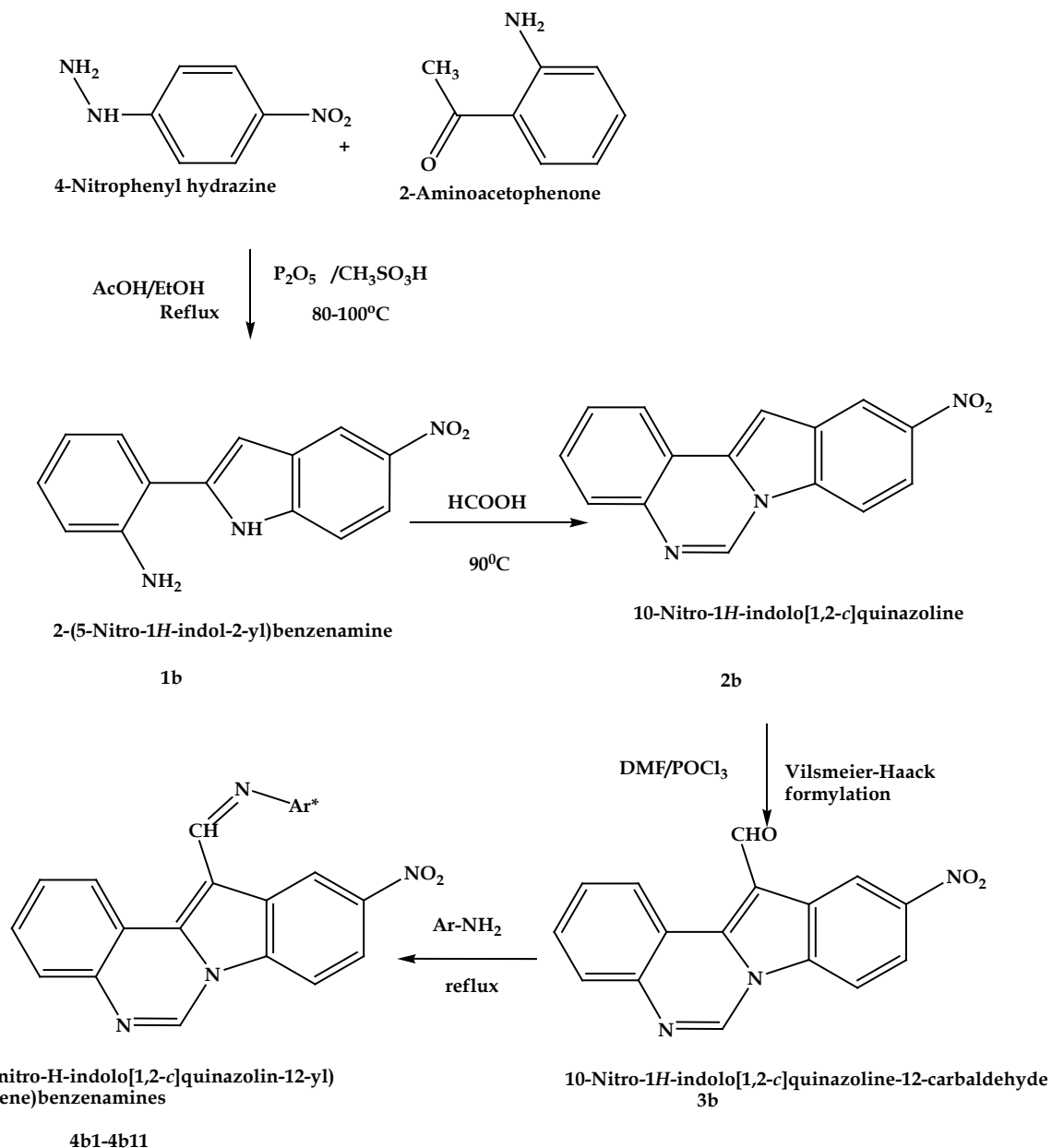
Hydrogen peroxide was used to produce hydroxyl radicals. All the solutions of test and standard compounds were prepared as above and concentrations of hydroxyl radicals were observed at 230 nm (Ningsih et al., 2016). The procedure was performed in a triplicate manner and the average of the three readings was shown in the results with standard deviation. Percent inhibition was calculated using **equation 1**.

## RESULTS AND DISCUSSION

### Chemistry

In the first step, phenyl hydrazone of 2-Aminoacetophenone was synthesized by the reflux of equimolar quantities of 4-Nitrophenyl hydrazine and 2-Aminoacetophenone in acetic acid/ethanol mixture for 3 h. Then, 2-(5-nitro-1*H*-indol-2-yl)benzenamine (**1b**) was synthesized after the cyclization reaction of phenylhydrazone of 2-Aminoacetophenone by phosphorous pentoxide and methanesulphonic acid. Then, cyclization of **1b** was carried out by 90% Formic acid, which produced 10-Nitro-1*H*-Indolo[1,2-*c*]quinazoline (**2b**). In the next step, compound **2b** was allowed to undergo formylation by Vilsmeier–Haack Formylation reaction to give 10-Nitro-12-formylindolo[1,2-*c*]quinazoline (**3b**). Compound **3b** was then reacted with various substituted anilines to give *N*-((10-nitro-1*H*-indolo [1, 2-*c*]quinazolin-12-yl)methylene)benzenamines (**4b1–4b11**). The synthetic **scheme** is given below.

The characterization of all derivatives was done by IR,  $^1\text{H}$  NMR,  $^{13}\text{C}$  NMR, mass spectral data, and elemental analysis. In the IR spectra of compounds **4b1–4b11**, the C-H stretching (aromatic) vibrations gave rise to a band at 3107–3020  $\text{cm}^{-1}$ . Stretching bands for C-H (aliphatic) were observed in between 2958–2800  $\text{cm}^{-1}$ . The stretching bands for C-Cl were observed between 752–685  $\text{cm}^{-1}$ . The stretching vibrations of the nitro group for symmetric and asymmetric vibrations gave rise to the bands between 1558–1451  $\text{cm}^{-1}$  and 1364–1308  $\text{cm}^{-1}$ . Stretching of C-F and C-Br bonds were observed at 1292  $\text{cm}^{-1}$  and 551  $\text{cm}^{-1}$  respectively. In the  $^1\text{H}$  NMR spectra of compounds **4b1–4b11**, the signals of protons of the aromatic rings appeared in the region of 7.00 and 9.23 ppm in the form of singlet, doublet, double doublet, and multiplet. The singlet due to the proton of C-H of methaniminyl group was observed at 7.50 ppm. Spectra of compounds showed the singlet due to the proton of quinazoline ring at 9.23 ppm.



\*Ar: -Phenyl, 2-Chlorophenyl, 3-Chlorophenyl, 4-Chlorophenyl, 2-Nitrophenyl, 3-Nitrophenyl, 4-Nitrophenyl, 4-Fluorophenyl, 4-Bromophenyl, 2-Chloro-4-nitrophenyl, 4-Chloro-2-nitrophenyl

In the <sup>13</sup>C NMR spectra of all compounds, carbons present in aromatic rings gave signals in the region of 102–160 ppm. The signal of N=C=N carbon atom of the quinazoline ring was observed at 136 ppm. The signal due to the C-Cl carbon was observed at 127–135 ppm. The signal due to the C-F carbon was observed at 161.40 ppm. The signal due to the C-Br carbon was observed at 121.63 ppm. Mass spectral data and elemental analysis were complying with the structures of all compounds. [M+ 2] peaks were found for compounds having Cl group.

### Biological activities

All indoloquinazoline derivatives (**4b1–4b11**) were tested for their potential as a better antioxidant and antibacterial agent. Antibacterial activity

The result for antibacterial activity was shown (Table 1), compound **4b9** showed 13 mm and 18 mm zone of inhibition at 100 µg/ml and 150 µg/ml concentrations, respectively against *B. subtilis* and it also showed 12 mm and 17 mm zone of inhibition at 100 µg/ml and 150 µg/ml concentrations, respectively against *E. coli*. Compound **4b10** showed

Table 1: Zone of inhibition values for derivatives (4b1-4b11) at 100 µg/ml and 150 µg/ml

Compounds	Zone of inhibition (mm)			
	B. subtilis		E.coli	
	100 µg/ml	150 µg/ml	100 µg/ml	150 µg/ml
<b>4b1</b>	2	7	3	5
<b>4b2</b>	2	8	4	9
<b>4b3</b>	4	8	6	10
<b>4b4</b>	5	10	4	9
<b>4b5</b>	3	7	4	9
<b>4b6</b>	6	10	7	10
<b>4b7</b>	6	12	7	12
<b>4b8</b>	5	10	7	13
<b>4b9</b>	13	18	12	17
<b>4b10</b>	12	15	13	17
<b>4b11</b>	6	14	8	14
<b>Ciprofloxacin (25 µg/ml)</b>	20		18	

good antibacterial activity against *B. subtilis* with a zone of inhibition of 12 mm and 15 mm at 100 µg/ml and 150 µg/ml concentrations, respectively and a zone of inhibition of 13 mm and 17 mm against *E. coli* at 100 µg/ml and 150 µg/ml concentrations, respectively. Ciprofloxacin showed better antimicrobial activity against *B. subtilis* and *E. coli* at lower concentration (25 µg/ml) with a zone of inhibition of 20 mm and 18 mm against *B. subtilis* and *E. coli* respectively.

### Antioxidant activities

#### DPPH radical scavenging activity

All the newly synthesized indoloquinazoline derivatives were screened for free radical scavenging activity by DPPH method. Sample solutions were prepared to have concentrations of 10, 20, 30, 40 and 50 µg/ml. Ascorbic acid was taken as a standard antioxidant. Compounds **4b7**, **4b8** and **4b11** were found to be good free radical scavengers with good percentage inhibition in all the concentrations and an IC<sub>50</sub> value of 25.18 µmol/L, 28.09 µmol/L and 44.22 µmol/L, respectively. The percentage inhibition for all the synthesized compounds is shown (Table 2).

#### H<sub>2</sub>O<sub>2</sub> radical scavenging activity

All the derivatives were also screened for antioxidant activity by the H<sub>2</sub>O<sub>2</sub> method. Sample solutions were prepared to have concentrations of 10, 20, 30, 40 and 50 µg/ml. Ascorbic acid was taken as a standard antioxidant. Compounds **4b7**, **4b8** and **4b11** were reported as good free radical scavengers with an IC<sub>50</sub> value of 39.46 µmol/L, 44.47 µmol/L and 35.61 µmol/L,

respectively. The percentage inhibition for all the synthesized compounds is shown in the tabular form (Table 3).

### Structure-Activity Relationship

The present study suggests that all the indole derivatives that were containing substituted anilines having electron-withdrawing groups at para positions were reported to have good antioxidant and antibacterial activities. Compounds **4b9** (4-Bromophenyl) and **4b10** (4-Chloro-2-nitrophenyl) were found to contain good antibacterial activity against gram-positive and gram-negative bacteria. Derivatives **4b7** (4-Nitrophenyl), **4b8** (4-Fluorophenyl) and **4b11** (4-Chloro-2-nitrophenyl) were having good potential as an antioxidant. It is also observed that the nitro group attached at 2<sup>nd</sup> position can also enhance the antioxidant activity and chloro group attached at 2<sup>nd</sup> position along with a nitro group at 4<sup>th</sup> position can enhance the antibacterial activity.

### CONCLUSION

Synthesis of some newer *N*-((10-nitro-1*H*-indolo [1, 2-*c*]quinazolin-12-yl)methylene)benzenamines (**4b1–4b11**) was done and the characterization of all the derivatives was done by the <sup>1</sup>H NMR, <sup>13</sup>C NMR, FTIR and mass spectrophotometry. Then their potential as an antioxidant and as an antibacterial was evaluated. Most of the derivatives have shown good antioxidant activity in all the concentrations. Compounds **4b7**, **4b8** and **4b11** were found to be the best free radical scavengers. Antibacterial studies showed that the compounds **4b9** and **4b10** have shown the best antibacterial action. By looking at these results, the conclusion can be made that

Table 2: DPPH free radical scavenging activity of compounds 4b1–4b11

Compounds	% Inhibition at $\mu\text{g/ml}^*$					IC <sub>50</sub> value ( $\mu\text{mol/L}$ )
	10	20	30	40	50	
Ascorbic acid	45.8 $\pm$ 1.21	54.01 $\pm$ 1.09	61.60 $\pm$ 0.98	66.89 $\pm$ 1.23	78.01 $\pm$ 2.31	87.67
4b1	17.26 $\pm$ 4.36	20.98 $\pm$ 0.43	26.20 $\pm$ 0.69	36.84 $\pm$ 2.86	41.26 $\pm$ 1.50	189.43
4b2	4.01 $\pm$ 2.43	14.75 $\pm$ 0.79	24.29 $\pm$ 1.71	35.24 $\pm$ 0.89	37.94 $\pm$ 1.67	150.70
4b3	14.75 $\pm$ 0.42	19.67 $\pm$ 0.91	27.60 $\pm$ 0.46	32.92 $\pm$ 0.75	36.64 $\pm$ 0.45	178.80
4b4	7.42 $\pm$ 0.75	15.66 $\pm$ 0.30	20.88 $\pm$ 0.62	30.82 $\pm$ 0.45	35.13 $\pm$ 0.75	174.22
4b5	16.06 $\pm$ 0.45	21.68 $\pm$ 0.30	28.01 $\pm$ 0.30	34.93 $\pm$ 1.08	45.98 $\pm$ 0.75	141.77
4b6	4.31 $\pm$ 0.75	13.65 $\pm$ 0.62	23.18 $\pm$ 1.50	26.70 $\pm$ 0.75	32.92 $\pm$ 0.62	176.32
4b7	50.19 $\pm$ 1.05	54.71 $\pm$ 0.45	65.45 $\pm$ 0.75	73.49 $\pm$ 0.90	76.70 $\pm$ 0.75	25.18
4b8	50.59 $\pm$ 1.17	53.61 $\pm$ 0.79	57.02 $\pm$ 0.62	60.94 $\pm$ 0.45	67.66 $\pm$ 0.75	28.09
4b9	12.74 $\pm$ 1.83	20.57 $\pm$ 0.96	28.41 $\pm$ 0.75	32.92 $\pm$ 0.92	36.04 $\pm$ 0.74	158.38
4b10	27.40 $\pm$ 0.21	30.41 $\pm$ 0.60	33.12 $\pm$ 0.79	35.63 $\pm$ 0.62	38.75 $\pm$ 0.45	203.73
4b11	44.67 $\pm$ 0.96	50.00 $\pm$ 0.62	56.62 $\pm$ 0.82	59.83 $\pm$ 0.45	67.46 $\pm$ 0.60	44.22

\*n = 3 (results are average of triplicate readings with standard deviation)

Table 3: H<sub>2</sub>O<sub>2</sub> free radical scavenging activity of compounds 4b1–4b11

Compounds	% Inhibition at $\mu\text{g/ml}^*$					IC <sub>50</sub> value ( $\mu\text{mol/L}$ )
	10	20	30	40	50	
Ascorbic acid	44.35 $\pm$ 1.21	55.32 $\pm$ 1.34	62.09 $\pm$ 1.51	66.72 $\pm$ 1.10	77.02 $\pm$ 1.33	88.23
4b1	4.02 $\pm$ 0.57	10.18 $\pm$ 0.75	18.11 $\pm$ 0.75	24.52 $\pm$ 0.37	32.32 $\pm$ 0.57	224.22
4b2	1.88 $\pm$ 0.37	7.67 $\pm$ 1.32	16.98 $\pm$ 0.37	20.37 $\pm$ 0.75	26.03 $\pm$ 0.75	220.12
4b3	9.68 $\pm$ 0.57	20.25 $\pm$ 0.57	24.02 $\pm$ 1.32	28.80 $\pm$ 0.57	34.08 $\pm$ 0.94	191.10
4b4	2.26 $\pm$ 0.37	8.55 $\pm$ 0.94	15.34 $\pm$ 0.78	20.00 $\pm$ 0.75	28.17 $\pm$ 0.94	213.82
4b5	1.25 $\pm$ 0.57	7.92 $\pm$ 1.13	12.20 $\pm$ 1.15	19.24 $\pm$ 0.37	23.52 $\pm$ 0.78	234.89
4b6	4.90 $\pm$ 0.99	10.06 $\pm$ 0.57	19.37 $\pm$ 0.57	23.64 $\pm$ 0.94	28.17 $\pm$ 0.57	205.62
4b7	44.90 $\pm$ 0.37	54.08 $\pm$ 0.57	60.37 $\pm$ 0.37	65.15 $\pm$ 0.94	76.10 $\pm$ 0.94	39.46
4b8	43.52 $\pm$ 0.57	54.00 $\pm$ 1.15	59.11 $\pm$ 0.57	66.03 $\pm$ 0.75	72.83 $\pm$ 1.13	44.47
4b9	8.30 $\pm$ 0.75	13.96 $\pm$ 0.37	20.12 $\pm$ 0.57	28.80 $\pm$ 0.57	30.81 $\pm$ 0.57	178.53
4b10	4.90 $\pm$ 0.75	8.30 $\pm$ 0.37	13.20 $\pm$ 0.37	20.75 $\pm$ 0.37	24.90 $\pm$ 0.75	219.88
4b11	47.04 $\pm$ 0.57	53.58 $\pm$ 1.13	57.10 $\pm$ 0.57	63.39 $\pm$ 0.75	74.08 $\pm$ 0.57	35.61

\*n = 3 (results are average of triplicate readings with standard deviation)

all those compounds having 4 substituted anilines (4-Nitro, 4-Fluoro, 4-Bromo & 4-Chloro-2-nitro) on the methaniminyl group of 12<sup>th</sup> position of indolo[1,2-*c*]quinazoline moiety possess good antioxidant and antibacterial activities.

#### FUNDING

This research received no external funding.

## ACKNOWLEDGMENTS

The authors would like to thank the management of Rajiv Academy for Pharmacy, Mathura for providing research facilities. IIT, Delhi is acknowledged for providing the spectral data of the synthesized compounds. National JALMA Institute for Leprosy & Other Mycobacterial Diseases, Agra is acknowledged for providing bacterial cultures.

## CONFLICTS OF INTEREST

The authors declare no conflict of interest.

## References

- [1] Al-Hiari YM, Qaisi AM, El-Abadelah MM, Voelter W. Synthesis and antibacterial activity of some substituted 3-(aryl)- and 3-(heteroaryl) indoles. *Monatshefte für Chemie/Chemical Monthly*. 2006 Feb 1;137(2):243–8.
- [2] Andreani A, Bunnelli S, Granaiola M et al. Antitumor activity of bis-indole derivatives. *J Med Chem*. 2008; 51: 4563–4570.
- [3] Bast A, Haenen G, Doelman C. Oxidants and antioxidants: state of the art. *Am J Med*. 1991; 92 (Suppl. 3C): 2–13.
- [4] Bhovi MG, Gadaginamath GS. 1,3-Dipolar cycloaddition reactions: Synthesis and antimicrobial activity of novel 1-triazolylindole and 1-triazolylbenz-[g]indole derivatives. *Indian J Chem*. 2005; 44B: 1068–1073.
- [5] Billimoria AD, Cava MP. Chemistry of Indole [1, 2-c]quinazoline: An approach to the marine alkaloid Hinckdentine A. *J Org Chem*. 1994; 59: 6777–6782.
- [6] Bulkley GB. Free radicals and other reactive oxygen metabolites: Clinical relevance and the therapeutic efficacy of antioxidant therapy. *Surgery*. 1993; 113: 479–483.
- [7] Chodvadiya VD, Pambhar KD, Parmar ND, Dhamsaniya AP, Chhatbar PV, Ram HN, Khunt RC, Patel PK. Synthesis and Characterization of N-Methyl Indole Derivatives via Desulfurative Displacement by Various Amines and Its Antimicrobial Activity. *World Scientific News*. 2019; 120(2):181–91.
- [8] Cihan-Üstündağ G, Naesens L, Şatana D, Erköse-Genç G, Mataracı-Kara E, Çapan G. Design, synthesis, antitubercular and antiviral properties of new spirocyclic indole derivatives. *Monatshefte für Chemie-Chemical Monthly*. 2019;150(8):1533–44.
- [9] Cross CE, Vliet A, Neill ACO, Eiserich JP. Reactive oxygen species and the lung. *Lancet*. 1994; 344: 930–933.
- [10] Dedon PC, Tannenbaum SR. Reactive nitrogen species in the chemical biology of inflammation. *Arch Biochem Biophys*. 2004; 423: 12–22.
- [11] Dekker WH, Selling HA, Overeem JC. Structure-activity relationships of some antifungal indoles. *J Agric Food Chem*. 1975; 23: 785–791.
- [12] Demurtas M, Baldisserotto A, Lampronti I, Moi D, Balboni G, Pacifico S, Vertuani S, Manfredini S, Onnis V. Indole derivatives as multifunctional drugs: Synthesis and evaluation of antioxidant, photoprotective and antiproliferative activity of indole hydrazones. *Bioorganic chemistry*. 2019 Apr 1;85:568–76.
- [13] Donawade DS, Gadaginamath GS. Some electrophilic substitution reactions on 1-substituted-3-acetyl/carbethoxy-5-hydroxy-2-methylindole and antimicrobial activity of these new indole derivatives. *Indian J Chem*. 2005; 44B: 1679–1685.
- [14] El Sayed MT, Sabry NM, Mahmoud K, Mahrous KF, Ali MM, Mahmoud AE, Voronkov A. Novel Nitro-Heterocycles Sugar and Indoles Candidates as Lead Structures Targeting HepG2 and A549 Cancer Cell Lines. *Current Bioactive Compounds*. 2018 Dec 1;14(4):434–44.
- [15] Gadaginamath GS, Kavali RR. Synthesis and antimicrobial activity of novel 4H-pyrano [2, 3-f]- indole derivatives. *Indian J Chem*. 1999; 38B: 178–182.
- [16] Gaikwad R, Bobde Y, Ganesh R, Patel T, Rathore A, Ghosh B, Das K, Gayen S. 2-Phenylindole derivatives as anticancer agents: synthesis and screening against murine melanoma, human lung and breast cancer cell lines. *Synthetic Communications*. 2019 Jun 17:1–2.
- [17] Ghosh AK, Gong G, Grum-Tokars V, Mulhearn DC, Baker SC, Coughlin M, Prabhakar BS, Sleeman K., Johnson ME, Mesecar AD. Design, synthesis and antiviral efficacy of a series of potent chloropyridyl ester-derived SARS-CoV 3CLpro inhibitors. *Bioorg Med Chem Lett*. 2008; 18: 5684–5688.
- [18] Gupta L, Talwar A, Chauhan PMS. Bis and tris indole alkaloids from marine organisms: new leads for drug discovery. *Curr Med Chem*. 2007; 14: 1789–1803.
- [19] Gurkok G, Altanlar N, Suzen S. Investigation of antimicrobial activities of Indole-3- Aldehyde Hydrazone/Hydrazone Derivatives. *Chemotherapy*. 2009; 55, 15–19.
- [20] Halliwell B, Gutteridge M. Free radicals in biology and medicine, third ed. Oxford Science Publications. Oxford University Press. 1998.
- [21] Halliwell B, Hoult JR, Blake DR. Oxidants, inflammation, and anti-inflammatory drugs. *FASEB J*. 1988; 2: 2867–2873.
- [22] Karah N, Gursoy A, Kandemirli F, Shvets N, Kaynak FB, Ozbey S, Kovalishyn V, Dimoglo A. Synthesis and structure-antituberculosis activity relationship of 1H-indole-2,3-dione derivatives. *Bioorg Med Chem*. 2007; 15: 5888–5891.
- [23] Kaushik N, Kumar N, Kumar A. Synthesis, antioxidant and antidiabetic activity of 1-[(5-substituted phenyl)-4,5-dihydro-1H-pyrazol-3-yl]- 5-phenyl-1H-tetrazole. *Indian J Pharm Sci*. 2016; 78(3): 352–359.
- [24] Kodisundaram P, Amirthaganesan S, Balasankar T. Antimicrobial evaluation of a set of heterobicyclic methylthiadiazole hydrazones: synthesis, characterization, and SAR studies. *Journal of agricultural and food chemistry*. 2013 Nov 27;61(49):11952–6

- [25] Macchia M, Manera C, Nencetti S, Rossello A, Broccoli G, Limonta D. Synthesis and antimicrobial activity of benzo[*a*] dihydrocarbazole and benzotetrahydrocyclohept [1,2*b*]indole derivatives. *Farmaco*. 1996; 51: 75–78.
- [26] Malesani G, Chiarelto G, Dallacqua F, Vedali D. Antimicrobial properties of some 3-acyl-4,7- disubstituted indoles. *Farmaco*. 1975; 30: 137–146.
- [27] Malviya R, Sharma PK, Dubey SK. Antioxidant potential and emulsifying properties of kheri (*Acacia chundra*, Mimosaceae) gum polysaccharide. *Marm Pharm J*. 2017; 21/3: 701–706.
- [28] Mathada BSD, Mathada MBH. Synthesis and antimicrobial activity of some 5-substituted-3-phenyl-Nb-(Substituted-2-oxo-2*H*-pyrano [2,3-*b*]quinoline-3-carbonyl)-1*H*-indole-2-carboxyhydrazide. *Chem Pharm Bull*. 2009; 57: 557–560.
- [29] McCord JM. Human disease, free radicals, and the oxidant/antioxidant balance, *Clin Biochem*. 1993; 26: 351–357.
- [30] Mouthys-Mickalad AML, Zheng SX, Deby-Dupont GP, Deby CM, Lamy MM, Reginster JY, Henrotin YE. In vitro study of the antioxidant properties of nonsteroidal anti-inflammatory drugs by chemiluminescence and electron spin resonance (ESR). *Free Radic Res*. 2000; 33: 607–621.
- [31] Nikolic D, Breemen RB. DNA Oxidation Induced by Cyclooxygenase-2, *Chem Res Toxicol*. 2001; 14: 351–354.
- [32] Ningsih IY, Zulaikhah S, Hidayat MA, Kuswandi B. Antioxidant activity of various Kenitu (*Chrysophyllum cainito* L.) leaves extracts from Jember. *Indonesia Agric Sci Procedia*. 2016; 9: 378–85.
- [33] Ran J, Huang N, Xu H, Yang Y, Lv M, Zheng YT. Anti HIV-1 agents 5: Synthesis and anti-HIV-1 activity of some *N*-arylsulfonyl-3-acetylindoles. *Bioorg Med Chem. Lett*. 2010; 20: 3534–3536.
- [34] Santrucek M, Krepelka J. Antioxidants from the aspect of their potential use in chemotherapy. *Drugs Future*. 1988; 37: 121–128.
- [35] Santrucek M, Krepelka J. Of particular interests are the potential protective effects of antioxidants on lipoproteins, since oxidized LDL is thought to be atherogenic, *Drugs Future*. 1988; 13: 973–996.
- [36] Shirinzadeh H, SÜZEN S, Altanlar N, Westwell AD. Antimicrobial Activities of New Indole Derivatives Containing 1, 2, 4-Triazole, 1, 3, 4-Thiadiazole and Carbothioamide. *Turkish Journal of Pharmaceutical Sciences*. 2018;15(3).
- [37] Slater MJ, Baxter R, Bonser RW, Cockerill S, Gohil K, Parry N, Robinson E, Randall R, Yeates C, Snowden W, Walters A. Synthesis of *N*-alkyl substituted indolocarbazoles as potent inhibitors of human cytomegalovirus replication. *Bioorg Med Chem Lett*. 2001; 11: 1993–95.
- [38] Somei M, Yamada F. Simple indole alkaloids and those with a nonrearranged monoterpenoid unit. *Nat Prod Rep*. 2003; 20: 216–242.
- [39] Sravanthi T, Rani S, Manju S. Synthesis and biological evaluation of 2-(2'/3'/4'/6'-substituted phenyl)-1*H*-indoles. *Int J Pharm Pharmac Sc*. 2015; 7(11): 268–73
- [40] Sreejayan N, Rao MN. Free radical scavenging activity of curcuminoids, *Drug Res*. 1996; 46: 169–171.
- [41] Sreenivasulu R, Reddy KT, Sujitha P, Kumar CG, Raju RR. Synthesis, antiproliferative and apoptosis induction potential activities of novel bis (indolyl) hydrazide-hydrazone derivatives. *Bioorganic & medicinal chemistry*. 2019 Mar 15;27(6):1043–55.
- [42] Tsotinis A, Varvaresou A, Calogeropoulou T, Siatra-Papastaikoudi T, Tiligada A. Synthesis and antimicrobial evaluation of indole containing derivatives of 1,3,4-triazole and their open-chain counterparts. *Drug Res*. 1997; 47: 307–310.
- [43] Turrens JF. Mitochondrial formation of reactive oxygen species. *J Physiol*. 2003; 552: 335–344.
- [44] Ugur A, Mercimek B, Ozler MA, Aahin N. Antimicrobial effects of bis (2-imidazolyl)-5,5*V*-dioxime and its mono- and tri-nuclear complexes. *Transit Met Chem*. 2000; 25, 421.
- [45] Vapaatalo H. Free radicals and anti-inflammatory drugs. *Med Biol*. 1986; 64: 1–7;
- [46] Varvaresou A, Tsantili-Kakoulidou A, Siatra-Papastaikoudi T, Tiligada E. Synthesis and biological evaluation of indole containing derivatives of thiosemicarbazide and their cyclic 1,2,4-triazole and 1,3,4-thiadiazole analogs, *Drug Res*. 2000; 50: 48–54.
- [47] Whitehead CW, Whitesitt AA. Effects of lipophilic substituents on some biological properties of indoles. *J Med Chem*. 1974; 17: 1298–1304.
- [48] Williams JD, Chen JJ, Drach JC, Townsend LB. Synthesis and antiviral activity of 3-formyl- and 3-Cyano-2,5,6-trichloroindole nucleoside derivatives, *J Med Chem*. 2004; 47: 5766–5772.
- [49] Xu H, Lv M. Developments of indoles as anti-HIV-1 inhibitors. *Curr Pharm Des*. 2009; 15: 2120–2148.

# Concentration-dependent effect of silymarin on concanavalin A-stimulated mouse spleen cells *in vitro*

Original research article/Review

Hrčková G.<sup>1</sup>✉, Mačák Kubašková T.<sup>1</sup>, Mudroňová D.<sup>2</sup>, Bardelčíková A.<sup>3</sup>

<sup>1</sup>Institute of Parasitology of the Slovak Academy of Sciences, Košice, Slovakia

<sup>2</sup>Institute of Microbiology and Immunology, The University of Veterinary Medicine and Pharmacy, Košice, Slovakia

<sup>3</sup>Annamária Bardelčíková, Department of Pharmacology, Faculty of Medicine, The University of P. J. Šafárik, Košice, Slovakia

Received 2 October, 2019, accepted 10 December, 2019

**Abstract** Aims: Silymarin (SIL), a mixture of phenolic compounds, has a pleiotropic mode of action on various cell types, including immune cells. In this study, we investigated the concentration-dependent effect of SIL on proliferation of concanavalin A (CoA)-stimulated mouse spleen T lymphocytes, their viability, and secretion of IFN- $\gamma$  and IL-4 cytokines *ex vivo* in relation to gene expressions of transcription factors nuclear factor kappa B and Foxp3. In addition, metabolic activity of T cells was determined as changes in the mitochondrial membrane potential and apoptosis.

Material/Methods: Isolated splenocytes were stimulated with lectin CoA and treated with SIL at the concentrations of 5, 10, 20, and 40  $\mu\text{g/ml}$  for 70 h and unstimulated cells served as the control. Cultures of splenocytes were evaluated for proliferation index following BrdU incorporation and viability of cells after trypan blue staining. Gene expressions of transcription factors and cytokines were assessed using real-time PCR, whereas ELISA test was applied to measure cytokine secretion. Mitochondrial membrane potential and apoptosis were determined by flow cytometry.

Results: We demonstrated that CoA-activated mouse spleen T lymphocytes show different susceptibilities to low ( $\leq 10 \mu\text{g/ml}$ ) and higher (20 and 40  $\mu\text{g/ml}$ ) SIL concentrations. Low concentrations resulted in increased proliferation, cytokine secretion, and mitochondrial membrane potential and reduced transition of cells to apoptosis. High concentration of SIL had the opposite effect without exerting significant cytotoxicity and upregulated genes for cytokines and transcription factors on mRNA level. It is possible that individual subpopulations of T cells induced by CoA were differentially affected by the various SIL concentrations and the dose of 40  $\mu\text{g/ml}$  had the profound suppressive effect. This correlated with the highest expression of Foxp3 factor, indicating that this dose stimulated preferential differentiation to Tregs lymphocytes.

Conclusions: Treatment with suitable doses of SIL can provide potential benefits in the modulation of host immune functions in various diseases.

**Keywords** silymarin – mouse – splenocytes – proliferation – mitochondrial potential – apoptosis

## INTRODUCTION

Numerous phytochemicals produced by plants as secondary metabolites are potent immunomodulators and their biological activity was demonstrated *in vitro* on isolated cells and *in vivo* on animal models of various diseases. One natural compound with a very long history of use in traditional medicine is silymarin (SIL), isolated from the seeds of *Silybum marianum* L. (Asteraceae). It contains a mixture of flavonolignans of which silybin A/B, silychristin A, silydianin, isosilybin A, and 2,3-dehydrosilybin form approximately 70%–

80% and other components are flavonoids, fatty acids, and some undefined molecules. SIL is subject to intensive research and has received great attention due to its wide range of pharmacological effects. SIL displays free radical scavenging and strong antioxidant abilities, which are associated with inducing superoxide dismutase activities and increasing cellular glutathione content (Kwon et al., 2013; Surai, 2015). A growing number of studies have shown that SIL and its main component, silybin A/B, exhibit hepatoprotective,

\* E-mail: hrcka@saske.sk

© European Pharmaceutical Journal

anticarcinogenic, immunomodulatory, and antiangiogenic activities (Saller et al., 2001; Fraschini et al., 2002; Gažák et al., 2007; Esmail et al., 2017), suggesting multiple molecular mechanisms regulated by SIL's components. Anticancer activities involve suppression of the inflammatory process that leads to neoplastic transformation, hyperproliferation, and downregulation of progression of carcinogenesis and angiogenesis (Ramasamy and Agarwal, 2008). Reports on immunomodulatory activities of SIL and silybin indicate that stimulation or suppression of inflammatory reactions in animal models of diseases is dependent on the concentration in medium as well as administered dose *in vivo*. It has been shown that SIL can modulate human T-lymphocyte proliferation and secretion of cytokines. *In vitro* treatment of peripheral blood mononuclear cells from  $\beta$ -thalassemia patients with low SIL concentrations up to 20  $\mu\text{g}/\text{ml}$  led to the restoration of glutathione levels and stimulated suppressed lymphocyte proliferation (Alidoost et al., 2006). On the contrary, *in vitro* treatment with higher doses (80  $\mu\text{M}/\text{ml}$ ) of SIL resulted in suppressed expression of T-cell activation- and exhaustion markers on CD4+ and CD8+ T cells from chronically infected HIV-positive subjects and also modulated functions of other human primary cells (Lovelace et al., 2017). SIL exerted significant inhibitory effect on proliferation of CD3-activated mouse spleen T-helper (CD4+) cells *in vitro* at a concentration of 50  $\mu\text{M}/\text{ml}$  or higher (Gharagozloo et al., 2010). Studies showed that anti-inflammatory activities of SIL are dependent on the inhibition of translocation of transcription nuclear factor kappa B (NF- $\kappa$ B) from the cytoplasm into the nucleus (Manna et al., 1999; Gharagozloo et al., 2010) where it regulates transcription of many genes for inflammatory mediators and cytokines.

Activation of T lymphocytes during an immune response is mediated by various T-lymphocyte receptors and triggers a series of programmed gene regulations, proliferation, and effector functions. Concanavalin A (CoA), a lectin isolated from the seeds of *Canavalia ensiformis* (the Jack bean), is a very potent mitogen for lymphocytes and can induce rapid cell proliferation, preferentially of T lymphocytes, including both helper and suppressor subsets (Dwyer and Johnson, 1981). It was shown that lymphocytes possess about  $10^6$  CoA receptors per cell on the cell membrane and bind to various glycosyl proteins and to  $\alpha$ -D-mannose residues on glycolipids (Wang et al., 1971). CoA also stimulates the energy metabolism of T cells via modulation of cell respiration localized in mitochondria and the overall effects are mostly mediated by modulation of ATP turnover (Krauss et al., 1999). Research accumulated in the past decade has revealed that immune cells change their metabolic programs which are tightly regulated via mitochondrial dynamics, to support activation and differentiation into individual subsets (O'Neill et al., 2016). Mitochondria are central organelles of metabolism that provide energy during the differentiation and maintenance of immune cell phenotypes (Ozay et al., 2018). Moreover, alterations of mitochondrial membrane

potential are important in apoptosis and may precede nuclear signs of apoptosis in several different cell types. Kulkarni et al. (1998) showed that CoA-induced apoptosis in human fibroblasts is associated with breakdown of mitochondrial membrane potential and loss of calcium homeostasis in mitochondria. Immunomodulatory activities of SIL have been evaluated in various cell models *in vitro*, but it is not clear whether SIL treatment of CoA-activated mouse spleen cells involves modulation of cytokines secretion and alterations in mitochondrial homeostasis and whether it can prevent cell apoptosis.

In this study, we aimed to investigate the concentration-dependent effect of SIL on proliferation of CoA-stimulated splenocytes, viability of cells, and secretion of IFN- $\gamma$  and IL-4 cytokines *ex vivo* in relation to gene expressions of transcription factors Foxp3 and NF- $\kappa$ B. In addition, metabolic changes in cells were evaluated by means of the mitochondrial membrane potential and apoptosis.

## MATERIAL AND METHODS

### Reagents

Spleen cells were incubated in RPMI medium (Biochrom-Merck, Germany) containing 2 mM of stable glutamine and supplemented with 10% heat-inactivated bovine fetal serum (Biochrom-Merck, Germany), 100 U/ml penicillin, 100  $\mu\text{g}/\text{ml}$  streptomycin, 10  $\mu\text{g}/\text{ml}$  gentamicin, and 2.5  $\mu\text{g}/\text{ml}$  amphotericin B (all from Sigma-Aldrich, St. Louis, USA). SIL was purchased from Sigma-Aldrich and was dissolved in 100% DMSO to obtain a concentration of 10 mg/ml. All the subsequent dilutions were made in RPMI medium and the final DMSO concentration was 0.1% or lower. Cells were treated with SIL concentrations of 2.5, 5, 10, 20, and 40  $\mu\text{g}/\text{ml}$  (final). The composition of SIL was determined by HPLC analysis (Hrčková et al., *in press*) and was as follows: taxifolin (4%), silychristin A/silychristin B and silydianin (33%), silybin A/B (52%), isosilybin A/B (11%). CoA, Rhodamine 123, and DMSO were purchased from Sigma-Aldrich.

### Animals and isolation of splenocytes

Male Balb/c mice were purchased from VELAZ (Prague, Czech Republic) and used at the age of 8 weeks. Spleens were aseptically isolated from three mice in each experiment ( $n = 3$ ). Suspensions of splenic cells were obtained by gentle squeezing spleen tissue between the glass slides in 5 ml of cold medium on ice and red blood cells were removed by incubation of suspension with lysis solution (8.02%  $\text{NH}_4\text{Cl}$ , 0.85%  $\text{NaHCO}_3$ , and 0.37% EDTA) on ice. Splenic cells were washed with PBS, filtered through 40  $\mu\text{m}$  nylon filters (BD Biosciences, Darmstadt, Germany), and resuspended in medium. Viability of the cells was more than 95% as determined by trypan blue exclusion.

## T-lymphocyte proliferation

The suspensions of naive splenocytes were diluted to a concentration of  $1 \times 10^6$  cells/ml and seeded into flat bottom 96-well plates in quadruplicates (Corning) for each treatment. They were used to examine the effect of SIL on the T-lymphocyte proliferation by BrdU Cell Proliferation ELISA Kit (Roche Diagnostics GmbH, Mannheim, Germany) and cytokine production *ex vivo*. Splenocytes were stimulated with CoA (3  $\mu\text{g/ml}$ ) for 70 h at  $37^\circ\text{C}$  and 5%  $\text{CO}_2$ . BrdU was added to the cell suspensions at 5  $\mu\text{M}$  final concentration for the last 18 h of cultivation. Stimulation of cell proliferation termed as proliferation index (PI) was determined as the ratio of absorbance of stimulated versus unstimulated cells for each cell sample plated in quadruplicates and data are expressed as means  $\pm$  SD from three mice/treatment.

## Cytokine concentrations

Supernatants from other CoA-stimulated splenocyte cultures (not supplemented with BrdU) were collected. Samples from identical treatments in wells were pooled and stored at  $-80^\circ\text{C}$  for determination of IFN- $\gamma$  and IL-4 by ELISA kits (Mouse Ready-SET-Go ELISA; eBioscience, Germany). Then cytokine concentrations were determined in triplicates for each treatment/mouse using MaxiSorp Nunc-immuno module strips (Thermo Fisher Scientific, Roskilde, Denmark) and calculated in picogram per milliliter and expressed as mean  $\pm$  SD.

## Viability assessment (trypan blue exclusion test)

Viability of CoA-stimulated splenocytes was evaluated after 70 h of incubation with increasing SIL concentrations using 0.05% solution of trypan blue (Sigma-Aldrich, Merck Sigma, UK) in PBS. Splenocytes were incubated in 24-well plates at a concentration of  $1 \times 10^6/\text{ml}$  in RPMI medium, stimulated with CoA, and treated with the same concentrations of SIL (in quadruplicates) as were used in the proliferation assay. After 70 h of incubation, nonadherent cells (lymphocytes) from each well were collected in tubes, and after addition of trypan blue, unstained live cells were counted using hemocytometer. Proportions (%) of live cells from total counted cells per well ( $n^3 \times 100$ ) were calculated for control sample and each SIL concentration and were expressed as mean  $\pm$  SD.

## Flow cytometric analysis of mitochondrial membrane potential

Naive, unstimulated, and CoA-stimulated cells treated with SIL were incubated in 24-well plates for 70 h as described previously. Then nonadherent cells were collected into tubes and used to measure mitochondrial membrane potential (Ym) using the fluorescent dye Rhodamine 123, which is taken by mitochondria of living cells. Changes in the uptake of this dye are believed to reflect the level of Ym (Darzynkiewicz et

al., 1982). The stock solution (1 mg/ml) of Rhodamine 123 was prepared in ethanol and added to the cell suspensions. Cells were incubated with Rhodamine 123 (10  $\mu\text{M}$  final) for 20 min at  $37^\circ\text{C}$  and immediately used to measure Ym without washing by flow cytometry. Flow cytometry was performed with excitation of Rhodamine 123 at 505 nm and emission at 535 nm using flow cytometer FACS Canto (Becton Dickinson Biosciences, USA). Data were analyzed using FACS Diva software and were expressed as the mean fluorescence intensity of Rhodamine 123 to establish the effect of CoA and SIL on splenocytes.

## Annexin V/propidium iodide apoptosis assay

Cell suspensions of nonadherent cells from cultivations in 24-well plates treated in the same way as were applied in other assays were used to study apoptotic process after 70 h of incubation. Apoptosis was detected with BD Pharmingen Annexin V-FITC Apoptosis Detection Kit (APO Alert Annexin V, ClonTech, California, USA) according to manufacturer's instructions. Briefly, treated cells were centrifuged for 10 min to remove the medium, then were washed and resuspended in 200  $\mu\text{l}$  of the binding buffer. Apoptotic cells were detected after staining with 5  $\mu\text{l}$  of Annexin V and 5  $\mu\text{l}$  of propidium iodide solutions at room temperature in the dark for 15 min. Analysis was performed by flow cytometry using BD FACS Canto (Becton Dickinson Biosciences) and data were analyzed using FACS Diva software. Data are expressed as proportions of apoptotic cells (%).

## Isolation of RNA from cells and real-time PCR

Quantitative transcription profiles of genes for IFN- $\gamma$ , IL-4, Foxp3, and NF- $\kappa\text{B}$  and housekeeping genes  $\beta$ -actin as well as GAPDH in spleen cells were determined by real-time PCR (RT-PCR). Cells ( $1 \times 10^6/\text{ml}$ ) were plated into 24-well plates in triplicate for each treatment and stimulated with CoA and/or SIL at increasing concentrations for 70 h. Then supernatants containing lymphocytes were collected into tubes, centrifuged, and pellets from three wells/treatment were pooled and used for extraction of RNA after adding Trizol reagent (Amresco, Solon, OH, USA). Then 3  $\mu\text{g}$  of total RNA was reverse transcribed with RevertAid H Minus M-MuLV Reverse Transcriptase and oligo dT primers (both from Thermo Fisher Scientific, St. Leon-Rot, Germany). Real-time quantitative analysis of the relative abundance of mRNA species was determined using the SYBR green master mix (BioRad, Hercules, CA, USA) on BioRad CFX thermocycler (BioRad). PCR was performed in 20- $\mu\text{l}$  reactions with detection primer pairs for IFN- $\gamma$  (forward: 5'-TCAAGTGGCATAGATGTGGAAGAA-3'; reverse: 5'-TGGCTCTGCAGGATTTTCATG-3'), IL-4 (forward: 5'-ACAGGAGAAGGGACGCCAT-3'; reverse: 5'-GAAGCCCTACAGACGAGCTCA-3'), Foxp3 (forward: 5'-AAT AGT TCC TTC CCA GAG-3'; reverse: 5'-GAT TTC ATT GAG TGT CCT-3'), NF- $\kappa\text{B}$  (forward: 5'-GGGAGTGCAGCGACG-3';

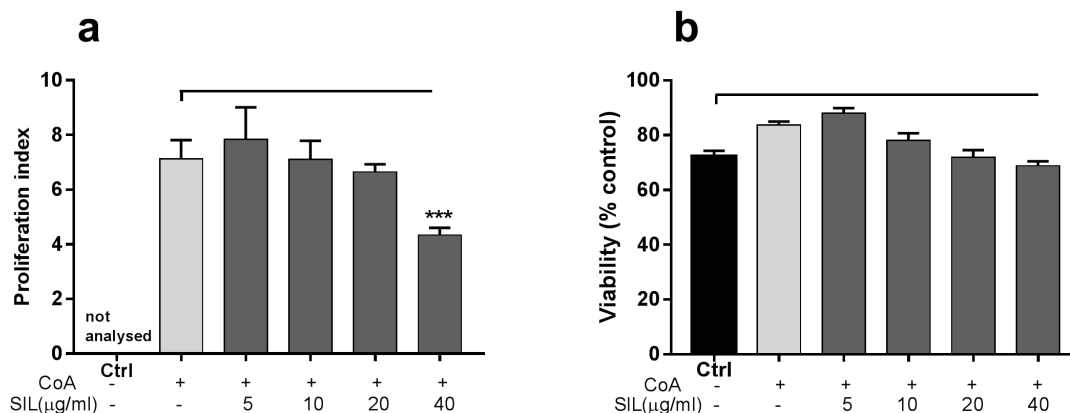


Figure 1: The effect of silymarin on CoA-activated mouse spleen cells *in vitro*: (a) proliferation index of T lymphocytes; (b) viability test of T lymphocytes using trypan blue staining. Significantly different values between CoA alone and CoA + silymarin treated groups are indicated as \* $p < 0.05$ , \*\* $p < 0.01$ , \*\*\* $p < 0.001$ .

reverse: 5'-AGCGCCCCTCGCATTATAG-3'),  $\beta$ -actin (forward: 5'-ACCAACTGGGACGACATGGAGAAAATC-3'; reverse: 5'-GTAGCCGCGCTCGGTGAGGATCTTCAT-3'), and GAPDH (forward: 5'-TCACCACCATGGAGAAGGC-3'; reverse: 5'-GCTAAGCAGTTGGTGGTGCA-3'). The results are expressed as fold amplification of the target gene compared with its expression in cells in naive mice by means of the comparative Ct method DDcT (Livak and Schmittgen, 2001).

### Statistical analysis

The results were analyzed either by using one-way ANOVA followed by Tukey's post hoc test or with the grouped analyses utilizing two-way ANOVA and the Sidak post hoc test. Data were evaluated by GraphPad Prism (version 7) (GraphPad Software, Inc., San Diego, CA, USA), and the differences were regarded as significant at least at  $p < 0.05$ .

## RESULTS

### The effect of silymarin on proliferation of CoA-stimulated lymphocytes and their viability

CoA is a strong mitogen, activating proliferation preferentially of T-cell subsets via cell membrane receptors. Splenocytes were treated with increasing concentrations of SIL and PI was determined in BrdU incorporation assay. As shown in Fig. 1a, SIL stimulated proliferation up to a concentration of 5  $\mu\text{g/ml}$  and significant elevation was detected in CoA-alone treated cells ( $p < 0.05$ ). On the contrary, high dose of 40  $\mu\text{g/ml}$  significantly ( $p < 0.001$ ) decreased PI of activated T lymphocytes.

To investigate whether highly reduced proliferation is due to the cytotoxic effect of SIL on lymphocytes, we counted viable cells after staining with trypan blue and calculated the proportions of live cells from total counted cells (Fig. 1b). In

comparison with unstimulated lymphocytes, the proportions of live cells increased significantly after CoA treatment and after CoA + 5  $\mu\text{g/ml}$  of SIL exposure, which correlated with the changes of PI. However, at 40  $\mu\text{g/ml}$  of SIL no cytotoxic effect was determined as non-significantly reduced numbers of live cells were observed, indicating that reduction of proliferation by SIL was caused by other mechanisms.

### The effect of silymarin on secretion and gene expression of cytokines

The effect of treatments on IFN- $\gamma$  and IL-4 cytokine levels and mRNA expression of both genes were examined by ELISA test and quantitative RT-PCR, respectively. As shown in Fig. 2 a, b concentration of cytokines was barely detectable in unstimulated cells, but has markedly increased after CoA stimulation. SIL significantly enhanced production of IFN- $\gamma$  at concentrations of 5 and 10  $\mu\text{g/ml}$  in comparison with CoA-alone-stimulated cells, but had no inhibitory effect at the highest concentration. In contrast, IL-4 levels were not significantly changed, except for the markedly suppressed secretion after exposure to 40  $\mu\text{g/ml}$  of SIL. However, SIL treatment had the opposite effect on mRNA transcript levels for both cytokines (Fig. 2 c, d). In unstimulated cells, the abundance of mRNA copies was several times higher than in CoA-stimulated cells. We found stimulation of genes expression with increasing concentrations of SIL in T-lymphocyte cell cultures, which was significantly higher ( $p < 0.01$ ) after treatment with 40  $\mu\text{g/ml}$  of SIL in comparison with CoA-treated cells.

### The effect of silymarin on gene expression of transcription factors

SIL can suppress nuclear transcription factor NF- $\kappa\text{B}$  on the protein level but it is not clear if SIL similarly suppresses NF- $\kappa\text{B}$

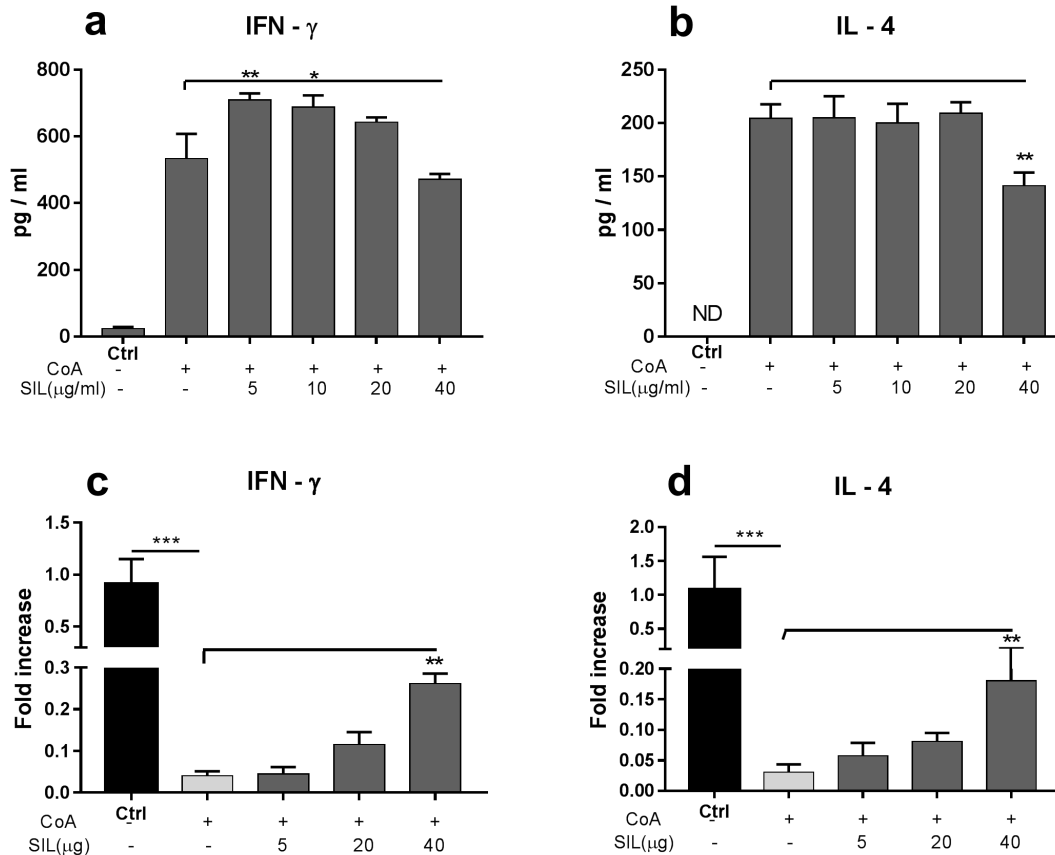


Figure 2: The effect of silymarin on cytokine secretion and mRNA levels in control unstimulated splenocytes and CoA-activated mouse spleen T lymphocytes *in vitro*: (a) concentration of IFN- $\gamma$  and (b) IL-4 in supernatants of cells after 70 h cultivation; (c) relative gene expression for IFN- $\gamma$  and (d) IL-4 in T lymphocytes after 70 h of cultivation. Significantly different values are indicated as: \* $p < 0.05$ , \*\* $p < 0.01$ , \*\*\* $p < 0.001$ .

on the mRNA level. To clarify concentration-dependent effect of SIL on CoA-stimulated T cells we examined the relative transcripts abundance of gene for p65 (RelA) which is one of the two subunits of NF- $\kappa$ B (Fig.3a). No difference was found between unstimulated and CoA-stimulated cells. Interestingly, SIL in dose-dependent manner stimulated expression of gene for this protein, and significantly elevated mRNA copies were found at a dose of 40  $\mu$ g/ml ( $p < 0.01$ ). Expression of transcription factors of T-helper cell subsets characterizes precisely their phenotype; therefore we evaluated the expression levels of gene encoding Foxp3, which is activated in regulatory T cells (Tregs) having suppressive effect on IFN- $\gamma$ -dependent inflammatory reactions (Hori et al., 2003). As shown in Fig.3 b, transcript levels increased significantly in CoA-activated cells in comparison with untreated cells ( $p < 0.001$ ). SIL enhanced the activity of gene for Foxp3 at transcriptional level at concentrations of 20 and 40  $\mu$ g/ml; however, low concentrations up to 5  $\mu$ g/ml slightly downregulated gene expression.

### The effect of silymarin on mitochondrial membrane potential

Upon activation, T cells utilize mitochondrial energy to differentiate into distinct T-helper cells (Ozay et al., 2018) and changes in mitochondrial dynamic can be assessed by mitochondrial membrane potential (Ym). The effects of SIL on Ym in CoA-stimulated T lymphocytes are demonstrated in Fig. 4 as the mean intensity of fluorescence (MIF), and representative plots of MIF are shown in the left panel. In comparison with freshly isolated lymphocytes, incubation of naive unstimulated cells for 70 h at standard conditions resulted in significant decrease of Ym ( $p < 0.05$ ). In contrast, CoA activation of cells led to moderate stimulation of Ym and significant activation was found at 5  $\mu$ g/ml concentration of SIL.

### The effect of silymarin on cell apoptosis

Impairment in mitochondrial biogenesis to a critical level might result in cell death in many pathological conditions. To get a deeper insight into the regulation of T-cell functions

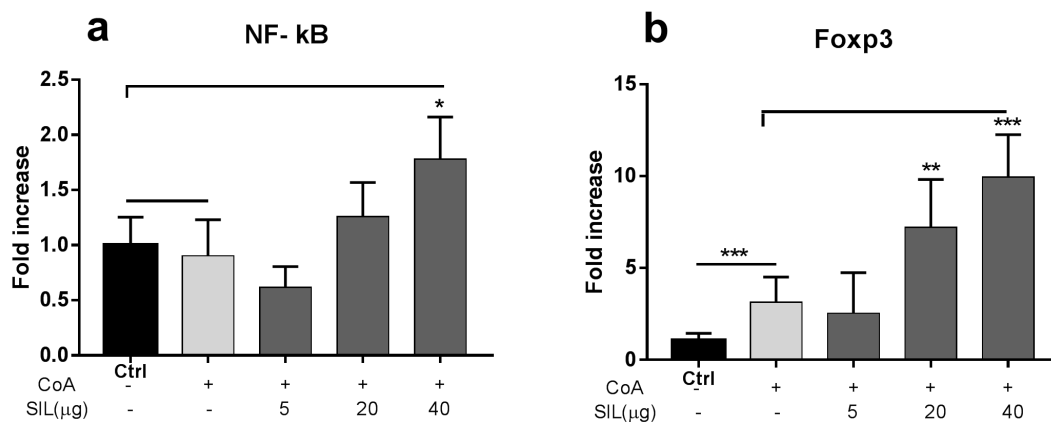


Figure 3: The effect of silymarin on mRNA levels in control unstimulated splenocytes and CoA-activated mouse spleen T lymphocytes *in vitro* for (a) transcription factor NF-κB and (b) transcription factor Foxp3. Significantly different values are indicated as \* $p < 0.05$ , \*\* $p < 0.01$ , \*\*\* $p < 0.001$ .

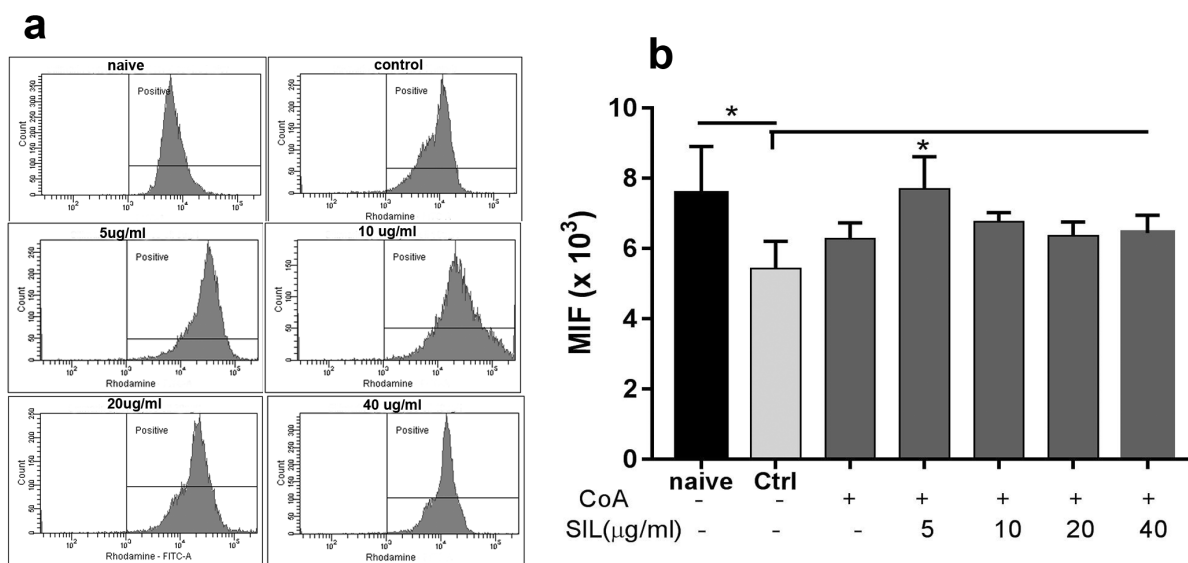


Figure 4: The effect of silymarin on mitochondrial membrane potential in naive and CoA-activated mouse spleen cells and after treatment with silymarin (b), expressed as the mean intensity of fluorescence (MIF) for Rhodamine 123: (a) representative plots of MIF for control and individual silymarin-treated groups. Significantly different values are indicated as: \* $p < 0.05$ .

and fate by various concentration of SIL, we determined the proportions of live cells, cells in the early stage of apoptosis, and dead cells by flow cytometry. Results of our analyses are summarized in Fig.5 and representative dot plots from analysis of freshly isolated naive spleen cells (upper left panel) and CoA-stimulated cells treated with 5 μg/ml of SIL for 70 h are on lower left panel. While in suspension of freshly isolated spleen cells, more than 93% of cells were live, cultivation for 70 h negatively influenced the physiological state of lymphocytes as manifested by their entry into the early phase of apoptosis. We found that  $86.2 \pm 2.7\%$  of unstimulated cells (control group) was at the early stage of apoptosis at the end of cultivation. Following CoA stimulation the proportion of

early apoptotic cells decreased, whereas the proportions of live cells significantly increased ( $p < 0.05$ ). In comparison with the control, further lowering of early apoptotic cells and elevation of live cells were observed after 5 μg/ml of SIL, which correlates with the elevation of mitochondrial membrane potential.

## DISCUSSION

SIL is a natural product widely studied for its numerous beneficial effects on health and prevention of many diseases (Gažák et al., 2007). It is considered very safe as after oral administration the 50% lethal dose was 10 g/kg in rats

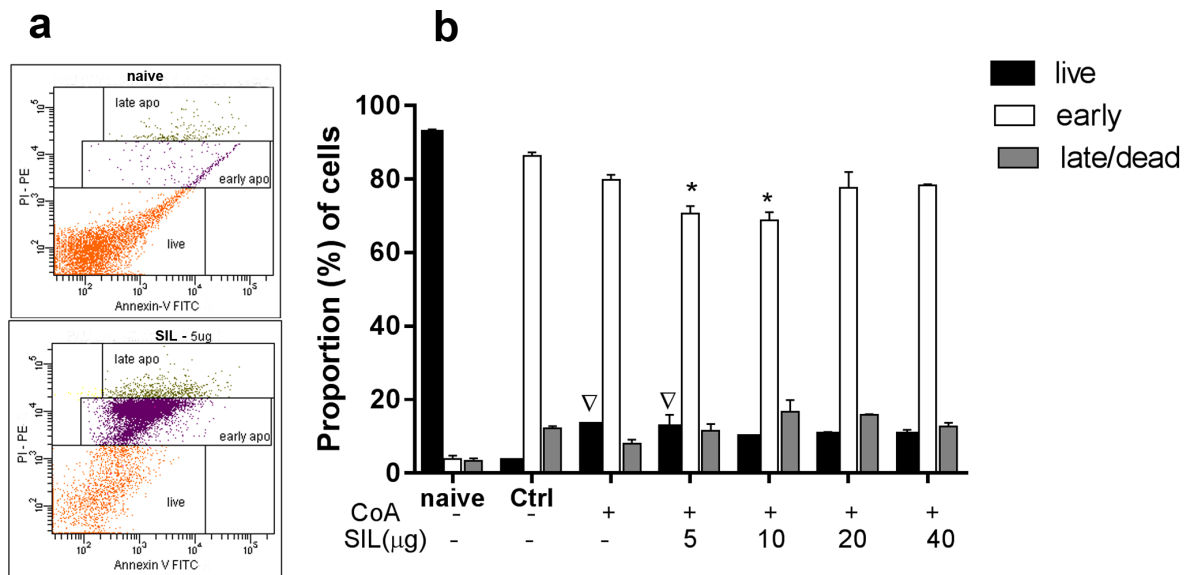


Figure 5: The proportions of live, early apoptotic, and late apoptotic/dead cells determined for the suspensions of naïve splenocytes, CoA-activated T lymphocytes, and following *in vitro* treatment with silymarin after 70 h of cultivation (b). Representative flow cytometric dot plots showing Annexin V and propidium iodide staining of naïve splenocytes and CoA-activated cells following silymarin treatment (a). Significantly different values between CoA alone and silymarin-treated groups for early apoptotic cells are indicated as \* $p < 0.05$  and for live cells are indicated as  $Np < 0.05$ .

(Fraschini et al., 2002). Studies on immunomodulatory activities indicate concentration-dependent effect at various *in vitro* and *in vivo* experimental conditions mostly reporting on suppression of inflammatory mediators (Esmail et al., 2017). In this study, we aimed to compare the effects of lower doses (5 and 10 μg/ml) and higher doses (20 and 40 μg/ml) of SIL preparation (Sigma) in which flavonolignans silybin A/B formed about 52%. We focused on spleen T lymphocytes isolated from healthy Balb/c mice following activation by plant mitogen CoA. We first investigated the dose-dependent effect on T-cell proliferation showing that low dose of 5 μg/ml can enhance proliferation and significant suppression was observed at a concentration of 40 μg/ml. Generally, upon priming of T cells with different stimuli, heterogeneous population is generated since naïve T cells have stem-like properties and can differentiate into virtually all different types of effector, memory, or regulatory cells. Higher sensitivity to suppressive effect of SIL was found when purified mouse spleen CD4+ T cells were used. Namdari et al. (2018) found that concentrations of 20 μg/ml of SIL and higher significantly reduced cell proliferation. By using CD4+ splenocytes from C57/Bl6 mice, proliferation assay revealed that SIL, at 50 μM concentration (approximately 25 μg/ml), significantly inhibited CD4+ cell proliferation (Gharagozloo et al., 2010). Suppressive effect of higher concentrations of SIL was not due to the direct induction of cell death, which was confirmed in our study by trypan blue test and in the study of Namdari et al. (2018) by propidium iodide staining. Moreover, we revealed that reduced proliferation was not due

to decreased cell viability as the proportions of live/dead cells remained similar as in untreated cells.

Reports on concentration-dependent effect of SIL administration to mice present various findings. Johnson et al. (2003) showed that the absolute numbers of splenic CD3+ T lymphocytes were reduced after intraperitoneal administration of 10 and 50 mg/kg of SIL; however, PHA-induced T-lymphocyte proliferation *ex vivo* was increased in 10 mg/kg of body weight-treated group. Wilasrusmee et al. (2002) studied the standardized milk thistle extract containing SIL and other phytochemicals in murine lymphocyte proliferation tests using CoA as the mitogen. They showed that the extract profoundly increased lymphocyte proliferation at doses of 250 μg/ml and only moderately at lower doses. This effect of milk thistle was associated with an increase in IFN-γ, IL-4, and IL-10 cytokines. Since SIL was found to form 70%–80% in the whole extract, the stimulatory activity after oral administration could be comparable with the results of another study on mice in which the purified SIL was used (Karimi et al., 2018). The authors showed that treatment of healthy mice with low dose of SIL (50 mg/kg) for 14 consecutive days stimulated both cellular and humoral immune functions. It increased the proliferation of phytohemagglutinin-A-stimulated spleen T-cell proliferation and IFN-γ secretion *ex vivo*. Pharmacokinetic studies on tissues distribution of silybin, the major active constituent of SIL, have revealed that in mice orally fed with silybin at dose of 50 mg/kg the peak levels were observed at 0.5 h after administration, and concentrations in tissues

were the following: 8.8 µg/g (liver), 4.3 µg/g (lung), 123 µg/g (stomach), and 5.8 µg/ml (pancreas) (Zhao and Agarwal, 1999). These low concentrations presented in these organs, except stomach, could support the stimulatory activities of SIL found in our *in vitro* study and *in vivo* studies mentioned earlier.

We further investigated the effect on cytokine secretion by CoA-stimulated cells and showed that only the highest concentration of SIL (40 µg/ml) leveled down the amount of IFN-γ and IL-4, probably due to diminished cell numbers as a consequence of reduced proliferation. The higher susceptibility to SIL was found for CD4+ T-helper cells activated with monoclonal anti-CD3/anti-CD28 antibodies, where SIL at concentrations of 20 and 30 µg/ml significantly decreased IFN-γ gene expression and upregulated Foxp3 transcription factor in Treg cells. Foxp3 factor plays a key role in the maintenance of lymphoid homeostasis in a number of immune circumstances, where Tregs guide immunosuppressive reactions (Feuerer et al., 2009).

In our study, SIL at the dose of 20 and 40 µg/ml stimulated expression of Foxp3 transcription factor in CoA-stimulated T lymphocytes, as well as mRNA levels for IFN-γ cytokine, suggesting that CoA probably induced a heterogeneous population of T cells with different transcriptional profiles and cytokine secretion. Stimulation of gene for NF-κB p65 subunit on mRNA level with increasing concentrations of SIL was also observed in our study. In the cytoplasm, NF-κB dimer is present in inactive form bound to inhibitory kappa B (IκB) protein and upon activation of cells the NF-κB is released from IκB and translocates to the nucleus. It was shown that SIL can block the translocation of NF-κB to nucleus via suppression of IκB degradation (Manna et al., 1999). We assume that although mRNA and probably also protein levels of NF-κB subunit were significantly elevated after 40 µg of SIL, simultaneous dose-dependent inhibition of IκB degradation occurred with increasing concentrations of SIL.

Interaction of CoA (concentration 3 µg/ml) with cell surface glycoproteins can induce apoptosis in fibroblasts and other nonimmune cells, and intrinsic pathway of apoptosis can be initiated by imbalance in the mitochondrial membrane potential Ym (Kulkarni et al., 1998). Mitochondrial control and guidance of cellular activities of T cells (Chao et al., 2017; O'Sullivan and Pearce, 2015) were recognized as a key factor in many diseases (Shinohara and Tsukimoto, 2018). In our study, cultivation of unstimulated splenocytes for 70 h decreased Ym and induced transition of naive splenocytes to early apoptosis (approximately 86%) and late apoptosis (approximately 11%). Activation with CoA stimulated Ym in T cells, which correlated with the decreased proportion of the early apoptotic cells (79%) indicating the metabolic reprogramming in activated cells. It was found that CoA bound to the cell membrane is internalized and accumulated primarily onto the mitochondria as early as

1 h posttreatment, and gradually increased mitochondrial membrane permeability. The increased mitochondrial membrane permeability would then lead to staining with Annexin V, the marker labeling the early stage, but no typical apoptosis was observed (Shinohara and Tsukimoto, 2018). We further showed that low concentrations of SIL (up to 10 µg/ml) positively modulated the mitochondrial dynamics in activated T cells which probably accounted for observed reduced proportions of the early apoptotic and late apoptotic/dead cells. Interestingly, higher concentrations (20 and 40 µg/ml) were not pro-apoptotic, in agreement with results of the study of Gharagozloo et al. (2010) on activated CD4+ T cells, supporting our hypothesis that antiproliferative effect of 40 µg/ml SIL (approximately 100 µM/ml) was not due to the cytotoxic effects on activated T cells. Detailed examination of the effect of SIL on proliferation revealed a significant G1 arrest in the cell cycle of CD3+ CD28+ activated T lymphocytes after 96 h of incubation with 100 µM SIL (approximately 50 µg/ml) without causing cell death (Gharagozloo et al., 2013). It is possible that the stimulated cells had an impaired respiratory capacity with a decreased mitochondrial membrane potential due to excess of produced reactive oxygen species. Addition of SIL to stimulated cells increased the mitochondrial membrane potential, suggesting that in CoA-stimulated cells the electron transfer, respiratory activity of the cells, and activity of the enzymes involved in oxidative phosphorylation have increased. Moreover, SIL is likely to prevent peroxidative damage of phospholipids, thereby preventing the initiation of apoptosis through cytochrome c release (Yuan, 2006; Robertson and Orrenius, 2000).

In conclusion, our study demonstrated that mouse spleen T lymphocytes activated by lectin CoA show different susceptibilities to low (10 µg/ml) and higher (20 and 40 µg/ml) SIL concentrations after 70 h of incubation *in vitro*. Treatment with low concentrations resulted in increased proliferation, cytokine secretion, and mitochondrial membrane potential and reduced transition of T cells to apoptosis. SIL at high concentration had the opposite effect without exerting significant cytotoxicity and upregulated genes for cytokines and transcription factors on mRNA level. It is possible that individual subpopulations of T cells induced by CoA were differentially affected by the various SIL concentrations and profound suppression of T lymphocyte functions was associated with the dose of 40 µg/ml. This correlated with the highest expression of Foxp3 factor indicating that this dose preferentially promoted differentiation to Tregs lymphocytes.

## CONFLICTS OF INTEREST

We wish to confirm that there are no conflicts of interest associated with this publication.

## ACKNOWLEDGMENTS

This study was supported by the project APVV No. 17-0410 and the project VEGA No. 02/0091/17 granted by the Ministry of Education, Science, Research and Sport of the Slovak Republic. The authors also gratefully acknowledge the bilateral mobility project SAV-AV ČR No. 18–24.

## References

- [1] Alidoost F, Gharagozloo M, Bagherpour B, et al. Effects of silymarin on the proliferation and glutathione levels of peripheral blood mononuclear cells from beta-thalassemia major patients. *Int Immunopharmacol.* 2006;6:1305-1310.
- [2] Chao T, Wang H, Ho PC. Mitochondrial control and guidance of cellular activities of T cells. *Front Immunol.* 2017;8:473.
- [3] Darzynkiewicz Z, Traganos F, Staiano-Coico L, Kapuscinski J, Melamed MR. Interaction of rhodamine 123 with living cells studied by flow cytometry. *Cancer Res.* 1982;42:799-806.
- [4] Dwyer JM, Johnson C. The use of concanavalin A to study the immunoregulation of human T cells. *Clin Exp Immunol.* 1981;46:237-249.
- [5] Esmaeil N, Anaraki SB, Gharagozloo M, Moayedi B. Silymarin impacts on immune system as an immunomodulator: One key for many locks. *Int Immunopharmacol.* 2017;50:194-201.
- [6] Feuerer M, Hill JA, Mathis D, Benoist C. Foxp3+ regulatory T cells: differentiation, specification, subphenotypes. *Nat Immunol.* 2009;10:689-695.
- [7] Fraschini F, Demartini G, Esposti D. Pharmacology of Silymarin. *Clin Drug Invest.* 2002;22:51-65.
- [8] Gažák R, Walterova D, Kren V. Silybin and silymarin—new and emerging applications in medicine. *Curr Med Chem.* 2007;14:315-338.
- [9] Gharagozloo M, Javid EN, Rezaei A, Mousavizadeh K. Silymarin inhibits cell cycle progression and mTOR activity in activated human T cells: therapeutic implications for autoimmune diseases. *Basic Clin Pharmacol Toxicol.* 2013;112:251-256.
- [10] Gharagozloo M, Velardi E, Bruscoli S, et al. Silymarin suppress CD4+ T cell activation and proliferation: effects on NF-kappaB activity and IL-2 production. *Pharmacol Res.* 2010;61:405-409.
- [11] Hori S, Nomura T, Sakaguchi S. Control of regulatory T cell development by the transcription factor Foxp3. *Science.* 2003;299:1057-1061.
- [12] Johnson VJ, He Q, Osuchowski MF, Sharma RP. Physiological responses of a natural antioxidant flavonoid mixture, silymarin, in BALB/c mice: III. Silymarin inhibits T-lymphocyte function at low doses but stimulates inflammatory processes at high doses. *Planta Med.* 2003;69:44-49.
- [13] Karimi G, Hassanzadeh-Josan S, Memar B, Esmaeili SA, Riahi-Zanjani B. Immunomodulatory effects of silymarin after subacute exposure to mice: A tiered approach immunotoxicity screening. *J Pharmacopuncture.* 2018;21:90-97.
- [14] Krauss S, Buttgerit F, Brand MD. Effects of the mitogen concanavalin A on pathways of thymocyte energy metabolism. *Biochim Biophys Acta.* 1999;1412:129-138.
- [15] Kulkarni GV, Lee W, Seth A, McCulloch CA. Role of mitochondrial membrane potential in concanavalin A-induced apoptosis in human fibroblasts. *Exp Cell Res.* 1998;245:170-178.
- [16] Kwon DY, Jung YS, Kim SJ, Kim YS, Choi DW, Kim YC. Alterations in sulfur amino acid metabolism in mice treated with silymarin: a novel mechanism of its action involved in enhancement of the antioxidant defense in liver. *Planta Med.* 2013;79:997-1002.
- [17] Livak KJ, Schmittgen TD. Analysis of relative gene expression data using real-time quantitative PCR and the 2(-Delta Delta C(T)) Method. *Methods.* 2001;25:402-408.
- [18] Lovelace ES, Maurice NJ, Miller HW, et al. Silymarin suppresses basal and stimulus-induced activation, exhaustion, differentiation, and inflammatory markers in primary human immune cells. *PloS one.* 2017;12:e0171139-e0171139.
- [19] Manna SK, Mukhopadhyay A, Van NT, Aggarwal BB. Silymarin suppresses TNF-induced activation of NF-kappa B, c-Jun N-terminal kinase, and apoptosis. *J Immunol.* 1999;163:6800-6809.
- [20] Namdari H, Izad M, Rezaei F, Amirghofran Z. Differential regulation of CD4(+) T cell subsets by Silymarin in vitro and in ovalbumin immunized mice. *Daru.* 2018;26:215-227.
- [21] O'Neill LA, Kishton RJ, Rathmell J. A guide to immunometabolism for immunologists. *Nat Rev Immunol.* 2016;16:553-565.
- [22] O'Sullivan D, Pearce EL. Targeting T cell metabolism for therapy. *Trends Immunol.* 2015;36:71-80.
- [23] Ozay EI, Sherman HL, Mello V, et al. Rotenone treatment reveals a role for electron transport complex i in the subcellular localization of key transcriptional regulators during T helper cell differentiation. *Front Immunol.* 2018;9:1284.
- [24] Ramasamy K, Agarwal R. Multitargeted therapy of cancer by silymarin. *Cancer Lett.* 2008;269:352-362.
- [25] Robertson JD, Orrenius S. Molecular mechanisms of apoptosis induced by cytotoxic chemicals. *Crit Rev Toxicol.* 2000;30:609-627.
- [26] Saller R, Meier R, Brignoli R. The use of silymarin in the treatment of liver diseases. *Drugs.* 2001;61:2035-2063.
- [27] Shinohara Y, Tsukimoto M. Adenine nucleotides attenuate murine T cell activation induced by Concanavalin A or T cell receptor stimulation. *Front Pharmacol.* 2018;8:986.
- [28] Surai PF. Silymarin as a Natural Antioxidant: An overview of the current evidence and perspectives. *Antioxidants (Basel).* 2015;4:204-247.
- [29] Wang JL, Cunningham BA, Edelman GM. Unusual fragments in the subunit structure of concanavalin A. *Proc Natl Acad Sci U S A.* 1971;68:1130-1134.

- [30] Wilasrusmee C, Kittur S, Shah G, et al. Immunostimulatory effect of *Silybum Marianum* (milk thistle) extract. *Med Sci Monit.* 2002;8:Br439-443.
- [31] Yuan J. Divergence from a dedicated cellular suicide mechanism: exploring the evolution of cell death. *Mol Cell.* 2006;2:1-12.
- [32] Zhao J, Agarwal R. Tissue distribution of silibinin, the major active constituent of silymarin, in mice and its association with enhancement of phase II enzymes: implications in cancer chemoprevention. *Carcinogenesis.* 1999;20:2101-2108.

# Study of qualitative and quantitative content of amino acids in pumpkin seeds for further standardization of the herbal drug

Original Paper

Kotova E.E.<sup>1</sup>, Kotov S.A.<sup>1</sup>, Gontova T.M.<sup>2</sup>, Kotov A.G.<sup>1✉</sup>

<sup>1</sup>Department of the State Pharmacopoeia of Ukraine,  
State enterprise "Ukrainian scientific Pharmacopoeial  
center for quality of medicines", 33, Astronomichna, Str.,  
Kharkiv, 61085, Ukraine

<sup>2</sup>Department of Botany, National University of  
Pharmacy, 4, Valentynivska Str.,  
Kharkiv, 61168, Ukraine.

Received 5 September, 2019, accepted 27 November, 2019

**Abstract** **Aim:** Literary sources on qualitative composition, quantitative content of biologically active substances, and standardization methods of pumpkin seeds have been studied. It has been established that, along with  $\Delta^7$ -sterols, whose action is associated with treatment of the prostate gland, pumpkin seeds contain amino acids, cucurbitin in particular, which are responsible for their antihelminthic effect. The aim is to study the qualitative and quantitative content of amino acids in domestic samples of pumpkin seeds in order to clarify the possibility of pumpkin seed standardization for this class of biologically active substances.

**Methods:** The investigation of the possibility of amino acids' identification in the herbal drug by the thin-layer chromatography (TLC) method was carried out on silica gel 60 F<sub>254</sub> plates, Merck and Silica gel 60, Merck, on aluminum and glass supports in a mixture of the following solvents: butanol–acetone–acetic acid–water (35:35:10:20). The conclusions have been made based on the presence of characteristic zones of amino acids in the chromatograms after the treatment with ninhydrin solution. Quantitative determination of amino acids in the herbal drug was carried out by absorption spectrometry using HP spectrophotometer HP-8453 UV-VIS, Hewlett Packard (USA).

**Results:** The chromatographic profile of the amino acid fraction of domestic samples of pumpkin seeds was studied using a TLC technique. In the chromatograms of test solutions from all samples, the zones were detected at the level of histidine, aspartic acid, glutamic acid, glycine, and leucine zones, as well as a zone with color (olive) that differs from the other zones of amino acids and which is possibly a zone of cucurbitin.

On the basis of the results of qualitative research, the quantitative content of the sum of amino acids according to a UV method developed has been determined, which including purification from the fatty oil, further extraction with an aqueous alcohol solution, selection of aliquots for the reaction with ninhydrin solution, and subsequent determination of the absorbance of the test solution and the solution of glutamic acid at a wavelength of 400 nm.

It has been established that the content of the sum of amino acids expressed as glutamic acid in domestic samples is about 2%. **Conclusions:** The research of the possibility of pumpkin seed standardization by the content of amino acids was carried out. The chromatographic profile of the amino acid fraction of domestic samples of pumpkin seeds was studied using a TLC method developed. The quantitative content of the amino acids sum by the absorption spectrophotometry method was investigated. The techniques developed will be recommended for inclusion in the draft of national monograph "Pumpkin seeds."

**Keywords** pumpkin seeds – amino acids – TLC method – UV-vis spectrophotometry method – standardization – SPhU

## INTRODUCTION

Pumpkin seeds (*Cucurbita pepo* L.) are a well-known traditional herbal medicine that has been widely used for centuries. Modern use of herbal drugs (HDs) of pumpkin seeds is primarily associated with functional disorders of the bladder, including enlarged prostate gland [1-3]. This pharmacological activity of the HD is associated primarily with the content of fatty oil components, in particular with the content of characteristic  $\Delta^7$ -steroles, and so on [4,5]. In addition, pumpkin seeds have been used for a long period

of time, and especially in countries of the former Soviet Union, as an antihelminthic. This pharmacological action is associated with a sufficient amount of amino acids in the raw material, among which special attention is given to cucurbitin (3-amino-3-carboxypiperidine) because of its antihelminthic properties. This amino acid is capable of destroying parasitic worms; it is an inhibitor of histidine decarboxylase by biological activity [6].

\* E-mail: fitex16@ukr.net

© European Pharmaceutical Journal

According to [7], raw pumpkin seeds (*C. pepo*) contain high concentrations of most essential amino acids, among which the highest concentrations are observed in arginine, glutamine, and aspartic acid. According to [8], the content of cucurbitin in the seeds of *C. pepo* ranges from 0.18% to 0.66% and in *Cucurbita moschata* Duch, from 0.4% to 0.84%.

Pumpkin seeds are described in several pharmacopoeias of the world, namely in the article of the State Pharmacopoeia of the USSR XI (GF XI), V. 2, art. 78 "Pumpkin seeds" [9], monograph of the State Pharmacopoeia of the Republic of Belarus "Pumpkin Seeds" (GF RB) [10], monograph of the German Pharmacopoeia (DAB 10) "Kurbissamen" [11], monograph of the British Herbal Pharmacopoeia (BHP) "Pumpkin seed" [12], and article of the State Pharmacopoeia of the Russian Federation, 14 edition (GF RF 14) "Pumpkin Seeds" [13].

At present, there is no monograph on this type of HD in the State Pharmacopoeia of Ukraine (SPHU) that conduct a research related to its development is relevant.

The analysis of normative documents, namely, articles/monographs in the pharmacopoeias listed above has revealed the following.

Articles GF XI and GF RB include the following HD quality indicators: identification (macroscopy, microscopy) and quantitative indicators (humidity, ash, and foreign matter). In monographs DAB 10 and BHP, a method of identification of steroid compounds by thin-layer chromatography (TLC) is presented additionally. In GF RF 14, the TLC method for identification of substances detected by the solution of ninhydrin is also presented.

The purpose of this work is to study the qualitative and quantitative content of amino acids in domestic samples of pumpkin seeds to determine the possibility of HD standardization for this class of biologically active substances.

## MATERIALS AND METHODS

For this experiment, we used seven batches of pumpkin seeds (*C. pepo* L.) (Fig. 1) collected in 2017–2018 and registered in the State Enterprise "Pharmacopoeia Center": No. 1: collected near Izum, Kharkiv region (RS 799); No. 2: collected near Chuguev, Kharkiv region (RS 800); No. 3: collected near Dergachi, Kharkiv region (RS 810); No. 4: collected near Valki, Kharkiv region (RS 802); No. 5: collected near Zmiev, Kharkiv region (RS 803); No. 6: collected near city Kharkiv (RS 804); and No. 7: collected near Merefa, Kharkiv region (RS 805). The identification and authentication of the plant material was carried out by Associate Prof. A.G. Vovk, Department of Experimental Support the Elaboration of Monographs on Herbal Drugs of the SE "Ukrainian Scientific Pharmacopoeial Center for Quality of Medicines" (Kharkov, Ukraine).

In the chromatographic study, TLC plates with a silica gel layer that meet the requirements of SPhU 2.0 "Chromatographic separating capacity" were used. Before use, the chromatographic plates were activated in a drying oven at 110°C for 1 h. The following equipment was used: Ultrasonic

bath SUPER RK100H "Bandelin" (Germany), glass vertical chamber, automatic spraying device ChromaJet DS20.

As standard substances, alanine, arginine, histidine, valine, glycine, leucine, glutamic and aspartic acids (>95%), pharmacopoeial reference standards of the State Pharmacopoeia of Ukraine were used.

Solvents (petroleum ether, alcohol [50%, v/v], methanol, butanol, acetone, water) and chemicals (acetic acid, ninhydrin) used in the experiments were of analytical grade.

The quantitative determination of amino acids in HD was carried out by absorption spectrometry using HP Spectrophotometer HP-8453 UV-VIS, Hewlett Packard (USA).

*Method for determination of the quantitative contents of amino acids.*

The basis for the determination of the amino acids' content was the technique described in [14] with changes that meet the requirements of SPhU 2.0.

*Stock solution.* Powdered herbal drug (500) (2.9.12) is pretreated with *petroleum ether* (bp: 50–70°C) and the residual raw material is dried at a temperature not higher than 50°C for complete removal of the residual solvent.

*Fat-free material (500) (2.9.12)* is extracted with a certain amount of *alcohol (50%, v/v)*.

*Test solution.* The stock solution is concentrated and 2-g/L *ninhydrin* solution is added and heated at 120°C for 20 minutes. The mixture is cooled and quantitatively transferred to a 100-ml volumetric flask.

*Reference solution.* It is prepared from accurately weighted mass of glutamic acid using the solution of 2 g/L *ninhydrin* and water.

The absorbance (2.2.25) of the test solution and the reference solution is measured in 40 min after the preparation at a wavelength of 400 nm using *water* as compensation liquid.

The content of amino acids, in percent, expressed as glutamic acid and fat-free material, is calculated using the following expression:

$$\frac{A_1 \times m_0 \times 40}{A_0 \times m}$$

where  $A_1$  is the absorbance of the test solution at 400 nm;  $A_0$  is the absorbance of the reference solution at 400 nm;  $m$  is the mass of the fat-free herbal drug to be examined, in grams.

## RESULTS AND DISCUSSION

Taking into account the literature data on the presence of a significant amount of amino acids in pumpkin seeds, which are responsible for the pharmacological activity of HD, studies on the possibility of identifying using TLC method according to the presence of amino acids' characteristic zones in the chromatograms have been conducted.

Conditions described in article GF RF 14 "Pumpkin Seeds"

that proposed to identify HD by TLC method were studied previously. In this normative document, the raw material is treated with heated water to extract water-soluble substances and then filtered, and the aliquot of the filtrate is treated with alcohol at a temperature of 5°C. After filtration, the obtained solution is applied on the chromatographic plate with a layer of silica gel and developed in the mobile phase: propanol–anhydrous formic acid–anhydrous acetic acid (16:5:5); after the development, the plate is treated with 0.4% solution of ninhydrin in acetone, and the presence of at least four zones of different colors in the chromatogram is observed. It should be noted that the position of these zones in the chromatogram is not described in any way.

A study of the hydrophilic fraction of pumpkin seeds is described in several scientific papers [15, 16], which also describe the method of isolating the amino acid complex (called cucurbin) and which almost correspond to the method presented in GF RF 14. In these works, TLC method using the plates of Sylufol (taken out of production in the 90s of the last century) in the mobile phase: methanol–water–pyridine–10 M HCl (80:11.5:10:2.5) with the detection of 0.4% solution of ninhydrin was used to identify ninhydrin-positive substances; the characteristic zone that got olive color was different from the other zones and probably corresponded to the amino acid cucurbitin was described, but it was determined without the use of the reference standard.

As a result of the analysis of the techniques described, as well as previous studies, the following conditions for identification of amino acids of pumpkin seeds by TLC method were selected.

#### 1) Preparation of the test solution.

Taking into account that seeds contain enough fatty oil (almost 50%), preliminary defatting of the raw material is obligatory because it allows separating the lipophilic part, which prevents chromatography. Conditions of the extraction of the amino acid complex (namely, the ratio of raw material to water is 1 g/10 ml and the heating conditions is 45 min on a water bath) are similar to those described in the abovementioned works, because they allow the quantitative extraction of the necessary substances [15]. After that, to remove high-molecular-weight substances from the water-soluble fraction, the aqueous extract is treated with methanol, filtered, and evaporated to remove alcohol to a volume of about 5 ml.

#### 2) Reference solutions.

Taking into account the literature data on the amino acid content of pumpkin seeds, the following solutions of reference samples (RS) of amino acids were prepared: 5 mg of glycine, alanine, arginine, histidine, valine, aspartic acid, glutamic acid, and leucine were dissolved in 10 ml of methanol.

#### 3) Mobile phase.

As a mobile phase, a mixture of solvents, butanol–acetone–acetic acid–water (35: 35: 10:20), was used, which is used in the SPhU monographs to identify amino acids in HDs [17].

#### 4) Stationary phase.



Figure 1: Pumpkin seeds: dried drug substance

Silica gel 60 F<sub>254</sub> and Silica gel 60, Merck on aluminum, and glass support were used.

#### 5) The volume of application.

As a result of the selection of different aliquots of the application volume for test solutions, as well as preliminary studies on sensitivity of amino acid zones to the detective reagent, the following application volumes have been chosen: for test solutions, 50 µl; for solutions of RS alanine, arginine, histidine, valine, glycine, and leucine, 10 µl; for solutions of glutamic and aspartic acids, 25 µl.

#### 6) Detection.

To detect amino acid zones, the plate is sprayed with ninhydrin solution (prepared by dissolving 1.0 g of ninhydrin in 50 mL of ethanol [96%] and adding 10 mL of glacial acetic acid), followed by heating at a temperature of (100–100°C) for 5 minutes; this detection is unified because it is used in the monographs of the SPhU to detect amino acid zones.

Figures 2 and 3 show the chromatograms obtained by identifying amino acids in pumpkin seed samples. As can be seen from the figures, the zones at the level of histidine, aspartic acid, glutamic acid, glycine and leucine zones are detected in chromatograms of the test solutions from all samples. In addition, in all chromatograms, the available zone is located close to the starting line, the color of which (olive) differs from other pink–purple zones of amino acids; we suppose this zone can be a zone of cucurbitin, taking into account similar descriptions given in works [15, 16].

Taking into account the results of the previous qualitative study, which showed the presence of amino acids in the studied samples of pumpkin seeds, the quantitative content of this group of biologically active compounds was determined.

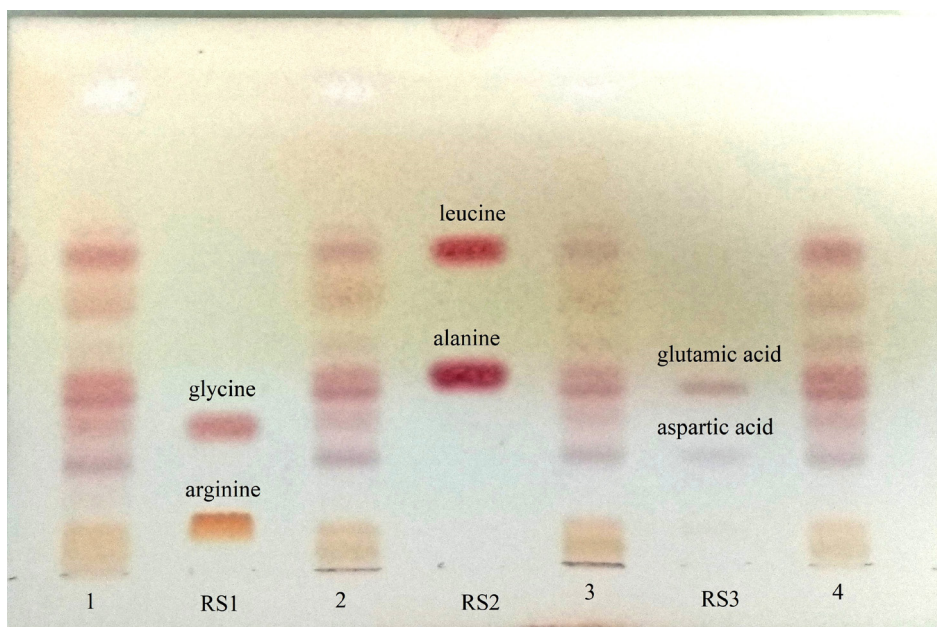


Figure 2: The chromatograms obtained for the identification of amino acids of various samples of pumpkin seeds under conditions of the procedure developed : 1,2,3,4, test solutions obtained from different series (RS 799, 800, 801, 802); RS 1, solution of arginine (zone with lower  $R_f$ ) and glycine (zone with higher  $R_f$ ); RS 2, solution of alanine (zone with lower  $R_f$ ) and leucine (zone with higher  $R_f$ ); RS 3, solution of aspartic acid (zone with lower  $R_f$ ) and solution of glutamic acid (zone with higher  $R_f$ )

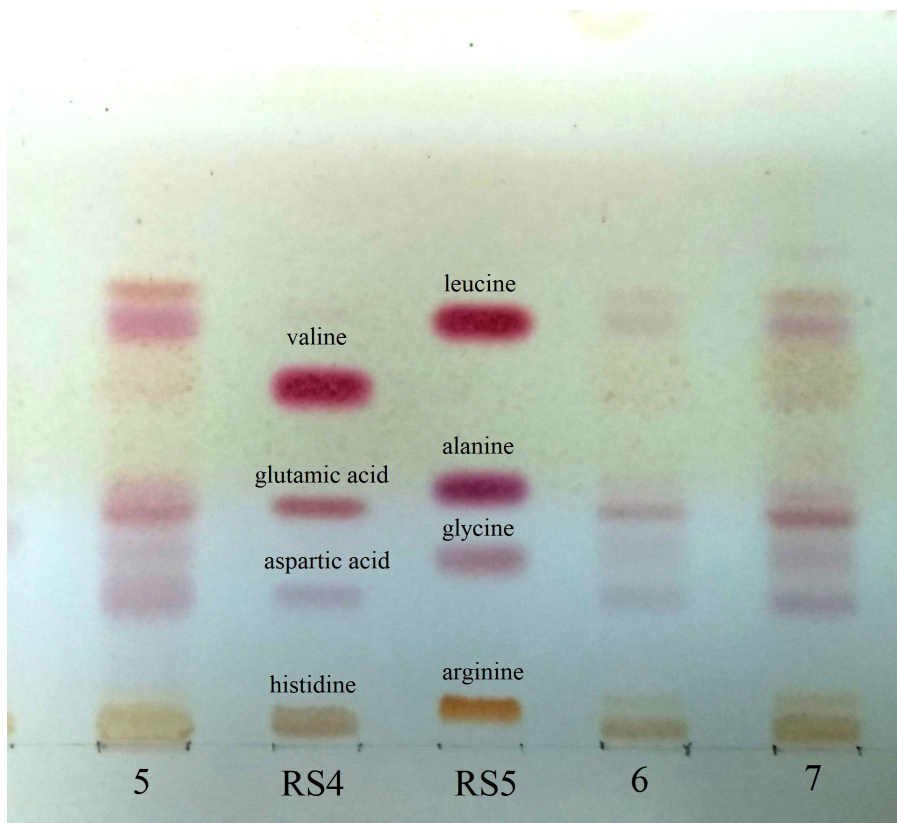


Figure 3: The chromatograms obtained for the identification of amino acids of various samples of pumpkin seeds under conditions of the procedure developed : 5,6,7, test solutions obtained from different series (RS 803, 804, 805); RS 4, solution of histidine, aspartic acid, glutamic acid, valine (in order of increasing  $R_f$ ); RS 5, solution of arginine, glycine, alanine, and leucine (in order of increasing  $R_f$ )

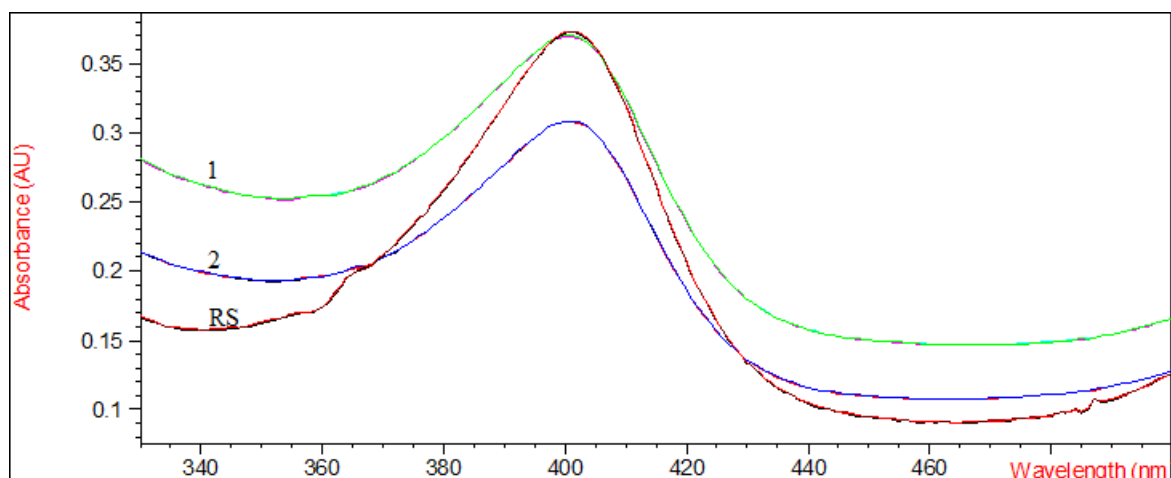


Figure 4: Typical absorption spectra obtained by assay amino acids content: 1,2, spectra of the test solutions obtained from the series of pumpkin seeds; RS, spectrum of solution of glutamic acid

Table 1: Results of amino acids assay expressed as glutamic acid and fat-free raw material in the different samples of pumpkin seeds

RS (batches of pumpkin seeds)	The content of the amino acids expressed as glutamic acid
799	$2.0 \pm 0.05$
800	$2.1 \pm 0.03$
801	$1.9 \pm 0.04$
802	$1.8 \pm 0.05$
803	$2.5 \pm 0.07$
804	$1.7 \pm 0.03$
805	$1.8 \pm 0.04$

The data (g/100 g fat-free raw material) are presented as mean  $\pm$  SEM ( $n = 3$ )

For the analysis of amino acids, methods based on the reaction with ninhydrin are widely used. In [14], the conditions for the ninhydrin reaction were optimized, and it was shown that the products of the reaction of  $\alpha$ -amino acids with aqueous ninhydrin solution are characterized by the highest stability in time and have a single maximum absorption at a wavelength of  $400 \pm 2$  nm. On this basis, the authors developed methods for the quantitative determination of  $\alpha$ -amino acids in medicines and plant materials, which are based on the reaction with 0.2% aqueous solution of ninhydrin. The developed technique differs with sufficient accuracy (relative error of the separate definition result does not exceed  $\pm 3\%$ ) and accessibility. Taking into account the results of these studies, the method described has been tested on seven samples of pumpkin seeds and the conditions for quantitative determination of the amino acids sum (with the changes indicated above) were selected. The research was carried out with the weights of defatted raw material, which was processed in a Soxhlet apparatus with petroleum ether for 5 h for the complete separation of fatty acid. As a standard, glutamic acid was used, the content of which is predominant in pumpkin seeds in accordance with

all literary sources. Figure 4 shows the absorption spectra of test solutions prepared from pumpkin seeds and a solution of glutamic acid obtained under conditions of the method developed. Table 1 shows the results of the quantitative determination of amino acids in the studied series.

## CONCLUSION

The research on the possibility of pumpkin seeds standardization by the content of amino acids was carried out.

The chromatographic profile of the amino acid fraction of domestic samples of pumpkin seeds was studied using a TLC method developed. In the chromatograms of the test solutions from all samples of raw materials, zones at the level of histidine, aspartic acid, glutamic acid, glycine, and leucine zones were detected, as well as a zone whose color was different from the other zones of amino acids, which is possibly a zone of cucurbitin, was also detected.

The quantitative content of the amino acids sum was investigated using the absorption spectrophotometry method. It has been established that the content of the amino

acids sum expressed as glutamic acid in domestic samples is about 2%. The techniques developed will be recommended for inclusion in the draft of national monograph "Pumpkin seeds."

## References

- [1] WHO Monographs on Selected Medicinal Plants. World Health Organization, Geneva. 4; 2009: 83-91.
- [2] Max Wichtl. Herbal drugs and phytopharmaceuticals: A handbook for practice on a scientific basis. Medpharm GmbH Scientific Publishers, Berlin. 2004: 163-165.
- [3] Cucurbitae semen (Pumpkin Seed). In: ESCOP Monographs. 2nd edition, supplement 2009. European Scientific Cooperative on Phytotherapy. Thieme Verlag, Stuttgart. 2009: 50-56.
- [4] Akihisa T., Shimizu N., Ghosh P. and al. Sterols of the Cucurbitaceae. *Phytochemistry* 26;1987: 1693-1700.
- [5] Phillips KM., Ruggio DM., Ashraf-Khorassani M. Phytosterol composition of nuts and seeds commonly consumed in the United States. *J. Agric. Food Chem.* 53; 2005: 9436-9445.
- [6] Wang Y., Qinchao Ma, Haonan Xu et al. Study on method of extraction and determination of Cucurbitin. *Advanced Materials Research.* 881-883; 2014: 823-826.
- [7] Kim MY., Kim EJ., Kim Y-N. et al. Comparison of the chemical compositions and nutritive values of various pumpkin (Cucurbitaceae) species and parts. *Nutr. Res. Pract.* 6; 2012: 21-27.
- [8] Blagrove RJ., Lilley G. Characterization of Cucurbitin from various species of the Cucurbitaceae. *Eur. J. Biochem.* 103; 1980: 577-584.
- [9] Gosudarstvennaya farmakopeya SSSR: Vyp. 2. Obshchie metody analiza. *Lekarstvennoye rastitel'noye syr'ye. Meditsina, Moscow.* 1990.
- [10] Gosudarstvennaya farmakopeya Respubliki Belarus'. T. 2. Obshchiye i chastnye farmakopeynyy stat'i. *Minskiy gosudarstvennyy PTK poligrafii im. V. Khoruzhey, Minsk.* 2007.
- [11] British Herbal Pharmacopoeia. British Herbal Medicine Association, London. 1996.
- [12] Deutsches Arzneibuch 10. Deutscher Apotheker Verlag, Stuttgart. 1999.
- [13] Gosudarstvennaya farmakopeya Rossiiskoy Federacii XIV ed. Available from URL: [http://resource.rucml.ru/feml/pharmacopia/14\\_4/HTML/index.html](http://resource.rucml.ru/feml/pharmacopia/14_4/HTML/index.html).
- [14] Simonyan A.V. Salamatov Yu.S., Pokrovskaya Yu.S. Ispolzovanie ningidrinovoi reakcii dlya kolichestvennogo opredelenia  $\alpha$ -aminokislot v razlichykh ob'ektah. *Volgograd.* 2007: 106.
- [15] Samylina I.A. Farmakognosticheskoe izuchenie, standartizacia syr'ya, lekarstvennykh sredstv boyaryshnika i tykvy: Dis. Doctor of Farmacy. *Moscow.* 1992: 88.
- [16] Mikhalev V.Yu. Razrabotka i standartizacia lekarstvennykh preparatov Tykveol i Tykvit, izgotovlyaemykh iz semyan tykvy po bezothodnoi tehnologii: abstract. Dis. Candidat of Farmacy. *Moscow.* 1997: 28 p.
- [17] Derzhavna Farmakopeia Ukrainy (2018). Kharkiv: Ukrainskiy naukoviy farmakopeyniy tsentr yakosti likarskykh zasobiv, 335.

# Therapeutic Drug Monitoring of Venlafaxine and Impact of Age, Gender, BMI, and Diagnosis

Original Paper

Krivosova M.<sup>1✉</sup>, Kertys M.<sup>1</sup>, Grendar M.<sup>2</sup>, Ondrejka I.<sup>3</sup>, Hrtanek I.<sup>3</sup>,  
Tonhajzerova I.<sup>4</sup>, Sekaninova N.<sup>4</sup>, Mokry J.<sup>1</sup><sup>1</sup>Department of Pharmacology<sup>2</sup>Bioinformatics Unit of Biomedical Centre Martin,<sup>3</sup>Psychiatric Clinic<sup>4</sup>Department of PhysiologyJessenius Faculty of Medicine, Comenius University in  
Martin and University Hospital Martin, Martin, Slovakia

Received 28 February, 2020, accepted 24 June, 2020

**Abstract** Depression is a common mental disorder affecting more than 264 million people in the world and 5.1% of the Slovak population. Although various antidepressant approaches have been used; still, about 40% of patients do not respond to a first-choice drug administration and one third of patients do not achieve total remission. Therapeutic drug monitoring (TDM) is a method used for quantification and interpreting the drug concentrations in plasma in order to optimize the pharmacotherapy. The aim of this study was to measure the plasma concentrations of venlafaxine, the fourth most prescribed antidepressant in Slovakia, as well as its active metabolite and interpret them with the relevant patients' characteristics. The study was of retrospective nature and 28 adult patients in total were included. The concentrations of venlafaxine and its active metabolite O-desmethylvenlafaxine (ODV) in plasma were quantified using the validated UHPLC-MS/MS method. The effects of potential influencing factors were evaluated by a multivariate linear regression model. Only 39% of patients reached the venlafaxine active moiety concentrations within the recommended therapeutic range. Plasma concentrations were dependent on age, gender, and duration of the therapy. Venlafaxine metabolism expressed as a metabolite-to-parent concentrations ratio was influenced by a combination of age, gender, and body mass index (BMI). We did not observe any significant difference in plasma concentrations between the patients with a single and recurrent diagnosis of depression. Combining variables made an additive effect on plasma concentrations, for example, active moiety plasma concentrations were higher in older women. In contrast, drug metabolism was higher in older men and men with lower BMI. TDM of venlafaxine is recommended in clinical practice, especially in the elderly when beginning the pharmacotherapy.

**Keywords** Venlafaxine – major depressive disorder – therapeutic drug monitoring

## INTRODUCTION

Depression is a relatively common mental disorder affecting nowadays more than 264 million people all around the world. The disorder is a leading cause of disability worldwide and significantly contributes to the overall global burden of disease (WHO, 2019). Prevalence in Slovakia is 5.1% in all age groups (WHO, 2017). Women have a higher prevalence rate of depression compared to men since adolescent age (Luppa et al., 2012). Although various antidepressant approaches have been used, about 40% of patients do not respond to a first-choice drug administration and one third of patients do not achieve total remission (Cai et al., 2017). Therapeutic

drug monitoring (TDM) is a beneficial patient management tool for quantification and subsequent interpretation of drug concentrations in blood in order to individualize and optimize pharmacotherapy. TDM enables individual dose adjustments according to the properties of the drug, patient characteristics, and measured concentration in blood. Therefore, it is considered as an important tool mainly in patients with variabilities in pharmacokinetics such as patients suffering from comorbidities, patients with impaired function of elimination organs as liver and kidneys, older patients, children, pregnant women or when

\* E-mail: krivosova6@uniba.sk

© European Pharmaceutical Journal

occurring drug-drug interactions (Hiemke et al., 2018). In neuropsychopharmacology, TDM provides a reasonable indirect estimation measurement of the relevant psychotropic drug levels in the central nervous system (CNS) as a result of the investigated correlation factors between concentrations in plasma and in CNS.

Although the plasma concentrations' quantification of a variety of neuropsychopharmacological drugs has become a clinical routine abroad, apart from the monitoring of the drugs with a narrow therapeutic range, it does not belong to standard care in Slovakia.

Venlafaxine (VEN) has been registered at the Slovak market for more than 20 years, and nowadays, it is the fourth most prescribed antidepressant in Slovakia (NHIC, 2019; SIDC, 2020). It belongs to the group of serotonin and norepinephrine reuptake inhibitors (SNRI) antidepressants as its mechanism of action is the inhibition of serotonin and norepinephrine reuptake from the synaptic cleft (Hansen et al., 2017). Venlafaxine is predominantly metabolized by cytochrome CYP2D6 enzyme to an active metabolite *O*-desmethylvenlafaxine (ODV). Half-lives of the extended-release formulations of venlafaxine are 4–14 hours and 10–20 hours for its metabolite ODV. Thus, steady-state concentrations are reached within 4 days of drug administration (Alventa SPC, 2019; Hiemke et al., 2018). It was found that both parent drug and active metabolite ODV penetrate well into the cerebrospinal fluid and the correlation between plasma and brain concentrations of venlafaxine, ODV and active moiety (sum of venlafaxine and ODV) was established. According to the study of Paulzen et al. (2015), the calculated correlation coefficients were 0.74, 0.88 and 0.84 for venlafaxine, ODV and active moiety, respectively.

The therapeutic plasma concentrations of active moiety should be within the range 100–400 ng/mL, and the critical levels are over 800 ng/ml (Hiemke et al., 2018). The concentrations over the critical levels should lead to dose adjustment if the adverse reactions are present. Hypertension, vasodilation leading to flushes, headaches, palpitations, nausea, constipation, dry mouth, insomnia, nervousness, and tachycardias are the most common side effects (Alventa SPC, 2019).

The aim of our study was to evaluate the plasma concentrations of venlafaxine and ODV in plasma of depressive patients treated in standard clinical settings and to explore factors influencing these concentrations.

## METHODS

Adult patients who were hospitalised with a diagnosis of depression at the Psychiatric Clinic of University Hospital Martin were included in this retrospective study. The Ethics Committee of Jessenius Faculty of Medicine, Comenius University approved the study as well as publication of the outcomes. The patients were administered venlafaxine or its combination with other psychotropic drugs. Two blood

samples (at admission day and at the day of discharge) were obtained from 28 adult patients (11 men, 17 women). The blood samples were collected at the trough level, that is, just before administering the next dose after a 24-hour interval and after reaching a stable state concentration of an applied medication and dose regimen. Immediately after the blood sampling and centrifugation, the plasma samples were stored at -80°C until the analysis. Developed and validated method based on ultra-high pressure liquid chromatography coupled with tandem mass spectrometry was used for the quantification of venlafaxine and ODV in plasma (for more details, see Kertys et al., 2020). Only the one-step sample preparation procedure was used as a sample pre-treatment method. The patients' basal characteristics, diagnosis, venlafaxine dose, duration of steady-state concentration of the drug in the applied daily dose, hepatic functions, and any information about co-medication were documented. Dose-corrected concentrations (DCC) of venlafaxine, ODV and active moiety were calculated to evaluate the influence of various dose regimens. The effect of potential influencing factors was quantified by a multivariate linear regression and the model was selected by Akaike Information Criterion (AIC). All the statistical analyses were performed in R (R Core Team, Vienna, Austria) ver. 3.5.2. P-value < 0.05 was considered as statistically significant.

## RESULTS

In total, 28 adult patients suffering from major depressive disorder (MDD) were included in the study (39% men, 61% women), with median age 50 years (range 18–70 years). The MDD diagnosis was confirmed by a specialist-psychiatrist according to DSM-5 (APA, 2018). Majority of patients (n = 25; 89%) were taking venlafaxine at the single daily dose of 300 mg, 2 patients at the single daily dose of 225 mg, and one patient at the single daily dose of 375 mg. Almost all patients were administered another psychomedication or combination of these; the most frequently co-administered antipsychotics were quetiapine, olanzapine, sulpiride, or a combination of two antidepressants venlafaxine and trazodone. Only 2 patients were taking venlafaxine alone. Therefore, we could not evaluate any potential effect of concomitant drugs on the levels of venlafaxine in plasma. Hepatic functions (alanine transaminase - ALT, aspartate aminotransferase - AST, gamma-glutamyltransferase - GMT) in all the patients were normal or slightly increased; however, no clinically important alterations were observed. The information about smoking habits and about renal functions of the patients was not available, as these tests were not performed as a routine examination.

The dose of venlafaxine was individually titrated for each patient according to its clinical efficacy and side effects' occurrence. Patients in our study reached a stable concentration of venlafaxine and the blood sample was collected on 4<sup>th</sup>–29<sup>th</sup> day.

Only 39% of the measured concentrations were within the therapeutic range (100–400 ng/mL) according to the

Table 1: Medians of plasma concentrations (VEN and ODV; ODV+VEN) and metabolite to parent drug ratios (ODV/VEN) in patients treated with venlafaxine at the single daily dose of 300 mg (F32 – single episode of MDD; F33 – recurrent episode of MDD)

	Patients	VEN [ng/mL]	ODV [ng/mL]	ODV/VEN	ODV+VEN [ng/mL]
<b>All</b>	<b>25</b>	<b>182</b>	<b>345</b>	<b>1.85</b>	<b>452</b>
Females	15	255	370	1.85	693
Males	10	148	261	1.75	389
Age < 65	21	132	304	1.92	417
Age ≥ 65	4	345	511	1.55	859
F32	7	128	280	2.00	435
F33	18	198	356	1.74	553

Table 2: Medians of dose-corrected plasma concentrations (DCC) of venlafaxine active moiety (F32 – single episode of MDD; F33 – recurrent episode of MDD)

	Patients	DCC [ng/mL/mg]
<b>All</b>	<b>28</b>	<b>1.46</b>
Females	16	2.07
Males	12	1.30
Age < 65	24	1.39
Age ≥ 65	4	2.86
F32	8	1.46
F33	20	1.61

Consensus Guidelines for TDM in Neuropsychopharmacology (Hiemke et al., 2018). 17 patients (61%) had active moiety concentrations above this range. The sum of the levels of venlafaxine and ODV ranged between 188 and 1426 ng/mL with median of 426 ng/mL. Median dose-corrected plasma levels were 0.59 ng/mL/mg for venlafaxine, 1.06 ng/mL/mg for ODV, and 1.46 ng/mL/mg for the sum of both.

The results of median plasma concentrations of venlafaxine, ODV and an active moiety at 300 mg dose regimen are summarized in Table 1. Dose-corrected plasma concentrations of venlafaxine active moiety in the subgroups of patients are shown in Table 2.

A statistically significant positive correlation of plasma concentration counted as DCC of active venlafaxine moiety with age was observed (in females  $p = 0.004$ , in males  $p = 0.04$ ). The increase was steeper in female patients than in male patients. We observed a negative and statistically significant correlation of DCC with the duration of the therapy (counted as days of stable concentration in the blood;  $p = 0.03$ ). Coefficient of determination of the AIC selected model was relatively high (adj.  $R^2 = 0.37$ ). The results are shown in Figure 1.

Metabolite to parent drug ratio (MPR, ODV/VEN), that is, a parameter reflecting the drug biotransformation, was significantly higher in older men ( $p = 0.0004$ ) and men with

lower BMI ( $p = 0.002$ ). For female patients, age did not seem to play a statistically significant role in the MPR parameter in our study ( $p = 0.06$ ). The adjusted  $R^2$  for this model was 0.36 and results are presented in Figure 2. According to these results, the combination of age, gender, and BMI exert some impact on the rate of venlafaxine metabolism. The difference in plasma concentrations between patients with a single depressive episode and recurrent episodes failed to reach statistical significance, although subjects diagnosed for the first time tend to have lower concentrations.

## DISCUSSION

In the present study, the measurements of venlafaxine plasma concentrations were performed in hospitalized depressive patients. A total of 28 patients were included in this retrospective study. Only 39% patients had venlafaxine active moiety plasma concentration within the recommended therapeutic range, the rest of the patients reached levels above the range, out of which 3 patients (11%) had the levels above laboratory alert level (800 ng/mL). However, no dramatic adverse effects were noticed, only abdominal pain and gastrointestinal discomfort with a short duration were reported. This means that even higher plasma concentrations of venlafaxine were well tolerated. The same conclusion reached Unterecker et al. (2012) in his study with 478 patients taking venlafaxine. Hiemke (2008) observed that interindividual variations in patients' pharmacokinetics led to 30–50% of sub- or supraoptimal concentrations in the blood even if the recommended dosage regimen was maintained. Because of the fact that only hospitalized patients were included in the study, patients' compliance was cautiously controlled by the health care providers (oral cavity check after the drug administration, observation of the patients' behaviour). The drugs were taken strictly at the scheduled dose and time.

According to our results, the venlafaxine plasma concentration is influenced by the combination of age, gender and duration of venlafaxine steady-state concentration. The last can be just an effect of the therapy adjustment in the beginning. Other

studies also confirmed the effects of gender and age, but they also included other factors, for example, smoking habits (Hiemke et al., 2008). Co-medication with other psychotropic drugs was associated with decreased MPR (Unterecker et al., 2012), suggesting inhibition of metabolism. As most of our patients also took other psychotropic drugs, we could not evaluate this as a potential influencing factor. The plasma concentration of ODV, as well as the value of MPR, depend on CYP2D6 metabolic activity (Otton et al., 1996).

Based on our results, the patients over 65 years, especially female patients, had higher concentrations of venlafaxine active moiety even if the same dose was administered as to the younger patients. This finding is in accordance with the results of other authors (Hansen et al., 2017; Reis et al., 2009; Sigurdsson et al., 2015; Unterecker et al., 2012). Additionally, weight-corrected doses with active moiety plasma concentrations were correlated and we found that they are non-significant predictors when controlling also for age and gender. MPR parameter was found significantly higher in men with lower BMI and in older men. The latter was likewise found in the study of Reis et al. (2009). In the same study, the negative correlation between the dose and MPR was observed, however, we could not confirm this as the majority of our subjects took the same dose of venlafaxine – 300 mg once daily.

Sex-related peculiarities influence different pharmacokinetic parameters such as gastric acidity, intestinal motility, body weight and composition, blood volume, liver enzymes, renal excretion and can also account for a different sensitivity to the positive but also unwanted effects and toxicity of psychotropic drugs (Marazziti et al., 2013). Women tend to have higher plasma concentrations of psychotropic drugs and one of the reasons might be a different expression of CYP enzymes and thus variable hepatic clearance of drugs (Reis et al., 2009).

Kloiber et al. (2007) demonstrated that depressive patients have on average higher BMI and the effect of antidepressants is decreased compared to the patients with lower BMI. Venlafaxine is a lipophilic drug and when body fat decreases,

the volume of distribution of these drugs is reduced (Turnheim, 2003). A negative correlation between BMI and MPR parameter was found in men, however, no correlation between plasma concentrations and BMI was observed.

According to the study of Reyes-Barron et al. (2016), response to antidepressants can be genetically determined from 42 to 50%. This might be also the case of our 3 patients with supratherapeutic or even toxic concentrations of the drug active moiety. CYP2D6, the major enzyme involved in venlafaxine metabolism as well as in other almost 20% most frequently prescribed medications, has a highly polymorphic gene. More than 100 variant alleles cause up to 200-fold variability in drug metabolism (Tirona & Kim, 2017).

In this study, the influence of the final diagnosis was assessed on the venlafaxine active moiety concentrations in plasma. Based on our results, a non-significant increase was observed in patients with recurrent episodes. However, the number of patients in this study could be considered as a limitation of our observation, and thus, this parameter should be revised in larger studies.

To summarize our findings, we confirmed that women and older patients reached higher plasma concentrations of venlafaxine active moiety, although none dose adjustments are mentioned in the summary of product characteristics of the relevant medicinal products. Dose adjustment seems to be advisable due to an additive effect of the variables, especially when administering the very first doses of venlafaxine to the elderly patients. The retrospective nature of this study provides only explorative data, but they confirm that TDM of venlafaxine therapy, controlling influences of the drug pharmacokinetics, should be recommended in clinical practice.

## ACKNOWLEDGEMENTS

We would like to thank Dr. Zuzana Macekova and Dr. Michal Kolorz, PhD for their advice based on clinical experience. The study was supported by grants VEGA 1/0255/18, APVV-18-0084 and UK/83/2019.

## References

- [1] Alventa SPC. (<https://www.adc.sk/databazy/produkty/spc/alventa-75-mg-304880.html>). Revised October 2019. Accessed December 20, 2019.
- [2] American Psychiatric Association (APA). DSM-5. (<https://www.psychiatry.org/psychiatrists/practice/dsm>). Revised October 2018. Accessed January 24, 2020.
- [3] Cai L, Xu L, Wei L, Chen W. Relationship of Mean Platelet Volume To MDD: A Retrospective Study. *Shanghai Arch Psychiatry*. 2017;29(1):21–29.
- [4] Hansen MR, Kuhlmann IB, Pottegård A, Damkier P. Therapeutic Drug Monitoring of Venlafaxine in an Everyday Clinical Setting: Analysis of Age, Sex and Dose Concentration Relationships. *Basic Clin Pharmacol Toxicol*. 2017;121(4):298–302.
- [5] Hiemke C. Clinical utility of drug measurements and pharmacokinetics – therapeutic drug monitoring in psychiatry. *Eur J Clin Pharmacol*. 2008;64:159–166.
- [6] Hiemke C, Bergemann N, Clement HW, et al. Consensus Guidelines for Therapeutic Drug Monitoring in Neuropsychopharmacology: Update 2017. *Pharmacopsychiatry*. 2018;51(1-02):9–62.
- [7] Kertys M, Krivosova M, Ondrejka I, Hrtanek I, Tonhajzerova I, Mokry J. Simultaneous determination of fluoxetine, venlafaxine, vortioxetine and their active metabolites in human plasma by

- LC-MS/MS using one-step sample preparation procedure. *J Pharm Biomed Anal.* 2020;181:113098.
- [8] Kloiber S, Ising M, Reppermund S, et al. Overweight and obesity affect treatment response in major depression. *Biol Psychiatry.* 2007;62(4):321–6.
- [9] Luppá M, Sikorski C, Luck T, et al. Age- and gender-specific prevalence of depression in latest-life--systematic review and meta-analysis. *J Affect Disord.* 2012;136(3):212–21.
- [10] Marazziti D, Baroni S, Picchetti M, et al. Pharmacokinetics and pharmacodynamics of psychotropic drugs: effect of sex. *CNS Spectr.* 2013;18(3):118–27.
- [11] National health information center (NHIC). Prescription Drug Use in Slovak Republic in 2018. ([http://www.nczisk.sk/Statisticke\\_vystupy/Tematicke\\_statisticke\\_vystupy/TOP-50-liekov/Pages/Spotreba-humannych-liekov-v-slovenskej-republike.aspx](http://www.nczisk.sk/Statisticke_vystupy/Tematicke_statisticke_vystupy/TOP-50-liekov/Pages/Spotreba-humannych-liekov-v-slovenskej-republike.aspx)). Revised December 2019. Accessed January 24, 2020.
- [12] Otton SV, Ball SE, Cheung SW, Inaba T, Rudolph RL, Sellers EM. Venlafaxine oxidation in vitro is catalysed by CYP2D6. *Br J Clin Pharmacol.* 1996;41(2):149–56.
- [13] Paulzen M, Groppe S, Tauber SC, Veselinovic T, Hiemke C, Gründer G. Venlafaxine and O-desmethylvenlafaxine concentrations in plasma and cerebrospinal fluid. *J Clin Psychiatry.* 2015;76(1):25–31.
- [14] Reis M, Aamo T, Spigset O, Ahlner J. Serum concentrations of antidepressant drugs in a naturalistic setting: compilation based on a large therapeutic drug monitoring database. *Ther Drug Monit.* 2009;31(1):42–56.
- [15] Reyes-Barron C, Tonarelli S, Delozier A, et al. Pharmacogenetics of antidepressants, a review of significant genetic variants in different populations. *Clin. Depress.* 2016;2(1):109.
- [16] Sigurdsson HP, Hefner G, Ben-omar N, et al. Steady-state serum concentrations of venlafaxine in patients with late-life depression. Impact of age, sex and BMI. *J Neural Transm (Vienna).* 2015;122(5):721–9.
- [17] State Institute for Drug Control (SIDC). Database of medicaments. ([https://www.sukl.sk/en/servis/search/searching-on-the-database-of-medicinal-products?page\\_id=410&lie\\_nazov=&atc\\_nazov=venlafax%C3%ADn&lie\\_kod=&atc\\_kod=&lie\\_rc=&drz\\_kod=](https://www.sukl.sk/en/servis/search/searching-on-the-database-of-medicinal-products?page_id=410&lie_nazov=&atc_nazov=venlafax%C3%ADn&lie_kod=&atc_kod=&lie_rc=&drz_kod=)). Revised January 2020. Accessed January 24, 2020.
- [18] Tirona RG, Kim RB. Introduction to Clinical Pharmacology. In: Robertson D, Williams GH. *Clinical and Translational Science*, 2<sup>nd</sup> ed. Academic Press; 2017.
- [19] Turnheim K. When drug therapy gets old: pharmacokinetics and pharmacodynamics in the elderly. *Exp Gerontol.* 2003;38(8):843–53.
- [20] Unterecker S, Hiemke C, Greiner C, et al. The effect of age, sex, smoking and co-medication on serum levels of venlafaxine and O-desmethylvenlafaxine under naturalistic conditions. *Pharmacopsychiatry.* 2012;45(6):229–35.
- [21] World Health Organisation (WHO). Depression and Other Common Mental Disorders. Global Health Estimates. (<https://apps.who.int/iris/bitstream/handle/10665/254610/WHO-MSD-MER-2017.2-eng.pdf?sequence=1&isAllowed=y>). 2017. Accessed January 24, 2020.
- [22] World Health Organisation (WHO). Depression. (<https://www.who.int/news-room/fact-sheets/detail/depression>). Revised December 2019. Accessed January 23, 2020.

# Comparative morphological studies of raw parts of the most common species of *Thymus* in Ukraine

Original research article/Review

Minarchenko V.<sup>1,4</sup>, Tymchenko I.<sup>2</sup>, Glushchenko L.<sup>3</sup>, Pidchenko V.<sup>4</sup>✉

<sup>1,2</sup>M.G. Kholodny Institute of Botany of the NAS of Ukraine, 2 Tereshchenkivska Street, 01004, Kyiv, Ukraine

<sup>3</sup>Experimental Station of Medicinal Plants, Institute of Agroecology and Nature Management of the National Academy of Agricultural Sciences of Ukraine, 16A Pokrovska Street, 37535, Berezotocha, Ukraine.

<sup>1,4</sup>Bogomolets National Medical University, Department of Pharmacognosy and Botany, 22 Pushkinska Street, 01004, Kyiv, Ukraine

Received 1 August, 2019, accepted 10 December, 2019

**Abstract** This study presents the results of our comparative evaluation of diagnostic morphological characteristics of raw material from 11 species of genus *Thymus* L. of medicinal and raw material importance occurring in Ukraine. The following taxa were evaluated: *T. serpyllum* L., *T. odoratissimus* Mill. (*T. glabrescens* Willd.), *T. borysthenticus* Klokov & Des.-Shost., *T. pallasius* Heinr. Braun, *T. moldavicus* Klokov & Des.-Shost., *T. calcareus* Klokov & Des.-Shost., *T. alpestris* Tausch ex A. Kern., *T. × dimorphus* Klokov & Des.-Shost., *T. pannonicus* All. s.l. (including *T. marschallianus* Willd.), *T. pulegioides* L. and *T. roegneri* K. Koch (*T. alternans* Klokov). Among wild species of thyme, only raw material of *Thymus serpyllum* is officially allowed for use with the purpose for production of pharmaceuticals and medicines. A comparison of the main characteristics is particularly important in view of the fact that raw material is represented by parts of plants (stems, leaves and flowers), which makes any whole comparison of species hardly possible. This study has revealed that stem pubescence, calyx structure, configuration/arrangement and type of leaf venation can provide valuable information for diagnostics of raw material of *Thymus* species. The results exhibited that according to characters of stem pubescence, calyx structure, shape and size of leaves the most similar are raw material samples of *T. serpyllum* and *T. moldavicus*. However, these species are rather well separated geographically, so the possibility of mixing of their raw material is negligible. Other species have significant morphological differences in certain characteristics by which they can be diagnosed in the raw material.

**Keywords** *Thymus* – morphology – characters – raw material – medicinal plants – Ukraine

## INTRODUCTION

Species of the genus *Thymus* are valuable natural sources of pharmaceutical raw materials for the pharmaceutical industry and medicine. The raw materials of wild and cultivated species of thyme have been used for a long time to treat and prevent respiratory and other diseases and malfunctions. Representatives of the genus *Thymus* are included in many pharmacopoeias of Europe, which recommend their use in medicines, balms and biologically active food supplements. Raw materials of wild *Thymus serpyllum* L. and cultivated *Thymus vulgaris* L., which are included in the State Pharmacopoeia of Ukraine, are mainly used for the production of medicines in Ukraine (SPhU, 2001, 2004, 2008, 2009, 2011). According to various data, there are from 15 to 40 species of the genus *Thymus* occurring in Ukraine, depending

on different taxonomic treatments and wide versus narrow species concepts applied by various taxonomists (see the list of accepted species and synonyms in Mosyakin and Fedoronchuk, 1999, with updates by Nachychko, 2015). In assessing the current taxonomic status of selected critical taxa, we also consulted the reliable online resources, such as POWO (Plants of the World Online – <http://www.plantsoftheworldonline.org>). These species differ by their morphological characteristics and territorial distribution. Still at this moment there are questions regarding the taxonomy of species, which belong to this genus due to high population variability and occasional hybridisation, despite the fact that there is abundant data on morphology and micromorphology (Bartolucci et al., 2013, Ložienė, 2006, Morales, 2002, Zeljković

\* E-mail: pidchenkovitalii@gmail.com

© European Pharmaceutical Journal

& Maksimović, 2015, etc.). Species of this genus have a comparatively small number of morphological features that can be used as diagnostic, so the question of interrelations species of thyme, and even the infraspecific *versus* specific status of some taxa, remains controversial at present.

Among the wide diversity of species and infraspecific entities of thyme in Ukraine, 11 species have the greatest distribution and native resources suitable for harvesting in natural habitats. Most of them are geographically restricted, although sometimes their geographic ranges overlap, and there are known cases of collecting of neighbouring or co-occurring species (Minarchenko, 2011). Such mixed or confused raw material may mistakenly get into production of medicines at pharmaceutical companies. Therefore, the identification of species-specific morphological features of these taxa is important for the diagnostics of raw material.

The main morphological characteristics of species of *Thymus* for the purposes of taxonomy are quite fully described by many scientists (Gogina, 1975, Ložiene, 2006, and references therein). But many systematically relevant and even reliable characteristics are not applicable to the purpose of identification of raw material, since the raw of thyme is a mixture of fragments of generative and vegetative shoots (stems with leaves), leaves, parts of inflorescences and flowers (or flower parts, such as the calyx and corolla). The aim of this comparative study was to determine morphological features required for the differentiation and identification in raw material of the most commonly occurring species of *Thymus* in Ukraine.

## MATERIAL AND METHOD

Taxa of research were above-ground (often termed *aerial*) parts of *T. serpyllum* L., *T. glabrescens* Willd., *T. borysthenticus* Klokov & Des.-Shost., *T. pallasianus* Heinr. Braun, *T. moldavicus* Klokov & Des.-Shost., *T. calcareus* Klokov & Des.-Shost., *T. alpestris* Tausch ex A. Kern., *T. × dimorphus* Klokov & Des.-Shost., *T. pannonicus* All. (*T. marschallianus* Willd.), *T. pulegioides* L. and *T. roegneri* K. Koch (*T. alternans* Klokov). Considering the fact reported in literature (see above) that the main diagnostic morphological characteristics of the raw materials of thyme species are the pubescence of different organs of plants, the shape and size of leaves, calyx and tooth of upper lip, the main attention was paid to analysing these characteristics.

The research is based on the materials and results of authors' long-term field research at different localities, as well as desktop studies, critical processing of literary sources, and herbarium specimens deposited at the National Herbarium of Ukraine (international acronym KW: <http://sweetgum.nybg.org/science/ih/herbarium-details/?irn=125430>). KW is the largest herbarium in Ukraine and the second largest in Eastern Europe; it contains trusted scientific collections of *Thymus* that were critically revised and identified by several distinguished experts in the taxonomy of the genus. For

the morphological studies, at least ten specimens of each species were investigated. All measurements were made ten times for each organ from different parts of a specimen. The photographs were taken using the Philip Harris Stereo Microscope and Levenhuk M1000 PLUS Microscope Camera.

## RESULTS AND DISCUSSION

This study is prepared for the purposes of diagnostic of raw material (so-called 'herb') of *Thymus* species under laboratory conditions using a simple microscope.

### Stem (Fig. 1, 2)

The main diagnostic feature for the stem of *Thymus* species is its pubescence and its peculiarities (pubescence on ribs, opposite margins or all faces, size and density of trichomes and so on), as well as the degree of the ribs manifestation, the presence of glandular trichomes and branching of generative shoots.

The character of stem pubescence is a rather stable morphological characteristic of *Thymus* species, although some species may vary by that character in their upper and lower parts of stems (Nachychko, 2015) or on generative and vegetative stems (Kamašina, Ložienė, 2009). While the raw material of thyme is the upper frondose (leaf-bearing, usually with inflorescences) part of the shoot, these differences are insignificant.

Comparative morphological analysis showed that the pubescence all around the stem is present in *T. serpyllum*, *T. borysthenticus*, *T. calcareus*, *T. dimorphus*, *T. glabrescens*, *T. moldavicus*, *T. pallasianus* and *T. pannonicus* (Fig. 1). Their stems are hairy all over with non-glandular, mostly multicellular, more or less curved hairs. The stems of vegetative shoots are pubescent with shorter trichomes than the stems of generative ones in all species. However, the stems of the analysed species have a number of distinctive features. Short and sparse stem trichomes are present in *T. borysthenticus* and *T. pallasianus*, while the stems of *T. calcareus* and *T. moldavicus* have short thick tectorial trichomes. Stems of *T. serpyllum*, *T. dimorphus*, *T. glabrescens* and *T. pannonicus* are thickly covered by the protruded long trichomes. Secretory (glandular) trichomes are rarely distinctly shown on the stems of *T. serpyllum*, *T. dimorphus*, *T. moldavicus* and *T. pannonicus* (Fig. 1a, d, f, h). The secretory trichomes on the stem are mostly represented by multicellular glands that are prominent above the verge of stem, and their density increases from the base to the apex of the stem. This is typical for many species of the genus, as well as the stem pubescence (Boz et al., 2009, Nachychko, 2015).

At the stems of generative shoots of *T. alpestris* and *T. pulegioides* the multicellular trichomes are present only along the ribs (Fig. 2a, b); the glandular trichomes are scarce. Stems of *T. roegneri* are pubescent with long multicellular hairs on

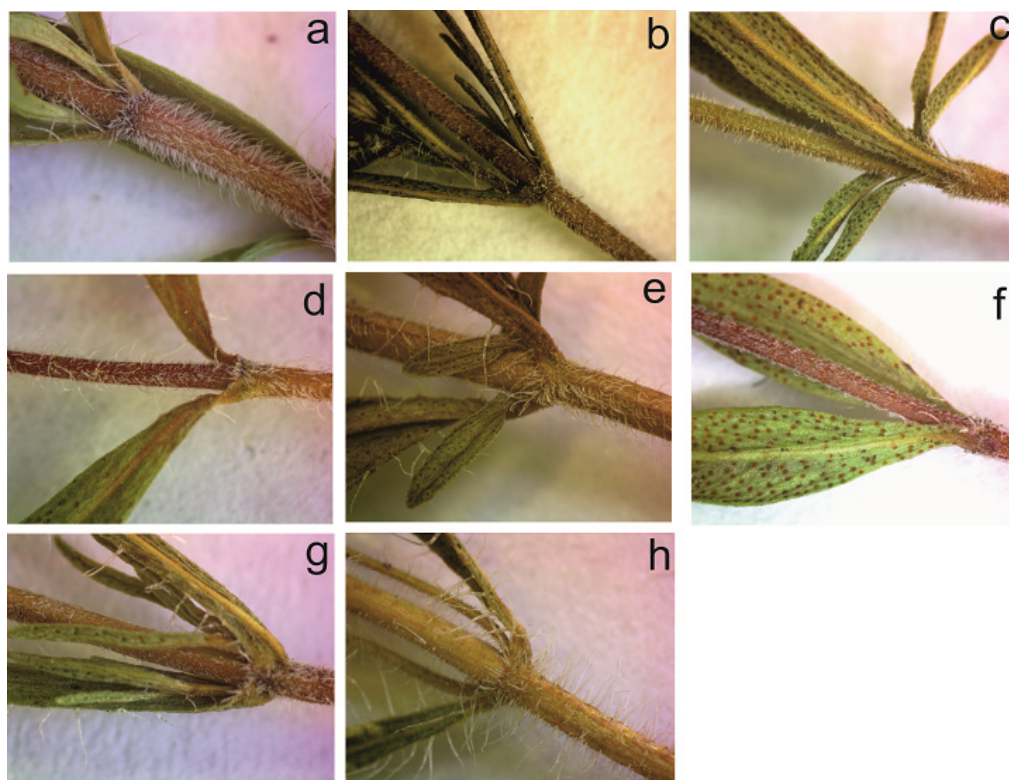


Figure 1: All-around stem pubescence of selected *Thymus* species,  $\times 20$ : a – *T. serpyllum*, b – *T. borysthenicus*, c – *T. calcareus*, d – *T. dimorphus*, e – *T. glabrescens*, f – *T. moldavicus*, g – *T. pallasianus*, h – *T. pannonicus*.



Figure 2: Stem pubescence along the ribs (a – *T. alpestris*, b – *T. pulegioides*, c – *T. roegneri*) and on opposite faces,  $\times 20$ .

two opposite faces (Fig. 2c), alternately from verge to verge; the glandular trichomes are less distinguished.

### Leaf blade (Fig. 3–5)

In raw materials of thyme the leaves are more distinguished. They differ in size, shape, pubescence of the leaf blade and edge of the blade, type of venation and frequency of occurrence of glandules. It has been established that the size of leaves in all species of thyme varies markedly depending on the stage of development and location on the stem. In addition, it is believed that the size of the leaves and the ratio of their length and width are significantly influenced

by environmental conditions (Ložiene, 2006). However, the shape of the leaf blade is a more stable feature.

The brevipedicelate (short-petioled) linearly elongated or elongated-elliptical leaf shape is present in *T. serpyllum*, *T. moldavicus* and *T. calcareus*, broadly-elliptical in *T. roegneri* and *T. glabrescens*. The manifestation of leaves polymorphism of different formations is customary for *T. glabrescens* (Nachychko, 2015). Though, within the limits of one generative shoot the leaves differ both in form and in degree of development of petioles on upside and basal part. The needle-shaped or narrow-linear leaves with involute edge of leaf blade are present in *T. borysthenicus* and *T. pallasianus* (Fig. 3). *Thymus dimorphus* and *T. pannonicus* have sessile

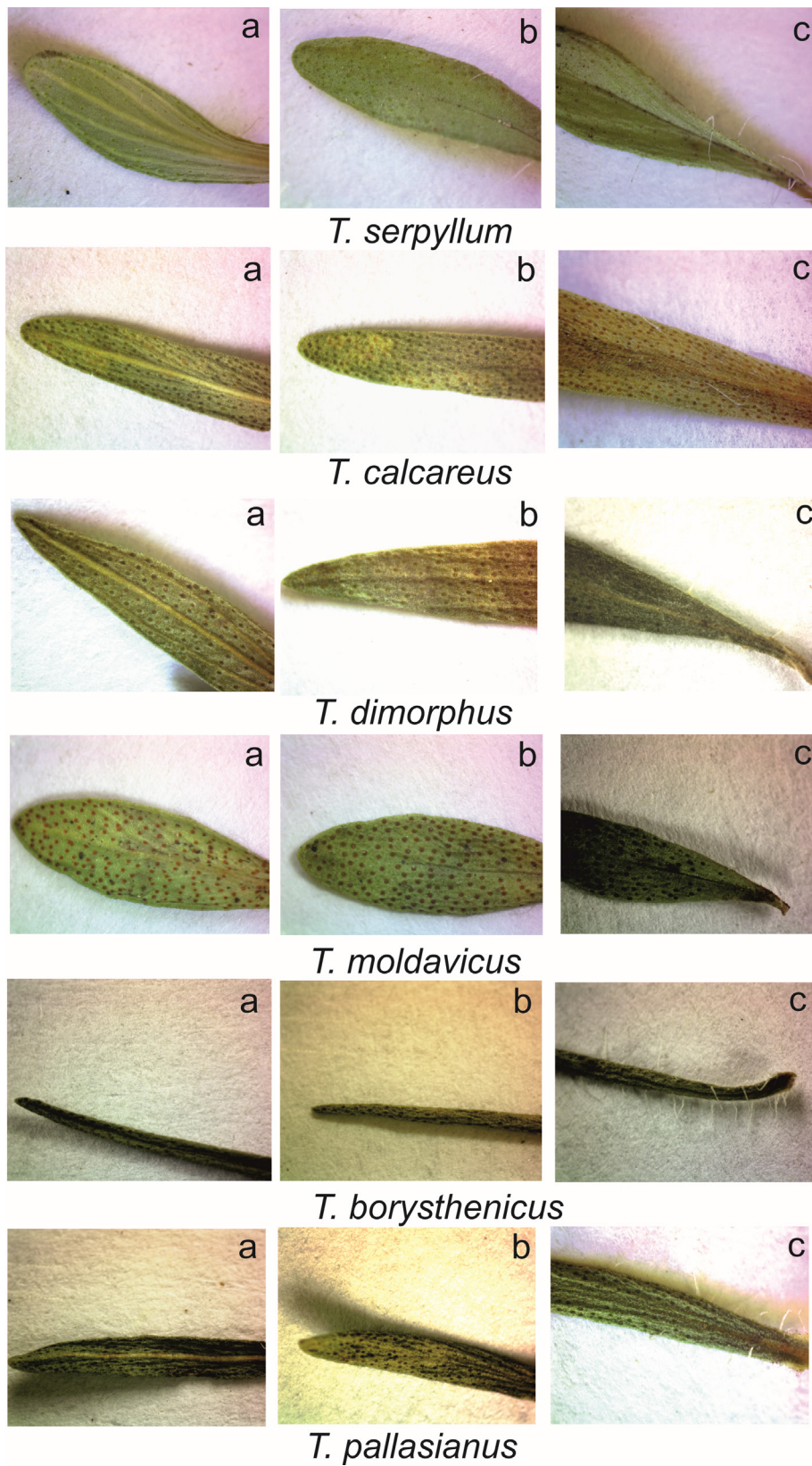


Figure 3: An important diagnostic characteristic of leaf blade of selected *Thymus* species,  $\times 20$ : a – abaxial leaf surfaces, b – adaxial leaf surfaces, c – leaf base.

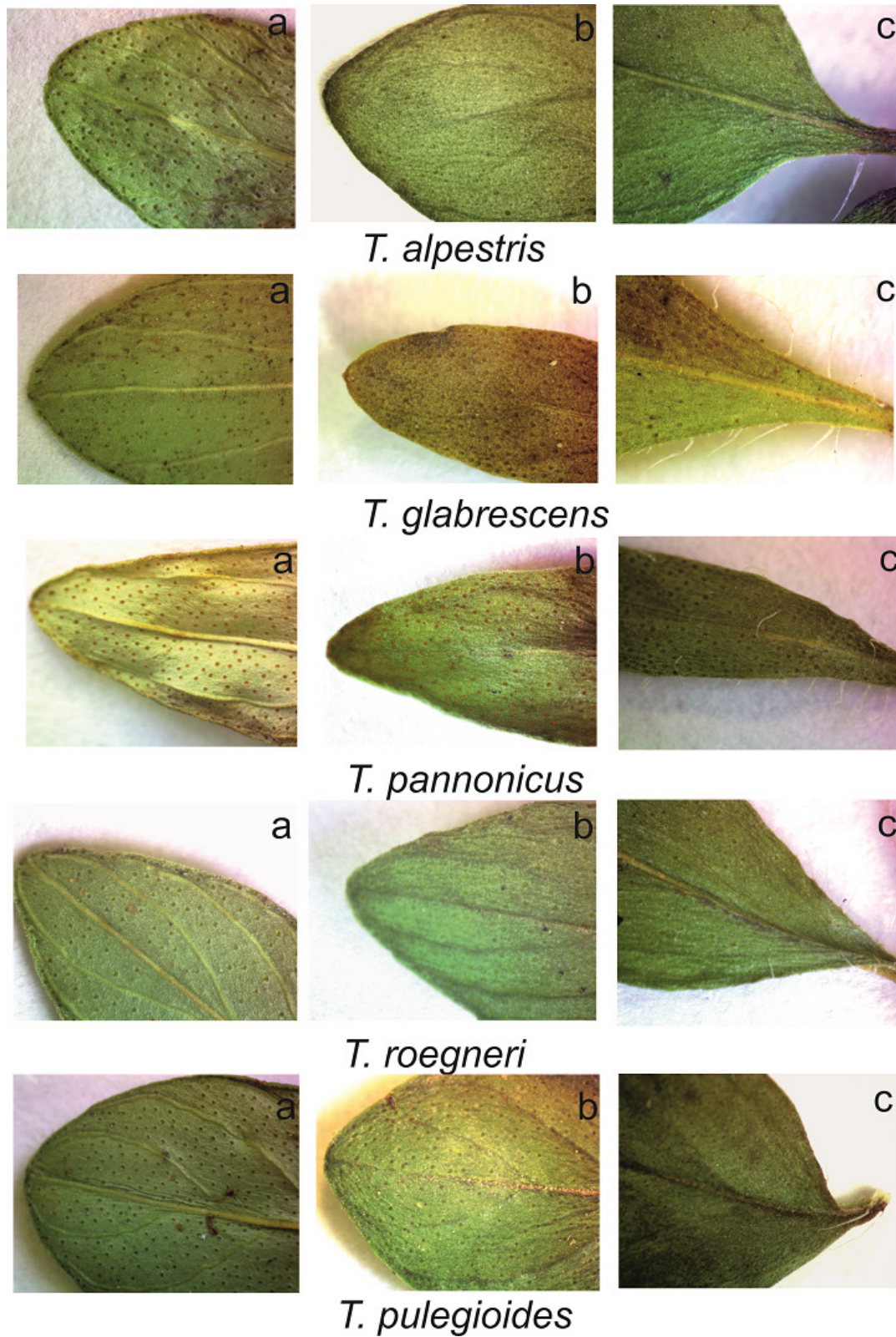


Figure 4: An important diagnostic characteristic of leaf blade of selected *Thymus* species,  $\times 20$ : a – abaxial leaf surfaces, b – adaxial leaf surfaces, c – leaf base.



Figure 5: Multicellular trichomes on both sides of the *T. pannonicus* leaf blade,  $\times 20$ .

(narrowed at the top, tapered at the base) or brevipetiolate elongated-elliptical leaves (Fig. 3, 4). The considerable variability of leaf blade pubescence of *T. pannonicus* was found in some populations. The leaves of some species are pubescent with multicellular trichomes on both sides of the leaf blade (Fig. 5), although in the most of analysed specimens these trichomes are present only on the edge of the leaf blade at the base. Leaves of *T. alpestris* and *T. pulegioides* are wide, egg-shaped with the largest width in the middle of the leaf blade and well-defined petiole.

The leaves of *Thymus* species are thickly covered by tectorial short non-glandular trichomes on both sides of the lamina (Fig. 3, 4) and, therefore, the leaves appear greyish. This is especially peculiar to leaves of *T. serpyllum*, *T. calcareus*, *T. dimorphus*, *T. moldavicus*, *T. borysthenticus* and *T. pallasianus* (Fig. 4). In other species it is less pronounced.

Multicellular unbranched trichomes along the edge of the leaf blade are present in all species. They usually occur in the lower third of the leaf, although sometimes they rise higher. Size, shape and colour of the glandular trichomes on the stems, adaxial and abaxial leaf surfaces and calyx differ in the studied species less.

The number and density of glands (capitate and peltate glandular trichomes) on both surfaces of the leaves vary considerably even in populations of one species (Arsenijević et al., 2019, Dajić-Stevanović et al., 2008), therefore these criteria have no significant diagnostic value for raw material of thyme. At both dorsal and ventral sides of leaves of most species, the glands are rather evenly distributed (Fig. 3, 4). It has been affirmed that two surfaces of leaves of *T. serpyllum* contain approximately the same quantity of these glandular trichomes, though the adaxial surface of *T. vulgaris* leaves has more glandular trichomes compared to the abaxial surface of ones (Svidenko et al., 2018). The density of glandular trichomes is distinguished for considerable diversity and variability; particularly it can depend on both ecological and genetic factors. In general, their density is higher in species

with small leaves except *T. serpyllum* (Fig. 1a, b).

The type of leaf venation is an important systematic characteristic of thyme leaves, but diagnosing of thyme raw materials only by this characteristic is complicated by blurriness or the weak expression of this trait and the lack of clear differences in the venation. For example, we can see that the central and lateral veins of leaf protrude above the abaxial surface of the leaf blade in *T. alpestris*, *T. glabrescens*, *T. pannonicus* and *T. roegneri*, and the lateral veins are arcuately curved, gradually thin out as they approach the edge of the leaf blade and do not merge together at the edge (eucaupitodromous venation) (Fig. 4a). In *T. pulegioides* and *T. serpyllum* the upper lateral veins merge together at the edge of the leaf blade. However, the lateral veins of *T. pulegioides* are arcuately bent, and acute angles to the central vein are present in *T. serpyllum*. The central and lateral veins are more or less distinguishable in *T. dimorphus*, and the lateral veins are scarce and elongated upwards at a slight angle to the central vein, but they do not merge at the apex, as in *T. serpyllum*.

The leaves of *T. borysthenticus*, *T. calcareus*, *T. moldavicus* and *T. pallasianus* are similar in venation, but even here some differences are present (Fig. 3). The lateral veins on the abaxial surface of *T. calcareus* and *T. pallasianus* leaves are better pronounced than in *T. moldavicus*. The distinguishing of the central and lateral veins in the leaves of *T. borysthenticus* is difficult. The results of our observations demonstrated that in some cases it is difficult to determine the distinctions in venation of leaves in different species. Therefore, this character (or, rather, set of characters) can only be used in combination with other diagnostic species-specific features.

#### Calyx (Fig. 6, 7).

Calyx structure is a species-specific feature in thyme, particularly length and shape of calyx, the shape of the teeth of upper lip of calyx and the pubescence of the teeth of lower lip of calyx. The trumpet elongated-campanulate calyx with numerous (more than 12 pairs) long trichomes on the teeth of the lower lip is present in *T. borysthenticus*, *T. calcareus*, *T. moldavicus*, *T. pallasianus* and *T. serpyllum* (Fig. 6). The glandular trichomes are present across all surfaces of the calyx of all analysed species.

The calyx of *T. alpestris*, *T. dimorphus*, *T. glabrescens*, *T. pannonicus*, *T. pulegioides* and *T. roegneri* has a predominantly widened extended-campanulate shape with a few (up to 12 pairs) scattered long trichomes on the teeth of the lower lip (Fig. 7).

It is believed that these structural features of the calyx within the genus of *Thymus* are quite conservative and rather constant at the section level, so they are often used for taxonomy purposes (Gogina, 1975, Nachychko, 2015). According to the results of our analysis, the characteristics of the calyx structure, especially its length and shape, have

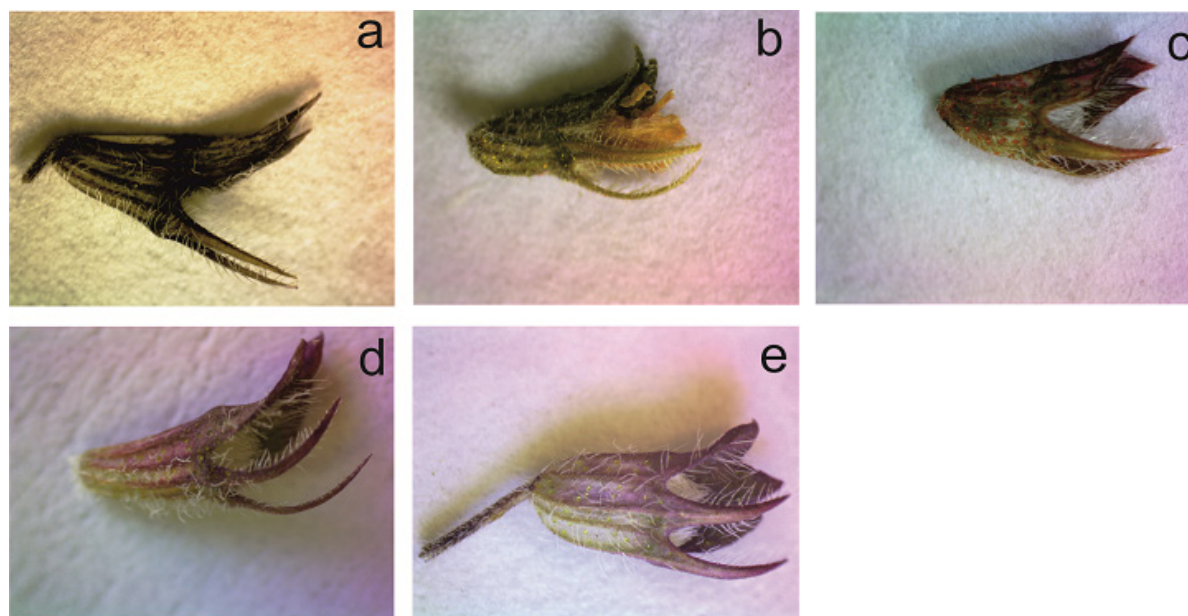


Figure 6: Calyx with numerous (more than 12 pairs) long trichomes on the teeth of the lower lip of selected *Thymus* species,  $\times 20$ : a – *T. borysthenticus*, b – *T. calcareus*, c – *T. moldavicus*, d – *T. pallasianus*, e – *T. serpyllum*.

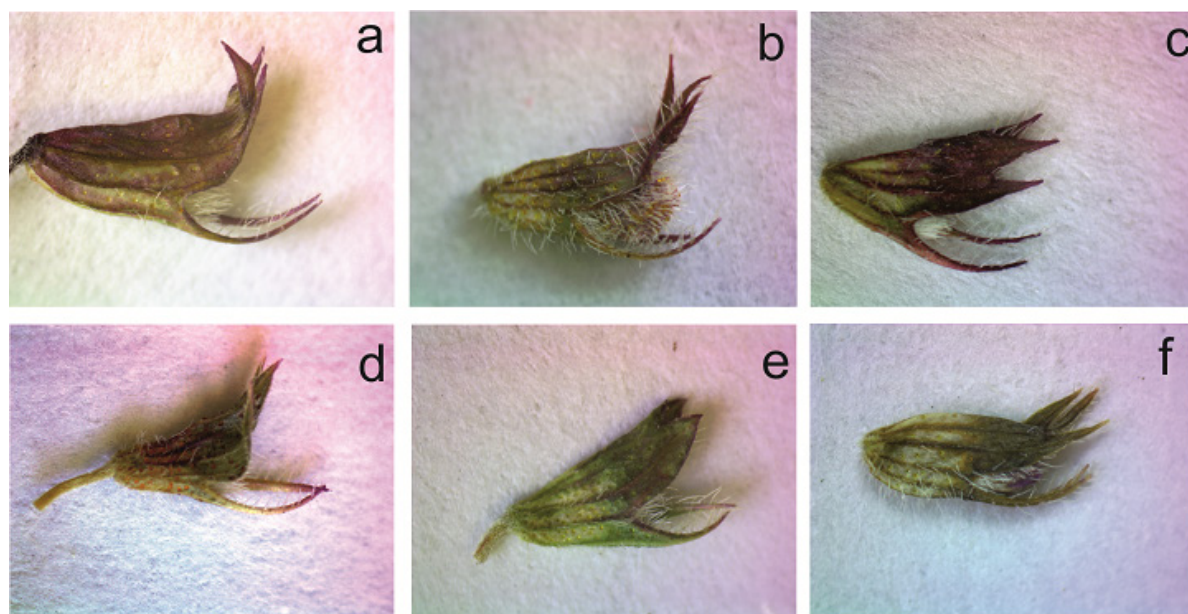


Figure 7: Calyx with few (up to 12 pairs) scattered long trichomes on the teeth of the lower lip of selected *Thymus* species,  $\times 20$ : a – *T. alpestris*, b – *T. dimorphus*, c – *T. glabrescens*, d – *T. pannonicus*, e – *T. pulegioides*, f – *T. roegneri*.

a significant range of variability and in species with multi-flowered inflorescences can vary greatly, depending on their position in the inflorescence, which complicates their comparison in raw material. Therefore, it has been found that structure of the thyme calyx could be useful for distinguishing the raw materials of *Thymus* species in addition to other morphological characteristics mentioned above.

## CONCLUSIONS

The investigation of the morphology of raw parts of 11 species of *Thymus* most commonly occurring in Ukraine was carried out using a light microscope. The diagnostic features of leaves, stem and calyx of these species from different regions were studied and described. The results of analyses demonstrated that raw material of *T. serpyllum* is similar to

that of other Ukrainian species of genus; however, it has a number of diagnostic morphological characteristics. The values of the analysed parameters do not have a universal range and are often variable within wide limits, depending on various environmental factors. Raw material of any of the studied species can be clearly distinguished from that of other taxa only through the use of the whole complex of species-specific morphological characteristics. This study is aimed at facilitating the identification of thyme raw material and might be further used for the development of regulatory documents on this herbal medicinal material, at least within the study area (Ukraine and adjacent areas).

## ACKNOWLEDGEMENTS

The authors are grateful to Sergei L. Mosyakin, Director of M.G. Kholodny Institute of Botany of National Academy of Sciences of Ukraine, and Natalia M. Shyian, Head Curator of National Herbarium of Ukraine (KW), for providing necessary research facilities. The valuable comments and suggestions of two anonymous reviewers on the earlier version of the manuscript are greatly appreciated, as well as comments of the editorial team, which greatly improved the text.

## References

- [1] Arsenijević J, Drobac M, Šoštarić I et al. Comparison of essential oils and hydromethanol extracts of cultivated and wild growing *Thymus pannonicus* All. *Industrial Crops and Products*. 2019;130:162–169.
- [2] Bartolucci F, Peruzzi L, Passalacqua N. Typification of names and taxonomic notes within the genus *Thymus* L. (Lamiaceae). *Taxon*. 2013;62(6):1308–1314.
- [3] Boz I, Burzo I, Zamfirache MM, Toma C, Padurariu C. Glandular trichomes and essential oil composition of *Thymus pannonicus* All. (Lamiaceae). *An. Univ. Oradea. Fasc. Biol.* 2009;16(2):36–39.
- [4] Boz I, Navarro L, Gales R, Padurariu C. *Morphology and structure of glandular hairs in development of Thymus vulgaris* L. *Scientific Annals of Alexandru Ioan Cuza University of Iasi. New Series, Section 2. Vegetal Biology*. 2009;55(2):81–86.
- [5] Dajić-Stevanović Z, Šoštarić I, Marin PD, Stojanović D, Ristić M. Population variability in *Thymus glabrescens* Willd. from Serbia: morphology, anatomy and essential oil composition. *Arch. Biol. Sci., Belgrade*. 2008;60(3):475–483.
- [6] Gogina EE. Genus thyme (thyme) *Thymus* L. *Biological flora of the Moscow region*. 1975;2:137–168. (in russian)
- [7] Kamašina V, Ložjeně K. The evaluation of phenotypic diversity of *Thymus × Oblongifolius* according to some anatomical characters and comparison with parent species. *Acta Botanica Hungarica*. 2009;51(1-2):105–117.
- [8] Ložjeně K. Instability of morphological features used for classification of *Thymus pulegioides* infraspecific taxa. *Acta Botanica Hungarica*. 2006;48(3-4):345–360.
- [9] Minarchenko V. Medicinal plants of Ukraine: diversity, resources, legislation. *Medicinal plant conservation*. 2011;14:7–13.
- [10] Morales R. The history, botany and taxonomy of the genus *Thymus*. In: Stahl-Biskup E, Sáez F, eds. *Thyme: the Genus Thymus*. London: Taylor and Francis; 2002:1–43.
- [11] Mosyakin SL, Fedoronchuk MM. *Vascular plants of Ukraine. A nomenclatural checklist*. Kiev; 1999. xxiii+345p.
- [12] Nachychko VO. Diagnostic features of representatives of *Thymus* sect. *Serpyllum* and T. sect. *Marginati* (Lamiaceae). *The Journal of V.N. Karazin Kharkiv National University. Series: biology*. 2015;25:77–89. (in ukrainian)
- [13] Svidenko L, Grygorieva O, Vergun O et al. Characteristic of leaf peltate glandular trichomes and their variability of some lamiaceae martinov family species. *Agrobiodiversity for improving nutrition, health and life quality*. 2018;2:124–132.
- [14] The State Pharmacopoeia of Ukraine. State Enterprise «Scientific and Expert Pharmacopoeial Centre». 1st ed. Kharkov: RIREH, 2001. Appendix 1. 2004. Appendix 2. Kharkov: State Enterprise «Scientific and Expert Pharmacopoeial Center»; 2008. Appendix 3. 2009. Appendix 4. 2011 (in Ukrainian).
- [15] Zeljković SČ, Maksimović M. Chemical composition and bioactivity of essential oil from *Thymus* species in Balkan Peninsula. *Phytochemistry Reviews*. 2015;14(3):335–352.